University Hospital Ulm
Department of Orthopaedics
Medical Director: Prof. Dr. med. Heiko Reichel
Division for Biochemistry of Joint and Connective Tissue Diseases
Head: Prof. Dr. med. Rolf E. Brenner

Involvement of anaphylatoxins and their corresponding receptors in cartilage calcification during osteoarthritis progression

Dissertation

submitted in partial fulfilment of the requirements for the
degree of “Doctor rerum naturalium” (Dr. rer. nat.)
of the International Graduate School
in Molecular Medicine Ulm

Leonie Ruths

Born in Stuttgart

Ulm, 2024

Current dean of the Medical Faculty: Prof. Dr. Thomas Wirth

Current chairman of the Graduate School: Prof. Dr. Bernd Knöll

Theses Advisory Committee:

- First Supervisor: PD Dr. Jana Riegger-Koch
- Second Supervisor: Prof. Dr. Markus Huber-Lang
- Third Supervisor: Prof. Dr. Gundula Schulze-Tanzil

External Reviewer: Prof. Dr. Anja Niehoff

Day doctorate awarded: 8th January, 2025

Publication index

Results gained in my thesis have previously been published in the following publication:

Ruths L, Huber-Lang M, Schulze-Tanzil G, Riegger J: Anaphylatoxins and their corresponding receptors as potential drivers in cartilage calcification during osteoarthritis progression. Osteoarthritis Cartilage 32: 514-525 (2024)

Licensed under CC BY 4.0, https://creativecommons.org/licenses/by/4.0/

Other publications with my contribution which are not associated with this thesis:

Riegger J, Schoppa A, **Ruths L**, Haffner-Luntzer M, Ignatius A: Oxidative stress as a key modulator of cell fate decision in osteoarthritis and osteoporosis: a narrative review. Cell Mol Biol Lett 28: (2023)

Maurer S, Kirsch V, **Ruths L**, Brenner RE, Riegger J: Senolytic therapy combining Dasatinib and Quercetin restores the chondrogenic phenotype of human osteoarthritic chondrocytes by promoting the release of pro-anabolic mediators. Aging Cell 24: (2025)

Ruths L, Hengge J, Teixeira GQ, Haffner-Luntzer M, Ignatius A, Riegger J: Terminal complement complex deposition on chondrocytes promotes premature senescence in age- and trauma-related osteoarthritis. Front Immunol 15: (2025)

Table of contents

Publication index I
Table of contents III
List of abbreviations V
1 Introduction 1
1.1 Hyaline cartilage under physiological conditions 1
1.2 The degenerative joint disease osteoarthritis (OA) 2
1.2.1 Pathophysiology 3
1.2.2 Treatment options 5
1.3 Complement system 7
1.3.1 Complement as potential driver of OA progression 11
1.4 Objectives of the thesis 13
2 Materials and methods 14
2.1 Materials 14
2.1.1 Human samples 14
2.1.2 Equipment 14
2.1.3 Consumables 16
2.1.4 Chemicals and reagents 17
2.1.5 Kits 21
2.1.6 Cell culture media and solutions 21
2.1.7 Antibodies 24
2.1.8 TaqMan Gene Expression Assays and conventional primers 24
2.1.9 Software 25
2.2 Methods 26
2.2.1 Isolation of primary cells and cell culture 26
2.2.2 Preparation, cultivation, and traumatization of cartilage explants 28
2.2.3 Differentiations 29
2.2.4 Gene expression analysis 32
2.2.5 Histology 38
2.2.6 Flow cytometry analysis 42
2.2.7 Preparation of cartilage conditioned medium 43
2.2.8 Preparation of cartilage homogenizate (HG) 43
2.2.9 C3 and C5 cleavage assay 44

2.2.10 Enzyme-linked immunosorbent assay (ELISA) 44
2.2.11 Statistical analysis 46
3 Results 47
3.1 Generation of C3a and C5a by hAC 47
3.2 Pro-osteogenic effects of C3a and C5a 50
3.3 Influence of C3a and C5a on chondrogenic differentiation of hAC 55
3.4 Trans-differentiation of hAC 59
3.5 Impact of anaphylatoxins on osteogenic differentiation of stem cells 63
3.6 Expression of C3aR and C5aR1 in cartilage tissue and isolated hAC, BM-MSC, and CSPC 65
3.7 Association of C3aR and C5aR1 expression and calcification processes 70
3.8 Influence of BMP-2 on C3aR and C5aR1 expression 72
3.9 Traumatic impact alters expression of complement associated proteins 74
3.10 Expression of complement regulatory proteins in hAC 77
4 Discussion 79
4.1 Generation of C3a and C5a by hAC 79
4.2 Influence of C3a and C5a on osteogenic and chondrogenic differentiation 81
4.3 Expression of C3aR and C5aR1 and association with calcification processes 85
4.4 Expression of complement associated proteins 89
4.5 Limitations of the study 92
5 Summary 93
6 List of references 95
Acknowledgment 112
Statutory declaration 113

List of abbreviations

ADAMTS	A disintegrin and metalloproteinase with thrombospondin motifs
ALP	Alkaline phosphatase
BM	Basal medium
BM-MSC	Bone-marrow derived mesenchymal stem cells
BMP-2	bone morphogenetic protein 2
C4BP	C4b-binding protein
CatD	Cathepsin D
CatL	Cathepsin L
CDM	Chondrogenic differentiation medium
cDNA	Complementary deoxyribonucleic acid
CR1	Complement receptor 1 (CD35)
CSPC	Chondrogenic stem/progenitor cells
Ct	Cycle threshold
DAF	Decay accelerating factor (CD55),
DAMPs	Damage-associated molecular patterns
dH_2O	Distilled water
DMEM	Dulbecco´s Modified Eagle Medium
DMOAD	Disease-modifying osteoarthritis drugs
DMSO	Dimethylsulfoxid
ECM	Extracellular matrix
EDTA	Ethylenedinitrilotetraacetic acid
ELISA	Enzyme-linked immunosorbent assay
FBS	Fetal bovine serum
FGF	Fibroblastic growth factor
FH	Factor H
hAC	Human articular chondrocytes
HG	Cartilage homogenizate
HRP	Horseradish peroxidase

ICC	Immunocytochemistry
IHC	Immunohistochemistry
IL	Interleukin
MASPs	MBL-associated serine proteases
MBL	Mannose-binding lectin
MCP	Membrane co-factor protein (CD46)
MMP	Matrix metalloproteinase
mRNA	Messenger RNA
OA	Osteoarthritis
ODM	Osteogenic differentiation medium
PBS	Phosphate-buffered saline
PTOA	Posttraumatic osteoarthritis
qRT-PCR	Quantitative real-time polymerase chain reaction
RNA	Ribonucleic acid
ROS	Reactive oxygen species
RUNX2	Runt-related transcription factor 2
SDS	Sodium dodecyl sulphate
SFM	Serum free medium
sTCC	Soluble terminal complement complex
TCC	Terminal complement complex
TNF	Tumor necrosis factor

1 Introduction

1.1 Hyaline cartilage under physiological conditions

The connective tissue cartilage can be subdivided into three groups, fibrous, elastic, and hyaline cartilage. All three consist of chondrocytes, proteoglycans and differ mainly in the composition and structure of various types of collagen fibres. Fibrous cartilage contains densely layered collagen type I (composed of two subunits, encoded by *COL1A1* and *COL1A2*) and is found in meniscus and intervertebral discs [148]. In contrast, elastic cartilage and hyaline cartilage are both predominantly made up of collagen type II (encoded by *COL2A1*). To provide its high elasticity, elastic cartilage further contains elastin fibres. Elastic cartilage supports structures which are frequently deformed, such as external ears and epiglottis [98]. Hyaline cartilage is the most common cartilage type in the human body and is found in the ribs, nasal septum, and trachea [8, 10]. Besides collagen type II, also collagen type IX and XI are present. Additionally, hyaline cartilage covers the ends of the long bones which enables smooth joint movements by providing a lubricating gliding surface [213]. This so-called articular cartilage is 2 - 4 mm thick and has a complex structure which facilitates its unique biomechanical properties. These include reversible deformation after a mechanical stimulation and shock absorption [49]. In the superficial zone, collagen fibres are aligned in parallel to the cartilage surface and are densely packed. Most of the water is found in this zone and located chondrocytes are generally smaller, flatter, and more frequent compared to cells in the deeper zones. Collagen fibres in the middle zone are structured diagonal or vertical and the sporadic chondrocytes have a spherical shape. The deep zone contains vertical arranged collagen fibres and located chondrocytes are oriented in a column in parallel to the collagen fibres. The last one is the calcified zone which connects the cartilage with the underlying subchondral bone by anchoring the collagen fibres with the bone. In this zone, collagen type X (encoded by *COL10A1*) is found and chondrocytes are sparse and if present, hypertrophic [8, 49]. Another important component of hyaline cartilage is the proteoglycan aggrecan which is also essential for the biomechanical properties [98]. Furthermore, hyaline cartilage is a hypocellular, avascular, alymphatic, and aneural tissue. Thus, nutrition of the

chondrocytes depends on diffusion and fluid flow. Consequently, chondrocytes have a slow metabolism and matrix turnover and remodelling is limited. Additionally, no cell proliferation is described under physiological conditions [201].

Furthermore, cartilage tissue and chondrocytes play a crucial role in bone development, growth, and healing. During embryogenesis, hyaline cartilage serves as a scaffold for future bones [128] and located chondrocytes undergo hypertrophic changes, characterised by a decreased expression of collagen type II and enhanced expression of collagen type I and X [110, 150, 163]. Further hypertrophic markers are runt-related transcription factor 2 (RUNX2, encoded by *RUNX2*), the main regulator of osteoblast genes like alkaline phosphatase (ALP, encoded by *ALPL*), which is involved in mineralisation, and zinc finger protein osterix (encoded by *SP7*) [71, 211, 216, 227]. These changes of the chondrogenic phenotype induce a mineralisation of the surrounding cartilage tissue [24]. Most of the chondrocytes die after mineralisation, however, also a trans-differentiation of hypertrophic chondrocytes into osteoblasts is observed [222, 236, 239]. Furthermore, blood vessels and additional osteoblasts infiltrate the cartilage, and the final bone is formed. This replacement of hyaline cartilage with bone tissue is called endochondral ossification. Hyaline cartilage remains only on the joint surface of the bone as articular cartilage and in the growth plate. Endochondral ossification is also observed in the growth plate after birth during longitudinal growth of the long bones. Remaining chondrocytes proliferate, differentiate into hypertrophic cells, and produced cartilage serves as a scaffold for bone matrix [128]. Similar processes can be observed during secondary bone healing. In this case, a fracture callus is formed out of hyaline cartilage which mineralises and is replaced by bone tissue [27, 61].

1.2 The degenerative joint disease osteoarthritis (OA)

OA is considered the most prevalent joint disease worldwide. More than 500 million people, which is 7% of the global population, were affected in 2019 [82]. The disease is more common in adults over 40 years and is the leading cause of disability and

chronic pain in older adults. According to the Robert Koch Institute´s GEDA 2014/2015-EHIS health interview survey, 48.1% of all women and around one third of all men (31.2%) over the age of 65 years are suffering in Germany from OA [108, 179]. Besides women and elderly people, individuals with obesity or genetic predisposition are more prone to be affected by OA [125]. Another risk factor is a preceding joint injury like intraarticular fracture, cartilage lesions, and instability or damage of the ligaments (e.g., anterior cruciate ligament injury) or menisci causing so called posttraumatic OA (PTOA) [126, 188]. Due to an aging society and increasing numbers of obese people, it is thought that OA numbers will increase even further in the future. Consequently, life quality of more and more people will be adversely affected. Additionally, the already high social and economic burden will go up as well. The United States Bone and Joint Initiative stated that between 2008-2014, a total of $71.3 billion work earnings were lost due to OA [131]. On average, individuals with OA earned $6,783 less than those without an OA diagnosis. Furthermore, the annual direct medial costs of OA are a total of $65.5 billion. These numbers underline the pressing urge to find sufficient treatment options to prevent OA in an early stage or delay progression of OA. So far, pain killers are the only clinically relevant medical option [32]. In severe cases or end stage OA, knee replacement surgery is the last resort to relief pain and to regain the ability to perform activities of daily living (see 1.2.2).

1.2.1 Pathophysiology

OA can affect all synovial joints in the human body, but especially the weight bearing joints like knee and hips have a greater risk. Focusing on the knee joint, pathological changes include synovial inflammation, degeneration of the articular cartilage, osteophyte formation, weakened ligaments, and sclerosis of the subchondral bone [125]. Another rather newly emerged hallmark of OA is cartilage calcification [17]. It is associated with cartilage degeneration and observed in end-stage OA patients [56, 80]. Furthermore, mineralisation of articular cartilage alters the unique biomechanical properties by increasing tissue stiffness [51].

Pathomechanisms of OA have been studied for decades and discovered pathways are complex and innumerous. Various biological, structural, and mechanical factors are described, which play a role in OA initiation and progression. Essentially, cartilage metabolism is disrupted, favouring catabolic over anabolic processes. This imbalance results sooner or later in the loss of cartilage matrix. Proteolytic enzymes involved in cartilage catabolism are matrix metalloproteinase (MMP) and a disintegrin and metalloproteinase with thrombospondin motifs (ADAMTS), which are expressed and secreted by chondrocytes and synovial cells [13, 62, 215]. Typical OA-associated proteases include the collagenases MMP-1 and MMP-13, the gelatinases MMP-2 and MMP-9, the proteoglycanase MMP-3, and the aggrecanases ADAMTS-4 and ADAMTS-5 [63, 235]. These enzymes degrade the extracellular matrix (ECM) of hyaline cartilage tissue, which consists mainly of collagen type II and the proteoglycan aggrecan (see 1.1). Resulting breakdown products are released into the synovial fluid and would be cleared under physiological conditions by phagocytosis by resident macrophages [23]. Elevated levels of proteolytic enzymes are often observed after an initial trigger such as a joint trauma and subsequent tissue damage results in the release of damage-associated molecular patterns (DAMPs). This pro-inflammatory cocktail promotes expression of inflammatory mediators like tumor necrosis factor (TNF), interleukin-6 (IL-6, encoded by *IL6*), IL-1β, and proteases [62, 72]. Consequently, excessive degradation of cartilage tissue exceeds macrophage clearance efficiency and results in a further increase of pro-inflammatory processes. Furthermore, an accumulation of reactive oxygen species (ROS) and thus oxidative stress is described during OA [111]. These catabolic processes are opposed under physiological conditions by ECM biosynthesis. However, under pathophysiological conditions, pro-inflammatory cytokines and oxidative stress have a negative impact on collagen type II and aggrecan expression by altering the chondrogenic phenotype [178]. The two most predominant forms of phenotypical alterations observed in OA tissue are senescence and hypertrophy. Cellular senescence is mainly characterised by a permanent cell cycle arrest and a senescence-associated secretory phenotype (SASP) [102]. SASP factors of senescent chondrocytes include proteases like MMP and ADAMPTS and cytokines such as IL-6 and IL-8 (encoded by *IL8*), which have

detrimental effects on the surround cells and tissue as described above [123, 175]. Additionally, enhanced ROS production due to mitochondrial dysfunction is described for senescent cells [240]. As a consequence, the senescent phenotype can spread from cell to cell through paracrine signalling resulting in an accumulation of dysfunctional chondrocytes in cartilage tissue [1, 29, 221]. Regarding hypertrophic alterations, some markers were already mentioned above (see 1.1). However, a hypertrophic phenotype is also accompanied by expression of catabolic enzymes like MMP-13 and chemokines such as CXCL-1 (encoded by *CXCL1)* and IL-8 [25]. Thus, the characteristics of senescent and hypertrophic cells overlap to some extent. Furthermore, it is proposed that pathological calcification occurs in cartilage tissue when the chondrocytes in the superficial zone shift towards a hypertrophic phenotype as described during endochondral ossification [25, 224, 234]. In addition, hypertrophy goes along with the formation and deposition of calcium containing crystals like basic calcium phosphate (BCP) [56]. BCP crystals in turn induce hypertrophic alterations of neighbouring chondrocytes [139] and are associated with synovial inflammation, cartilage degradation and chondrocyte apoptosis [43].

Overall, oxidative stress, accumulation of cartilage degrading enzymes and enhanced levels of pro-inflammatory cytokines act in a synergistic manner. This vicious cycle results in chronic inflammation and cartilage destruction and thus drives OA progression.

1.2.2 Treatment options

Despite decades of research and clinical experimentation, no current surgery-based, drug-based, material-based, or cell-based therapy can reliably restore or maintain the function and structure of hyaline cartilage in the long-term [64, 143, 175]. This is mainly due to the complex collagen structure and the unfavourable conditions (hypocellularity and slow metabolism) regarding intrinsic regeneration of hyaline cartilage itself. A further challenge is the rather late diagnosis of OA. Early diagnosis is nearly impossible as cartilage changes involved in the beginning of the diseases do not cause pain

(aneural nature of hyaline cartilage). In an advanced and symptomatic stage, the joint damage is almost irreparable [19]. Additionally, the accessibility of the knee joint is limited. Intra-articular administration of drugs can cause multiple complications ranging from pain and bleeding at the injection side to sepsis [208]. In the case of an oral application, local drug concentrations in the joints are low. Thus, higher dosages are required which are accompanied by an increasing risk of side effects [161]. Overall, current treatment options are limited to symptom-relieving approaches to reduce pain and maintain joint function, which delay OA progression only slightly, if at all.

Non-pharmaceutical strategies include exercise which should be individualised depending on the OA severity [114, 130]. As obesity is one general risk factor of OA, also health education and lifestyle changes to lose weight is promising to slow down OA progression [94]. Further approaches for patients with mild symptoms are strength training and physiotherapy [130, 200].

Current primary pharmaceutical treatments of symptomatic OA are the oral or topical administration of non-steroidal anti-inflammatory drugs or paracetamol [32, 106, 237]. Associated adverse effects of a constant pain medication are gastrointestinal irritations, cardiovascular problems, and hepatic toxicity [53, 169]. Another approach is the intra-articular injection of corticosteroids, hyaluronic acid, or platelet-rich plasma. However, long-term beneficial effects of these injections are controversially discussed [14, 38, 39, 44, 90]. Since these mainly symptomatic treatments do not prevent further degradation of cartilage tissue, a total joint replacement is advisable in severe cases or end stage OA. But the surgical procedure of arthroplasty is accompanied by a high infection rate [34]. Additionally, prosthetic devices have a limited lifespan and thus, a revision surgery might be necessary. Revisions in turn possess unique challenges, and increased complications and mortality rates are described [41, 65, 117].

Furthermore, cell-based approaches using either autologous chondrocytes or bone-marrow derived mesenchymal stem cells (BM-MSC) are a frequently used method to treat cartilage defects [35, 95, 164]. Short-term, beneficial effects are described [230]. However, resulting cartilage tissue is often hypertrophic or the formation of

fibrocartilage was observed [8, 136, 219]. Other disadvantages are the need of a second surgery to isolate autologous chondrocytes and the phenotypical alterations of chondrocytes and BM-MSC during *in vitro* expansion [8, 33, 147].

Latest research focused on disease-modifying osteoarthritis drugs (DMOADs) which stop joint structural changes and improve symptoms [154]. DMOADs include among others anti-cytokine therapy to reduce inflammation, protease inhibitors to prevent cartilage degradation, senolytic therapy to eliminate senescent cells, and growth factors to support anabolic processes [115, 180]. Many drugs were promising in *in vitro* and *in vivo* experiments. However, none passed clinical trials so far successfully due to major adverse reactions or the beneficial effects were not sufficient [143, 180].

Targeting the hypertrophic phenotype and mineralisation of cartilage tissue is a relatively unexplored, but potentially promising therapeutic strategy to treat OA [17, 25]. So far, the underlying molecular processes of cartilage calcification are not completely unravelled and need to be studied more intensively to discover pathological triggers and determine new potential targets.

1.3 Complement system

The complement system is an essential part of the innate immune system. It detects and eliminates pathogens and dysfunctional or damaged cells. More than 50 different proteins, often zymogens which are activated upon proteolytic cleavage, are part of the complement system [129]. It is organised in a cascade-like fashion and can be initiated by three different pathways (**Figure 1**). The first discovered one is the classical pathway which is activated by bound IgG and IgM. C1q recognizes antigen-antibody complexes and recruits the proteases C1r and C1s. The latter is able to cleave C4 and C2 which results in the formation of the classical pathway C3 convertase C4b2b (according to the revised nomenclature [20]). The same convertase is formed upon complement activation through the lectin pathway. In this case, pattern recognition molecules such as ficolins and mannose-binding lectin (MBL) bind to microbe-

associated molecular patterns. Subsequent activation of MBL-associated serine proteases (MASPs), which are functionally equivalent to C1r and C1s, results in C4 cleavage [57]. In contrast to the classical and lectin pathway, which are specifically activated, the alternative pathway is permanently active at a low level. C3 (encoded by *C3*) is continuously cleaved and the alternative pathway C3 convertase C3bBb assembles eventually in the presence of factor B, factor D, and Mg^{2+} [79, 105]. All three pathways converge at the proteolytic cleavage of the central protein C3 into a smaller fragment C3a and a larger C3b. Consequently, new formed C3b is the basis of further C3bBb, resulting in an increased C3b density by the alternative pathway amplification loop [46]. This induces the formation of a convertase containing an additional C3b molecule which shifts the product specificity from C3 to C5 (encoded by *C5*). The C5 convertases C4b2bC3b and C3bBbC3b cleave C5 into C5a and C5b. The larger fragment C5b in turn assembles with C6, C7, C8, and several C9 molecules to generate a lytic pore (C5b-9) in the cell membrane of the target cell [170]. The so-called terminal complement complex (TCC) lyses and thus eliminates the cell. Sublytic TCC deposition is associated with intracellular signalling and cell activation resulting in expression of pro-inflammatory proteins [142, 231]. Besides the classical, lectin, and alternative activation pathways, several other complement activation factors emerged in recent years. It was shown that thrombin, plasmin, and cathepsin L (CatL) are able to cleave C3 [28, 119]. Thrombin and plasmin, as well as cathepsin D (CatD) can additionally cleave C5 [70, 75, 76, 99, 112]. It is not surprising that haemostasis-associated proteases such as thrombin and plasmin are involved in complement activation, as the haemostatic system depends, like the complement system, on the activation of proteases [79].

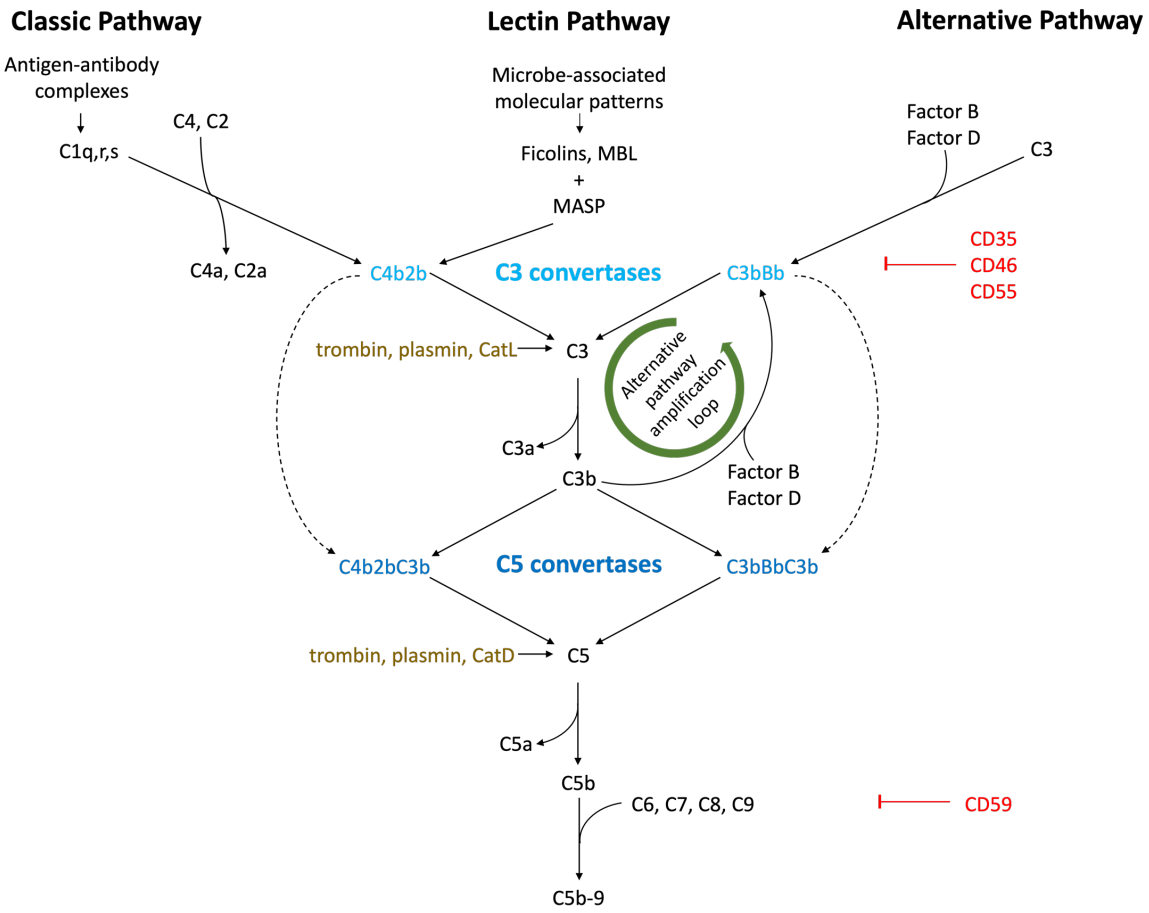

Figure 1: Simplified scheme of the complement cascade. The complement system can be activated by the classical, lectin, and alternative pathway. All three converge at the proteolytic cleavage of C3. Generated C3b forms a complex with a C3 convertase which is able to cleave C5. Finally, C5b assembles with C6, C7, C8, and several C9 in a lytic pore (C5b-9). Furthermore, the haemostasis-associated proteases thrombin and plasmin can activate the complement system by cleavage of C3 and C5. Additionally, cathepsin L (CatL) and cathepsin D (CatD) can cleave C3 or C5, respectively. Proceeding of the complement cascade can be impaired by the membrane bound proteins CD35, CD46, and CD55 at the level of the C3 convertases. CD59 inhibits C5b-9 assembly. MBL = mannose-binding lectin; MASP = MBL-associated serine proteases. Based on Huber-Lang et al. 2021 [79], Silawal et al. 2018 [196], and Orsini et al. 2015 [157].

The small peptides C3a and C5a (77 and 74 amino acids, respectively) are named anaphylatoxins and are generated during complement activation but are it-self not relevant for the proceeding of the complement cascade. However, they are powerful bioactive molecules and play a major role in immune modulatory processes. In general, C5a is more potent than C3a [45, 47]. Originally, only pro-inflammatory properties were described such as the release of histamine from mast cells [47]. Additionally, C3a and

C5a serve both as chemotactic factors by attracting leukocytes, macrophages, mast cells and activated B- and T-cells [66, 146, 158, 187]. In an acute setting, also anti-inflammatory effects were described for C3a (e.g., prevents mobilization of neutrophils) [228]. C3a and C5a signalling is mediated by binding to the respective anaphylatoxin receptors. For C3a, only one receptor (C3aR) is known and activation of C3aR (encoded by *C3AR*) has both pro- and anti-inflammatory effects. In contrast, two receptors (C5aR1 and C5aR2) are described for C5a. C5aR1 (encoded by *C5AR1*) signalling is predominantly pro-inflammatory [30]. The role of C5aR2 is not well understood and currently controversially discussed [92, 116, 187]. At structural level, C3aR and C5aR1 are both G-protein-coupled receptors, while C5aR2 lacks a coupled G protein [92].

In general, the complement system is tightly regulated at various points by both membrane-anchored and soluble factors. Strict control is necessary to allow cascade progression on damaged, altered, or foreign cells while progression is attenuated on healthy host cells. Focusing on the central proteins C3 and C5, the responsible convertase can be dissociated by complement receptor 1 (CR1; also known as CD35, encoded by *CR1*), decay accelerating factor (DAF; also known as CD55, encoded by *CD55*), factor H (FH; specific for alternative pathway), or C4b-binding protein (C4BP; specific for classical and lectin pathway) [129]. Additionally, the membrane co-factor protein (MCP; also known as CD46, encoded by *CD46*) is involved in C3b cleavage [118]. These complement regulatory proteins can significantly reduce the half-life of the convertases from 1 - 3 minutes to only a few seconds [159]. Consequently, further downstream processes are diminished, including the generation of C3a and C5a. However, activity of anaphylatoxins is not only regulated by generation, but also by inactivation and clearance. Inactivation of both peptides is rather quick and controlled by carboxypeptidase which cleave the C-terminal arginine. It results in C3a-desArg and C5a-desArg, respectively [21, 137]. Furthermore, anaphylatoxins are cleared by binding to their specific receptors, which are internalised subsequently [155, 187]. Another membrane-anchored complement regulator is CD59 (encoded by *CD59*) which circumvents the assembly of the pore-forming C9 molecules [31].

1.3.1 Complement as potential driver of OA progression

In the last decades, dysregulation of the complement system has been associated with multiple different diseases. Patients with complement protein deficiencies are more prone to be affected by bacterial, fungal or viral infections [209]. On the other hand, uncontrolled complement activation can cause devastating effects by inducing acute inflammation as described for sepsis or by attacking host cells [171]. An enhanced activation of the complement system is also observed during OA progression and is considered to be crucially involved in OA pathogenesis [187, 196]. Wang et al. 2011 detected elevated levels of C3a-desArg and soluble TCC (sTCC) in synovial fluid of early-stage OA patients, compared to healthy individuals [223]. Additionally, a study showed that C4d, C3bBbP (C3bBb with an bound properdin which leads to a 5 - 10 fold higher enzyme stability [50]), and sTCC was enhanced in the synovial fluid of OA patients [205]. The authors reported further that the same was true after a knee injury, especially within the first 83 days after the injury. Articular chondrocytes and synovial cells are an important source of complement components [160, 196]. Components of the classical complement pathways (i.e., C1q, C1s, C4, and C2) as well as the alternative pathway (i.e., C3, factor B) were synthesised by human articular chondrocytes (hAC) [9, 22]. C3, C4, and factor B were also expressed in isolated synoviocytes [9]. Furthermore, gene expression of the anaphylatoxin receptors C3aR and C5aR1 and the complement regulatory proteins CD46, CD55, and CD59 was found in hAC [153, 192]. C5aR2 expression has not yet been detected in cartilage or chondrocytes and the receptor is considered as irrelevant in the context of OA [11, 192, 223]. Another source of complement components is intra-articular bleeding after a knee trauma [187]. As the synovial joint is an isolated environment, complement components circulating in the blood stream can only infiltrate the joint after an injury. In line with this, Cheng et al. 2022 showed that only synovial and not blood plasma C3 levels correlated with histological assessed severity of primary knee OA [26].

In the knee joint, the complement system can be activated via all three pathways. Potential triggers are degraded ECM components accumulating during cartilage degeneration and DAMPs released after a cartilage trauma, for example due to

consequent necrosis of chondrocytes [129, 175, 196]. Additionally, high ROS levels contribute to complement activation [77] and cartilage expresses the proteases CatD and CatL which were found together with thrombin and plasmin in the synovial fluid of OA patients [36, 212]. Harmful consequences of complement activation are described in the context of OA. Surgical meniscectomy caused in C5- and C6-deficient mice after 6 weeks a reduced cartilage degeneration compared to mice which were sufficient for the respective complement components [223]. Accordingly, the authors reported that a CD59-deficiency increased in the same surgical model the observed cartilage degeneration. Furthermore, TCC deposition induced phenotypical alterations in hAC [176] and absence of TCC partially protected from OA progression in an injury-induced OA model in C6-deficient rabbits [177]. Additionally, it is described that C1s is able to degrade collagen type II [233] and cleave the proenzyme of MMP-9 in its active state [184]. Therefore, C1s is not only involved in the classical pathway but might also contribute directly and indirectly to the degradation of cartilage tissue.

Previous research of the complement system in OA dealt so far mainly with the consequences of TCC deposition. Less attention was on the anaphylatoxins C3a and C5a and the corresponding receptors C3aR and C5aR1. In the context of collagen-induced rheumatoid arthritis, *in vivo* studies demonstrated that cartilage damage was observed in $C3aR^{-/-}$ and $C5aR^{-/-}$ mice to a lesser extent and intraperitoneal injection of anti-mC5aR antibody reduced joint destruction [4, 11]. Regarding mineralisation processes, multiple studies showed that C3aR and C5aR1 are upregulated during osteogenic differentiation of MSC [83, 84, 89]. Inhibition of C5aR1 with PMX53 or silenced C5aR1 with siRNA resulted in a reduced osteogenic differentiation [89]. Furthermore, most osteoblasts in the fracture callus of rats were positive for C5aR1 [83]. As the endochondral ossification described during fracture healing (see 1.1) can be compared to the processes which take place during cartilage calcification [25, 224, 234], C5aR1 can also be relevant in the mineralisation of cartilage tissue. Additionally, C3a, C5a, and C5aR1 are associated with vascular calcification [89, 133, 144, 225]. Despite these indications, no one addressed so far whether the anaphylatoxins C3a and C5a and the receptors C3aR and C5aR1 are involved in cartilage calcification.

1.4 Objectives of the thesis

The musculoskeletal disease OA is considered the most prevalent joint disease worldwide and the quality of life of affected patients is severely impaired. Despite decades of research, adequate therapy does not exist. In recent years, evidence accumulated that the complement system plays a crucial role in OA pathogenesis. However, the consequences of complement activation during OA progression are not completely understood and, until now, it is not known in which pathological processes the complement system is involved. Multiple studies in the field of fracture healing and vascular calcification indicate that the anaphylatoxins C3a and C5a and the corresponding receptors C3aR and C5aR1 might be involved in the mineralisation of cartilage tissue. In the present theses, either primary hAC *in vitro* or cartilage explants *ex vivo* were used to elucidate whether the complement system contributes to cartilage calcification.

The main objectives were:

- To examine the influence of anaphylatoxins C3a and C5a on the chondrogenic and osteogenic differentiation of hAC.

- To investigate the expression of the anaphylatoxin receptors C3aR and C5aR1 in cartilage tissue and hAC.

- To explore a potential association of anaphylatoxin receptors with mineralisation processes.

Of further interest was:

- To elucidate if hAC can cleave the complement components C3 and C5 in the respective anaphylatoxins.

- To determine the expression of complement associated proteins in cartilage tissue and hAC.

2 Materials and methods

2.1 Materials

2.1.1 Human samples

Human samples were obtained from donors undergoing either knee replacement or triple osteotomy surgery at the University Hospital Ulm, Department of Orthopaedics. Cartilage tissue and bone marrow was only used when patients signed a written informed consent according to the terms of the Ethics Committee of the University of Ulm following the instructions of the Declaration of Helsinki (ethical approval number 353/18).

Chondrogenic stem/progenitor cells (CSPC), hAC, and full-thickness cartilage explants were isolated from macroscopically intact human femoral condyles (OARSI grade ≤ 1) [220]. Additionally, cartilage tissue was collected from highly degenerated human cartilage tissue (OARSI grade ≥ 3).

Bone-marrow derived mesenchymal stem cells (BM-MSC) were routinely isolated from bone marrow.

2.1.2 Equipment

Table 1: Equipment.

Equipment	Manufacturer
Autoclave Systec DE-45	Systec GmbH, Linden, Germany
Automatic tissue dehydration TB1020	Leica, Nussloch, Germany
Axioshop 2 mot plus microscope	Zeiss, Oberkochen, Germany
Balance 400 M	Precisa, Dietikon, Switzerland
Balance CPA225D	Sartorius, Goettingen, Germany
BD FACSCalibur Flow Cytometer	Becton Dickinson GmbH, Heidelberg, Germany
Canon EOS 700D camera	Canon, Krefeld, Germany
CASY 1 cell counter	Schärfe-System GmbH, Reutligen, Germany

Centrifuges: Allegra 64R Allegra X-30R Biofuge 13 Megafuge 1.0 Mini Star silverline	 Beckman Coulter, Brea, USA Beckman Coulter, Brea, USA Heraeus Holding GmbH, Hanau, Germany Heraeus Holding GmbH, Hanau, Germany VWR, Leuven, Belgium
Cold Plate EG1140 C	Leica, Nussloch, Germany
Dewar vessel	KGW Isotherm, Karlsruhe, Germany
Drop-tower	Manufactured by Feinwerkstatt, University Ulm
Freezer Premium NoFrost	Liebherr, Biberach an der Riß, Germany
Fridge Comfort	Liebherr, Biberach an der Riß, Germany
Incubator BBD 6220	Heraeus, Hanau, Germany
Incubator HERAcell 240	Heraeus, Hanau, Germany
Infinite M200 Pro	Tecan Germany GmbH, Crailsheim, Germany
Magnetic stirrer IKAMAG RCT	IKA, Staufen, Germany
Microdismembrator S	B. Braun, Melsungen, Germany
Microtome 2050	Reichert-Jung, Depew, USA
Paraffin Embedding Center EG1140 H	Leica, Nussloch, Germany
Pipet aid pipetus	Hirschmann Laboratory, Eberstadt, Germany
Pipettes (10 µL, 20 µL, 100 µL, 200 µL, 1000 µL)	Gilson, Berlin, Germany
ProFlex thermocycler	Life Technologies GmbH, Darmstadt, Germany
Steel beads (∅ 9 mm)	Sartorius, Ratingen, Germany
StepONEPlus	Life Technologies GmbH, Darmstadt, Germany
Sterile bench HERAsafe	Heraeus, Hanau, Germany
Teflon vessel	Manufactured by Feinwerkstatt, University Ulm
Ultrasonic Cleaning USC - THD	VWR, Leuven, Belgium
Unitherm Hybridization Oven 6/12	Uniequip, Planegg, Germany
Vortex	neoLab Migge GmbH, Heidelberg, Germany
Waterbath GFL 1083	Gesellschaft für Labortechnik mbH, Burgwedel, Germany

2.1.3 Consumables

Table 2: Consumables.

Consumables	Manufacturer
0.2 mL reaction tube	VWR, Leuven, Belgium
0.5 mL safe-lock tubes	Eppendorf, Hamburg, Germany
1.5 mL reaction tube	Greiner Bio-One, Frickenhausen, Germany
1.5 mL reaction tube, RNase-free	VWR, Leuven, Belgium
15 mL tube	Corning, Glendale, USA
15 mL tube, filter cap	Greiner Bio-One, Frickenhausen, Germany
5 mL polystyrene round-bottom tube	Becton, Dickinson and Company, Franklin Lakes, USA
50 mL tube	Greiner Bio-One, Frickenhausen, Germany
Biopsy punch (∅ 6 mm)	Stiefel Laboratories, Offenbach am Main, Germany
Cell culture flask T175	Greiner Bio-One, Frickenhausen, Germany
Cell culture flask T75	Greiner Bio-One, Frickenhausen, Germany
Cell culture plates: 6-well 12-well 24-well 48-well 96-well	 Corning, Tewksbury, USA Corning, Tewksbury, USA Greiner Bio-One, Frickenhausen, Germany Corning, Tewksbury, USA Brand, Wertheim, Germany
Cell scraper	Greiner Bio-One, Frickenhausen, Germany
Cell strainer 40 μm	Corning, Tewksbury, USA
Cryogenic vial	Fisher Scientific GmbH, Schwerte, Germany
Cryotubes	Greiner Bio-One, Frickenhausen, Germany
CultureSlide 4-well	Corning, Glendale, USA
ImmEdge pen	Vector Laboratories, Newark, USA
MicroAmp Fast Optical 96-Well Reaction Plate	Life Technologies GmbH, Darmstadt, Germany
MicroAmp Optical Adhesive Film	Life Technologies GmbH, Darmstadt, Germany
Microscope Cover Glasses	Marienfeld, Lauda Königshofen, Germany
Microtome Blade S35	Feather, Osaka, Japan
Nitrile gloves	Hartmann group, Heidenheim, Germany

Pipette tips: 10 µL 20 µL 100 µL 200 µL 1000 µL	 Greiner Bio-One, Frickenhausen, Germany Greiner Bio-One, Frickenhausen, Germany Greiner Bio-One, Frickenhausen, Germany Fisher Scientific GmbH, Schwerte, Germany Fisher Scientific GmbH, Schwerte, Germany
Protein LoBind Tube	Eppendorf, Hamburg, Germany
Single-use syringes	Braun, Melsungen, Germany
Single packed serological pipettes: 1 mL 5 mL 10 mL 25 mL 50 mL	 Corning, Glendale, USA Greiner Bio-One, Frickenhausen, Germany Greiner Bio-One, Frickenhausen, Germany Greiner Bio-One, Frickenhausen, Germany Greiner Bio-One, Frickenhausen, Germany
Styrene 96-well plate, V-bottom	Fisher Scientific GmbH, Schwerte, Germany
Superfrost Plus Adhesion Microscope Slides	Epredia, Dreieich, Germany
Surgical blade No.11	Feather, Osaka, Japan
Surgical blade No.23	Feather, Osaka, Japan
Syringe filter 0.22 µm	VWR, Leuven, Belgium

2.1.4 Chemicals and reagents

Table 3: Chemicals and reagents.

Chemical	Manufacturer
2-Mercaptoethanol	Carl Roth GmbH + Co. KG, Karlsruhe, Germany
2-Phospho-L-ascorbic acid trisodium salt	Sigma-Aldrich, Darmstadt, Germany
Acetic acid glacial	VWR, Leuven, Belgium
Acidum citricum	Caesar & Loretz GmbH, Hilden, Germany
AEC Chromogen	Dako, Hamburg, Germany
Alcian blue	Carl Roth GmbH + Co. KG, Karlsruhe, Germany
Alizarin Red S	Sigma-Aldrich, Darmstadt, Germany

Aluminium potassium sulfate dodecahydrate	Merck KGaA, Darmstadt, Germany
Aluminium sulfate-18-hydrate	Merck KGaA, Darmstadt, Germany
Antibody diluent	Dako, Hamburg, Germany
Aquatex	Sigma-Aldrich, Darmstadt, Germany
BD CellFix	Becton, Dickinson and Company, Franklin Lakes, USA
Biocoll	Bio&Sell, Feucht, Germany
Biotinylated goat anti-polyvalent	Dako, Hamburg, Germany
BMP-2	PeproTech, Cranbury, USA
Brij	Merck KGaA, Darmstadt, Germany
C3	Quidel, San Diego, USA
C3a	Complement Technology, Tyler, USA
C5	Quidel, San Diego, USA
C5a	Complement Technology, Tyler, USA
CASY ton	OMNI Live Science GmbH & Co KG, Bremen, Germany
Cetylpyridinium	Sigma-Aldrich, Darmstadt, Germany
Chloral hydrate	Merck KGaA, Darmstadt, Germany
Chloroform	Sigma-Aldrich, Darmstadt, Germany
Cleaner for ultrasonic bath	Dr H Stamm, Berlin, Germany
Collagenase	Sigma-Aldrich, Darmstadt, Germany
Dexamethasone	Sigma-Aldrich, Darmstadt, Germany
Disodium hydrogen phosphate	Merck KGaA, Darmstadt, Germany
Dimethylsulfoxid (DMSO)	AppliChem GmbH, Darmstadt, Germany
dNTP Mix	Biozym Scientific GmbH, Hessisch Oldendorf, Germany
Dulbecco´s Modified Eagle Medium (DMEM)	Live Technologies, Paisley, UK
ELISA Wash Buffer Powder	Life Technologies GmbH, Darmstadt, Germany
Eosin	Chroma, Köngen, Germany
Ethanol denatured	Pharmacy University Hospital Ulm, Ulm, Germany
Ethanol undenatured absolute	SERVA Electrophoresis GmbH, Heidelberg, Germany
Ethylenedinitrilotetraacetic acid (EDTA)	Sigma-Aldrich, Darmstadt, Germany

Eukitt	ORSAtec GmbH, Bobingen, Germany
Fast Green	Sigma-Aldrich, Darmstadt, Germany
Fetal bovine serum (FBS)	PAN Biotech GmbH, Aidenbach, Germany
Fibroblastic growth factor-2 (FGF-2)	PeproTech, Cranbury, USA
Formaldehyde 36%	VWR, Leuven, Belgium
Ham´s F12	PAN Biotech GmbH, Aidenbach, Germany
Hematoxylin monohydrate	Merck KGaA, Darmstadt, Germany
Hyaluronidase	Sigma-Aldrich, Darmstadt, Germany
Hydrchloric acid	Merck KGaA, Darmstadt, Germany
Hydrogen peroxide 30%	Merck KGaA, Darmstadt, Germany
Insulin-Transferrin-Selenium	Live Technologies, Paisley, UK
Iron(III) chloride	Merck KGaA, Darmstadt, Germany
Isopropyl alcohol	Pharmacy University Hospital Ulm, Ulm, Germany
L-glutamine	PAN Biotech GmbH, Aidenbach, Germany
L-prolin	Sigma-Aldrich, Darmstadt, Germany
Non-essential amino acids	Bio&Sell, Feucht, Germany
Nuclear fast red	Fluka, Steinheim, Germany
Nuclease-free water	Qiagen, Hilden, USA
OligodT	Biomers.net GmbH, Ulm, Germany
Paraffin	Leica, Nussloch, Germany
PBS for histology	Sigma-Aldrich, Darmstadt, Germany
Penicillin/ Streptomycin	PAN Biotech GmbH, Aidenbach, Germany
Pepsin	Sigma-Aldrich, Darmstadt, Germany
Phosphate-buffered saline (PBS) for cell culture	Live Technologies, Paisley, UK
PMX53	Sigma-Aldrich, Darmstadt, Germany
Power SYBR Green PCR Master Mix	Life Technologies GmbH, Darmstadt, Germany
Power SYBR Green PCR Mastermix	Life Technologies GmbH, Darmstadt, Germany
Pronase	Sigma-Aldrich, Darmstadt, Germany
Protein block	Dako, Hamburg, Germany
Pyrogallol	Merck KGaA, Darmstadt, Germany
QIAzol Lysis Reagent	Qiagen, Hilden, USA
rhBMP6	PeproTech, Cranbury, USA
rhTGF-β3	PeproTech, Cranbury, USA

RNase Inhibitor	GeneOn GmbH, Ludwigshafen am Rhein, Germany
Safranin O	Chroma, Köngen, Germany
SB290157	Sigma-Aldrich, Darmstadt, Germany
Silver nitrate	Carl Roth GmbH + Co. KG, Karlsruhe, Germany
Sodium dihydrogen phosphate monohydrate	Merck KGaA, Darmstadt, Germany
Sodium dodecyl sulphate (SDS)	Carl Roth GmbH + Co. KG, Karlsruhe, Germany
Sodium iodate	Merck KGaA, Darmstadt, Germany
Sodium pyruvate	Sigma-Aldrich, Darmstadt, Germany
Sodium thiosulfate	Merck KGaA, Darmstadt, Germany
STOP Solution	R&D Systems, Minneapolis, USA
Streptavidin peroxidase	Dako, Hamburg, Germany
TagMan Gene Expression Mastermix	Life Technologies GmbH, Darmstadt, Germany
TaqMan Fast Advanced Master Mix	Life Technologies GmbH, Darmstadt, Germany
Trisodium citrate (dihydrate)	Fluka, Steinheim, Germany
Trypsin/EDTA	PAN Biotech GmbH, Aidenbach, Germany
Tween 20	Carl Roth GmbH + Co. KG, Karlsruhe, Germany
UltraPure Distilled Water	Life Technologies GmbH, Darmstadt, Germany
Xylene	Fisher Scientific GmbH, Schwerte, Germany
β-glycerophosphate disodium salt hydrate	Sigma-Aldrich, Darmstadt, Germany

2.1.5 Kits

Table 4: Kits.

Solution	Manufacturer
Alizarin Red S (pH 4.0)	Morphisto, Offenbach am Main, Germany
C3a Human ELISA Kit	Life Technologies GmbH, Darmstadt, Germany
C5a Human ELISA Kit	Life Technologies GmbH, Darmstadt, Germany
Human IL-6 Uncoated ELISA	Life Technologies GmbH, Darmstadt, Germany
Omniscript RT Kit	Qiagen, Hilden, USA
RNeasy Lipid Tissue Mini Kit	Qiagen, Hilden, USA
RNeasy Mini Kit	Qiagen, Hilden, USA

2.1.6 Cell culture media and solutions

Table 5: Composition of cell culture media.

Medium	Composition
Basal medium (BM)	DMEM 10% FBS 1 g/L Glucose 100 U/mL Penicillin 100 μg/mL Streptomycin 2 mM L-glutamine
Chondrocyte BM	1:1 DMEM and Ham´s F12 10% FBS 1 g/L Glucose 1 mM L-glutamine 50 U/mL Penicillin 50 μg/mL Streptomycin 40 μM 2-Phospho-L-ascorbic acid trisodium salt

Chondrogenic differentiation medium (CDM)	DMEM 2 mM L-glutamine 4.5 g/L Glucose 100 U/mL Penicillin 100 μg/mL Streptomycin 0.1 μM Dexamethasone 200 μM 2-Phospho-L-ascorbic acid trisodium salt 40 μg/mL L-prolin 1 mM Sodium pyruvate 10 μg/mL Insulin 5.5 μg/mL Transferrin 6.7 ng/mL Selenium 10 ng/mL rhTGF-β3 10 ng/mL rhBMP6
Osteogenic differentiation medium (ODM)	DMEM 10% FBS 2 mM L-glutamine 1 g/L Glucose 100 U/mL Penicillin 100 μg/mL Streptomycin 0.1 μM Dexamethasone 10 mM β-glycerophosphate disodium salt hydrate 200 μM 2-Phospho-L-ascorbic acid trisodium salt
Serum free medium (SFM)	DMEM 1 g/L Glucose 1 mM Sodium pyruvate 1% Non-essential amino acids 1 mM L-glutamine 50 U/mL Penicillin 50 μg/mL Streptomycin 40 μM 2-Phospho-L-ascorbic acid trisodium salt 10 μg/mL Insulin 5.5 μg/mL Transferrin 6.7 ng/mL Selenium

Table 6: Composition of solutions.

Solution	Composition
1% Alcian blue	0.5 g Alcian blue Fill up to 50 mL with 0.1 N HCl
10 mM citrate buffer (pH 6)	2.94 g Trisodium citrate (dihydrate) Fill up to 1,000 mL with dH_2O 0.5% Tween 20
40 mM Alizarin Red S (pH 4.2)	0.684 g Alizarin Red S Fill up to 50 mL with dH_2O
5 mM EDTA solution (pH 7.3)	930.6 mg EDTA Fill up to 1,000 mL with PBS
Fast Green staining solution	0.02 g Fast Green Fill up to 100 mL with dH_2O
Formalin according to Lilie (pH 7)	40 g Sodium dihydrogen phosphate monohydrate 65 g Disodium hydrogen phosphate 1,000 mL Formaldehyde 36% Fill up to 10,000 mL with dH_2O
Hämalaun solution (MAYER)	1.0 g Hematoxylin monohydrate 50 g Aluminium potassium sulfate dodecahydrate 0.2 g Sodium iodate 50 g Chloral hydrate 1.0 g Acidum citricum Fill up to 1,000 mL with dH_2O
Hämatoxylin solution (WEIGERT)	Solution A: 1.0 g Hematoxylin monohydrate 100 mL 96% Ethanol → needs to mature for 4 weeks Solution B: 95 mL dH_2O 1 mL Hydrchloric acid (25%) 4 mL Iron(III) chloride (29%) Mix 25 mL Solution A with 75 mL Solution B
Nuclear fast red solution	5 g Aluminium sulfate-18-hydrate 100 mL dH_2O → heat until dissolved 0.1 g nuclear fast red
Safranin O staining solution	0.1 g Safranin O Fill up to 100 mL with dH_2O

2.1.7 Antibodies

Table 7: Antibodies used for flow cytometry analysis and histology.

Target	Conjugate	Isotype	Reference #	Provider
Human C3aR	-	Rabbit IgG	Ab126250	Abcam, Cambridge, UK
Human C3aR	FITC	Mouse IgG2b	130-108	Milentyi Biotec, Bergisch Gladbach, Germany
Human C5aR1	-	Rabbit IgG	Ab59390	Abcam, Cambridge, UK
Human C5aR1	APC	Mouse IgG2a	130-104	Milentyi Biotec, Bergisch Gladbach, Germany
Human Collagen type II	-	Mouse IgG1	AF5710	Acris, Herford, Germany
Human Collagen type X	-	Mouse IgG1	031501005	Quartett, Potsdam, Germany
-	APC	Mouse IgG2a	IC003A	R&D Systems, Minneapolis, USA
-	FITC	Mouse IgG2b	IC0041F	R&D Systems, Minneapolis, USA
-	-	Rabbit IgG	011-000-003	Jackson ImmunoResearch, Ely, UK

2.1.8 TaqMan Gene Expression Assays and conventional primers

Table 8: TagMan Gene Expression Assays and conventional primers.

Gene	Primer sequence / Assay ID
18S rRNA	forward (5´-CGCAGCTAGGAATAATGGAATAGG-3´) reverse (5`-CATGGCCTCAGTTCCGAAA-3´)
ALPL	Hs01029144_m1
BMP2	Hs00154192_m1
C3	Hs00163811_m1
C3AR	Hs00377780_m1
C5	Hs00156197_m1
C5AR1	Hs00383718_m1

CD46	Hs00611257_m1
CD55	Hs00892618_m1
CD59	Hs00174141_m1
COL10A1	Hs00166657_m1
COL1A1	Hs00164004_m1
CR1	Hs00559348_m1
CXCL1	Hs00605382_gh
GAPDH	Hs02758991_g1
HPRT1	Hs02800695_m1
IL6	Hs00174131_m1
IL8	Hs00174103_m1
RUNX2	Hs01047973_m1
SP7	Hs01866874_s1

2.1.9 Software

Table 9: Software.

Software	Company
AxioVision 4.8.2	Zeiss, Oberkochen, Germany
BD CellQuest Pro 5.2.1	Becton Dickinson GmbH, Heidelberg, Germany
GraphPad Prism 10	GraphPad Software, Boston, USA
i-control 2.0	Tecan Germany GmbH, Crailsheim, Germany
ImageJ 2.9.0	U. S. National Institutes of Health, Bethesda, Maryland, USA
Magellan 7.2	Tecan Germany GmbH, Crailsheim, Germany
Microsoft Office 16.80	Microsoft Corporation, Redmond, USA
StepOne Software v2.3	Life Technologies GmbH, Darmstadt, Germany

2.2 Methods

2.2.1 Isolation of primary cells and cell culture

To isolate hAC, macroscopically intact cartilage, obtained after knee replacement surgery (see 2.1.1), was cut in small pieces and was digested with 0.2% pronase (in DMEM) for 45 min. Pronase was removed by washing cartilage pieces three times with PBS. Afterwards, remaining cartilage matrix was digested with 0.025% collagenase (in DMEM + 0.5% Penicillin/ Streptomycin) overnight at 37 °C rotating. On the next day, undigested pieces were removed by means of a 40 μm cell strainer and the cell suspension was centrifuged to separate the collagenase. Isolated cells were seeded (5,000 cells/cm^2) into a suitable cell culture flask in chondrocyte BM (see 2.1.6) [176]. After 24 h, cell debris and dead cells were removed by gently washing with PBS.

CSPC were isolated according to Koelling et al. 2009 [93]. For this purpose, cartilage slices of macroscopically intact tissue were placed on a 6-well culture dish. A 40 μm cell strainer was placed on top of the cartilage slices to keep them on the bottom of the well which is required for a successful outgrowth of CSPC. 2.5 mL BM (see 2.1.6) was added and the cartilage was cultured for up to 14 days. Medium was replaced twice a week and outgrowth of CSPC was frequently examined by means of a light microscope.

To isolate human BM-MSCs, a density gradient centrifugation with Biocoll was performed with bone marrow, which was obtained after triple osteotomy surgery (see 2.1.1) [68]. Bone marrow was 1:2 diluted with BM and 4 mL of this mixture was slowly overlaid onto 6 mL of Biocoll. After centrifugation (600*g*, 30 min), the interphase, containing the BM-MSC, was collected and seeded into a T75 cell culture flask in BM, supplemented with 10 ng/mL FGF-2. On the next day, BM-MSCs can be distinguished from other mononuclear cells by their ability to bind to bottom of the culture flask. Nonadherent cells were removed by medium change.

All cells were cultured in an incubator at 37 °C, 95% humidity and 5% CO_2. CSPC and hAC were passaged (see 2.2.1.1) at 80% confluence, BM-MSC at 60 % confluence. hAC were used up to passage 5, CSPC and BM-MSC up to passage 4.

2.2.1.1 Passaging of cells

When a confluence of either 80% (CSPC and hAC) or 60% (BM-MSC) was reached, cells were passaged. At first, medium was removed and cells were washed with PBS. Next, trypsin/EDTA was incubated for 7 min at 37 °C to detach the cells. The enzyme was inactivated by adding medium and the resulting cell suspension was centrifuged at 180*g* for 10 min. The supernatant was discarded and the remaining cell pellet was suspended in a suitable volume to count the cells using a CASY cell counter. For this, 100 µL cell suspension was added in 10 mL CASY ton. The CASY cell counter calculates the number of cells per mL in the initial cell suspension. Finally, the required number of cells can be seeded either for experiments, as described in the respective method section, or for expansion into cell culture flasks (5,000 cells/cm^2).

2.2.1.2 Cryopreservation and thawing

For long-term storage, the resulting cell suspension (see 2.2.1.1) was centrifuged (180*g*, 10 min) once more. This time, the cell pellet was resuspended in prechilled medium (4 °C) supplemented with 5% DMSO. 1 mL of this suspension, containing 0.5 – 1 x 10^6 cells, was added in a cryotube, which was placed overnight in the gas phase of liquid nitrogen. On the next day, cryotubes were put for long-time storage in liquid nitrogen.

To thaw cryopreserved cells, the cryotube was at first incubated in a water bath at 37 °C for 2-3 min. When most of the content was melted, cells were diluted in 37 °C warm medium, centrifuged (180*g*, 10 min), and seeded on a suitable cell culture flask.

2.2.2 Preparation, cultivation, and traumatization of cartilage explants

Full-thickness cartilage explants were extracted with a biopsy punch (∅ 6 mm) from macroscopically intact cartilage, obtained after knee replacement surgery (see 2.1.1). The explants were washed with PBS and cultured in an incubator at 37 °C, 95% humidity and 5% CO_2 in 1 mL serum free medium (SFM) (see 2.1.6) on a 24-well plate. Medium was changed at least twice a week. Prior stimulation, cartilage explants were weighed and, depending on the experimental set-up, traumatised with an established drop-tower device (**Figure 2**) with a defined impact energy of 0.59 J [172, 173].

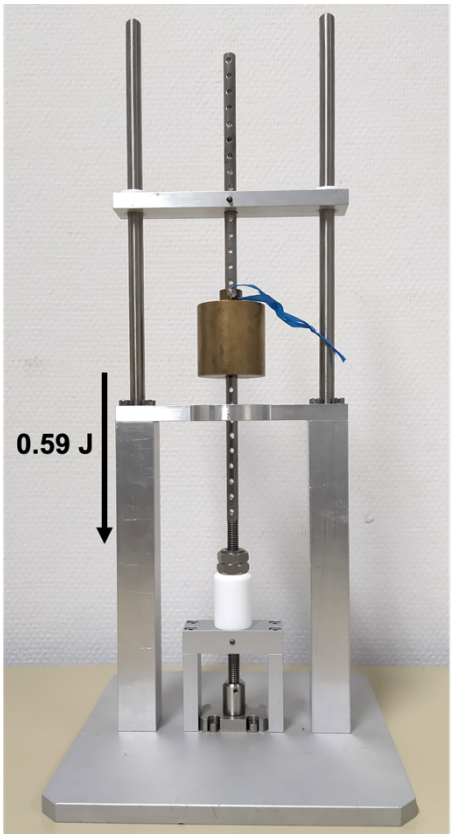

Figure 2: Image of the drop-tower device. The cartilage explant is placed below the indenter and a previously installed weight of 600 g is released. Consequently, the weight falls down 10 cm, gains energy due to gravity, and the impact energy (0.59 J) is transmitted in the sample.

During running experiments, cartilage explants were stimulated in 500 µL SFM on a 48-well plate for 4 days with 50 or 1,000 ng/mL C3a or 50 ng/mL C5a. Concentrations of a similar range were used in previous experiments and were found in the serum of

patients with a posttraumatic systemic inflammation [68, 84]. Medium was collected at day 1 and day 4 and stored at -80 °C. Furthermore, some explants were cultured for 21 days in either 1 mL BM or 1 mL ODM (see 2.1.6) with and without bone morphogenetic protein 2 (BMP-2) on a 24-well plate. Medium was changed at least twice a week. Depending on the usage of the explants, they were either placed in formalin and used for histology (see 2.2.5) or in liquid nitrogen to isolate ribonucleic acid (RNA) (see 2.2.4). Additionally, cartilage explants were collected from highly degenerated cartilage tissue and were directly prepared for histology or RNA isolation without further cultivation.

2.2.3 Differentiations

2.2.3.1 Osteogenic differentiation and evaluation

To evaluate osteogenic differentiation potential, either hAC, CSPC, or BM-MSC were seeded in monolayer in passage 3 or 4 with a density of 1 x 10^4 cells/cm^2. When a confluence of 80% was reached, the respective medium was replaced by ODM. Furthermore, cells were stimulated with 50, 500 or 1,000 ng/mL C3a, 50 ng/mL or 500 ng/mL C5a, 10 μM SB290175, 10 μM PMX53, and/or 100 ng/mL BMP-2 for 21 days. Additionally, cells cultured in BM served as undifferentiated, negative control. Medium was changed twice a week and supplements were refreshed every time.

Alizarin Red S staining was applied after 21 days to analyse the calcification during osteogenic differentiation. Alizarin Red S forms with calcium a complex, which is visible in a bright red staining. Thus, calcification appears red [18]. All steps were carried out at room temperature. At first, cells were washed 3 times with PBS and subsequently fixated with prechilled (4 °C) 70% ethanol. After an incubation of 1 h, 40 mM Alizarin Red S solution was added for 10 min. This incubation was carried out on a shaker. Next, staining solution was removed and cells were washed multiple times with dH_2O to remove all remaining, unbound Alizarin Red S. Images were taken from the stained cells with a Canon EOS 700D camera. To quantify the amount of bound Alizarin Red S, stained cells were incubated on a shaker in 10% cetylpyridinium for 15 min.

Additionally, a two-fold serial dilution of an Alizarin Red S standard (600 μg/mL to 0 μg/mL) was prepared. The measurement was carried out at an absorbance at 652 nm by means of a multimode microplate reader Infinite M200 Pro. The program Magellan was used to calculate the Alizarin Red S concentration based on a standard curve.

Osteogenic differentiation was also assessed on messenger RNA (mRNA) level. For this purpose, cell lysates were prepared with RLT-buffer on day 7 and day 14 and further processed as described in 2.2.4.1. Furthermore, C3aR and C5aR1 protein expression was evaluated on day 14 by means of immunocytochemistry (see 2.2.5.5).

Additionally, a modified osteogenic differentiation was carried out. The experimental procedure was based on the trans-differentiation protocol (see 2.2.3.3). In this case, chondrogenic differentiation was skipped and hAC were cultured in BM for the first 7 days instead. To ensure a successful osteogenic differentiation, culture time in ODM with/without 100 ng/mL BMP-2 was increased from 3 to 10 days. Medium was changed three times a week and required additives (1,000 ng/mL C3a, 50 ng/mL C5a, or 10 μM PMX53) were added as needed.

2.2.3.2 Chondrogenic differentiation and evaluation

To investigate the influence of anaphylatoxins on the chondrogenic differentiation potential, 3.9 x 10^5 hAC (passage 4 or 5) were put in a 15 mL tube with a filter cap. After centrifugation (180*g*, 10 min), the resulting cell pellets were put in an incubator (37 °C, 95% humidity, 5% CO_2) overnight. On the next day, BM was replaced by 1 mL CDM (see 2.1.6). Depending on the experimental set-up, the following supplements were added to CDM: 50 or 1,000 ng/mL C3a, 50 ng/mL C5a, 10 μM SB290175, and/or 10 μM PMX53. Additionally, cells cultured in BM served as undifferentiated, negative control. Medium was changed twice a week and supplements were refreshed every time. Furthermore, the growth factors rhTGF-β3 and rhBMP6 were added daily during the first 7 days. After 28 days of cultivation, cell pellets were processed for histological analysis (see 2.2.5).

For evaluation, histological staining of proteoglycans by means of Safranin O staining (see 2.2.5.2) and collagen type II immunohistochemistry (see 2.2.5.1) was carried out. An adapted scoring system was applied which was first described in Riegger et al. 2018 [174]. The same categories (pellet size, collagen type II, Safranin O staining intensity, cell-cell distance, and cell morphology) were used, however the score of the pellet size was adjusted as shown in **Table 10** [182]. A score ranged from 0 (failed chondrogenic differentiation) to 3-5 (evidence for successful chondrogenic differentiation). The individual scores of all categories were added up to calculate the overall score.

Table 10: Assessment of neo-cartilage formation. Adapted from Ruths et al. 2024 [182]. Licensed under CC BY 4.0, https://creativecommons.org/licenses/by/4.0/

Scoring categories	Score
1) Pellet size (diameter)	
< 900 µm	0
> 900 µm	1
> 1,200 µm	2
> 1,500 µm	3
> 1,800 µm	4
> 2,200 µm	5
2) Collagen type II/ Safranin O staining intensity	
No staining	0
Weak staining (> 5% positive)	1
Scattered moderate staining (> 25% positive)	2
Even moderate stain (> 50% positive)	3
Even intensive stain (> 85% positive)	4
3) Cell-Cell distance (matrix production)	
High cell density; no matrix between cells	0
High cell density; little matrix between cells	1
Moderate cell density; little matrix between cells	2
Low cell density; extensive matrix between cells	3
4) Cell morphology	
Condensed/necrotic/pycnotic bodies	0
Spindel/fibrous	1
Mixed spindle/fibrous and rounded/chondrogenic	2
Majority rounded/chondrogenic	3

2.2.3.3 Trans-differentiation and evaluation

During a trans-differentiation, hAC were first re-differentiated in monolayer towards a chondrogenic phenotype and subsequently an osteogenic differentiation was performed [211]. 2.5 x 10^4 hAC/cm^2 were seeded in passage 2 and on the next day, chondrogenic differentiation was induced by cultivation in CDM supplemented with 2% FBS. At day 3 and 6, medium was replaced by CDM (+ 1% FBS). After 7 days, cells were cultured for 3 further days in ODM with/without 100 ng/mL BMP-2. Differentiation was carried out in presence of 50 or 1,000 ng/mL C3a, 50 ng/mL C5a, 10 μM SB290175, and/or 10 μM PMX53. Supplements were refreshed with every medium change.

Chondrogenic differentiation in monolayer was evaluated by means of Alcian blue staining. All steps were carried out at room temperature. Cells were at first washed twice with PBS and fixated with formalin. After 15 min, formalin was removed and 0.1 N HCl was incubated for 10 min. Next, Alcian blue staining solution was added. 30 min later, the staining solution was removed by washing the cells multiple times with 0.1 N HCl. For quantification, remaining Alcian blue was dissolved for 1 h in 1% SDS solution and absorbance at 595 nm was measured with a multimode microplate reader Infinite M200 Pro. Alizarin Red S staining (see 2.2.3.1) was used to assess osteogenic differentiation.

2.2.4 Gene expression analysis

2.2.4.1 Isolation of total RNA

Total RNA was extracted from cryopreserved cartilage explants with the RNeasy Lipid Tissue Mini Kit according to manufacturer´s instructions. At first, steel beads were cleaned twice in an ultrasonic bath for 10 min. Initially with a cleaner specific for ultrasonic baths and subsequently with 100% undenatured absolute ethanol. Cartilage samples assigned for RNA isolation were stored at -80 °C in a cryogenic vial, which was put in liquid nitrogen prior the disintegration. One cleaned steel bead was added

in each vial which was then put back in liquid nitrogen. Also, a teflon vessel was prechilled in liquid nitrogen and 4 vials were put in one teflon vessel. A Microdismembrator S was used to pulverize the cartilage explants. All remaining steps were carried out at room temperature. Next, 750 µL QIAzol Lysis Reagent was added, thoroughly mixed with cartilage debris, and incubated for at least 30 min. Next, the suspension was transferred to a 1.5 mL reaction tube and 200 µL Chloroform was added. The resulting suspension was vortex for 30 sec, incubated for 3 min, and subsequently centrifuged (12,000*g*, 1 h, 4 °C). In the next step, the upper, aqueous phase (approx. 300-350 µL) was carefully transferred to a new 1.5 mL reaction tube and mixed with 350 µL 70% ethanol. This mixture was transferred to a Mini Spin Column, which was included in the kit, and columns were centrifuged (8,000*g*, 15 sec). After the flow-through was discarded, 250 µL RW1 (included in kit) was added and the columns were again centrifuged (8,000*g*, 15 sec). This procedure was repeated three more times, first once again with 350 µL RW1 and then twice with 500 µL RPE (included in kit). Subsequently, the column was transferred in a new collection tube and centrifuged (12,000*g*, 1 min). In the last step, 33 µL nuclease-free water was added directly on the membrane and the columns were centrifuge one last time (8,000*g*, 1 min). Eluted RNA was directly placed on ice and stored at -80 °C.

To extract total RNA from monolayer cultured cells, the RNeasy Mini Kit was used. In this case, cells were lysed with RLT-buffer (included in kit) containing 1% 2-Mercaptoethanol, transferred in a 1.5 mL reaction tube, and vortexed thoroughly for 1 min. Next, 350 µL 70% ethanol was added and mixed with the RLT-buffer. The resulting solution was added to a Mini Spin Column and the following isolation was carried out as described above.

2.2.4.2 cDNA synthesis

Reverse transcription of isolated RNA into stable complementary deoxyribonucleic acid (cDNA) was conducted using the Omniscript RT Kit. For this purpose, master mix I was

prepared as depicted in **Table 11** in a 0.2 mL reaction tube in which 8 µL RNA was added. After manual mixing, tubes were shortly centrifuged and placed into a ProFlex thermocycler. The thermocycler protocol is shown in **Table 12** and was carried out till the first hold step at 4 °C to allow the primers to anneal to the RNA. Next, reaction tubes were removed from the thermocycler and 7 µL of master mix II (**Table 13**), containing the reverse transcriptase, was added. The solution was again mixed manually, centrifuged shortly and placed back into the thermocycler. The protocol was continued and obtained cDNA was stored at -20 °C.

Table 11: Master mix I for primer annealing

Component	Concentration	Volume [µL]
OligodT	100 pmol/µL	0.5
dNTP Mix	5 mM	2
RNase Inhibitor	40 U/µL	0.25
Nuclease-free water		2.25
Total		5

Table 12: Thermocycler protocol for cDNA synthesis

	Temperature [°C]	Duration [min]
Primer annealing	65	5
	4	2
	4	∞
Reverse Transcription	42	50
Inactivation of enzyme	70	15
Hold	4	∞

Table 13: Master mix II for cDNA synthesis

Component	Concentration	Volume [µL]
First Strand Puffer	5x	4
DTT	100 mM	2
Reverse Transcriptase	200 U/µL	1
Total		7

2.2.4.3 Quantitative real-time polymerase chain reaction (qRT-PCR)

Synthesised cDNA was used for qRT-PCR. Either target-specific conventional primers or TaqMan Gene Expression Assays were used (**Table 8**) to amplify a sequence within the target gene and simultaneously quantify the target gene.

To detect *18S rRNA* with conventional primers, cDNA was diluted 1:30 in nuclease-free water and the master mix as shown in **Table 14** was prepared. 2 µL of diluted cDNA or 2 µL nuclease free water as negative control was mixed with 8 µL of the prepared master mix on a MicroAmp Fast Optical 96-Well Reaction Plate. Measurements were performed in duplicates. Next, the plate was properly sealed with MicroAmp Optical Adhesive Film, centrifuged (250*g*, 2 min) and placed in the StepONEPlus. Applied PCR protocol is shown in **Table 15**. The Power SYBR Green PCR Master Mix contains a SYBR Green I dye binding double-stranded DNA. Thus, the dye provides a fluorescence signal that is equivalent to the amount of double-stranded DNA generated during PCR. The absence of non-specific amplification was confirmed by means of a melt curve.

Table 14: Master mix for qRT-PCR with Power SYBR Green PCR Master Mix

Component	Concentration	Volume [µL]
Power SYBR Green PCR Master Mix	2x	5
Nuclease-free water		2
Primer mix (forward and reverse)	10 µM	1
Total		8

Table 15: Protocol for qRT-PCR with Power SYBR Green PCR Master Mix

	Temperature [°C]	Duration [min]	
Polymerase activation	95	10:00	
Denaturation	95	0:15	40 cycles
Annealing/Extension	60	1:00	
Melt curve	95	0:15	
	60	1:00	
	60 → 90 0.3 °C steps		
	95	0:15	

To quantify gene expression with TaqMan Gene Expression Assays, cDNA was diluted 1:3 in nuclease-free water. In this case, a master mix containing TaqMan Fast Advanced Master Mix (**Table 16**) was prepared. 8 µL of the master mix was added with 2 µL of diluted cDNA or 2 µL nuclease free water on a MicroAmp Fast Optical 96-Well Reaction Plate. The protocol is shown in **Table 17**. TaqMan Gene Expression Assays consist of primers and a probe which both bind within the target gene. The probe has a fluorescent dye on the 5´ end and a quencher on the 3´end. In the beginning, the signal of the dye is quenched and no signal can be detected. During synthesis of the complementary DNA strand, the bound TaqMan probe is cleaved due to the endogenous 5´ nuclease activity of the polymerase. Thus, the fluorescent dye is separated from the quencher resulting in an increased fluorescence intensity proportional to the amount of newly synthesised DNA.

Table 16: Master mix with TaqMan Fast Advanced Master Mix

Component	Concentration	Volume [µL]
TaqMan Fast Advanced Master Mix	2x	5
Nuclease-free water		2.5
TaqMan Gene Expression assay		0.5
Total		8

Table 17: Protocol for qRT-PCR with TaqMan Fast Advanced Master Mix

	Temperature [°C]	Duration [min]	
Polymerase activation	95	00:20	
Denaturation	95	0:01	40 cycles
Annealing/Extension	60	0:20	

qRT-PCR was evaluated by means of the ΔΔCt method. At first, the cycle threshold (Ct) was determined for each well. The Ct value describes how many cycles were needed to reach a defined threshold of fluorescence intensity. Thus, a low Ct value indicates a high expression of the target gene while a high Ct value represents a low expression. For the following calculations, the mean of the duplicates was used. Normalised gene expression was calculated by subtracted the Ct value of each individual housekeeping gene (*18S rRNA*, *GAPDH*, *HPRT1*) from the Ct value of the target gene:

$$\Delta Ct = Ct_{\text{target gene}} - Ct_{\text{housekeeping gene}}$$

To calculate the ΔΔCt, a reference sample was defined as calibrator. The respective calibrators are indicated in the figure legends. The ΔCt of the calibrator was subtracted from the ΔCt of the sample:

$$\Delta\Delta Ct = \Delta Ct_{\text{sample}} - \Delta Ct_{\text{reference}}$$

The relative gene expression was calculated with the following formular:

$$\text{Gene expression} = 2^{(-\Delta\Delta Ct)}$$

Finally, the mean of the relative gene expressions was calculated on the basis of the three housekeeping genes and used for statistical analysis.

2.2.5 Histology

Cartilage explants which were used for histologic analysis were stored in formalin for 24 h. Afterwards, explants were placed for 1 h under running tap water to remove excessive formalin. Subsequent dehydration was carried out at room temperature with an automatic tissue dehydration TB1020 with the following program: 2x 1.5 h 75% isopropyl alcohol; 2x 1.5 h 96% isopropyl alcohol; 2x 1.5 h 100% isopropyl alcohol; 2x 1.5 h xylene; 2x 1.5 h paraffin. Next, explants were embedded in paraffin and sections of 3.5 μm were prepared and transferred on microscope slides. Slides were dried overnight at 40 °C and stored at room temperature till further use.

Cell pellets obtained after chondrogenic differentiation (see 2.2.3.2) were washed with PBS and fixated with formalin for 15 min. All steps were carried out at room temperature. Formalin was removed by washing twice with PBS. Next, the pellets were dehydrated manually: 1x 30 min 50% isopropyl alcohol; 2x 15 min 75% isopropyl alcohol; 1x 15 min 96% isopropyl alcohol (+0.01% Eosin); 1x 15 min 96% isopropyl alcohol; 2x 30 min 100% isopropyl alcohol; 2x 30 min xylene; 2x 60 min paraffin. Pellets were embedded in paraffin and sections of 3.5 μm were prepared as described above.

2.2.5.1 Immunohistochemistry (IHC)

IHC was used to detect and localize proteins in paraffin sections. If not indicated otherwise, all steps were carried out at room temperature. To perform IHC, microscope slides with tissue sections were at first placed in a 65 °C incubator to allow the paraffin to melt. Next, sections were deparaffinised with xylene (2x 10 min) and rehydrated with the following steps: 2x 5 min 100% isopropyl alcohol; 2x 5 min 96% isopropyl alcohol; 2x 5 min 75% isopropyl alcohol. The slides were washed in dH_2O and transferred in 0.01% Brij in PBS. In case of C3aR , C5aR1 , and rabbit IgG IHC, antigen retrieval was performed by means of 10 mM citrate buffer overnight at 65 °C. For collagen type II staining, antigen retrieval was carried out with pepsin (1 mg/mL in 0.5 M acetic acid) for 30 min at 37 °C. At first hyaluronidase (2 mg/mL; 30 min; 37 °C) and then pepsin

(1 mg/mL; 40 min; 37 °C) was needed to demask collagen type X. After the individual procedures, slides were left to cool down to room temperature and placed in PBS. Next, samples were blocked for 30 min with protein block and the respective antibodies were diluted in antibody diluent (C3aR: 1:400; C5aR1: 1:500; rabbit IgG: 1:400; collagen type II: 1:100; collagen type X: 1:10) and subsequently incubated overnight at 4 °C. On the next day, unbound primary antibody was removed by washing the slides twice in PBS and placing them in 0.01% Brij for 10 min. To suppress endogenous peroxidase activity, slides were placed for 30 min in 3% hydrogen peroxide, which blocks peroxidases. Subsequently, slides were washed in PBS and the staining procedure was continued by incubating the slides for 30 min with biotinylated goat anti-polyvalent solution. After another washing step (PBS, PBS, 10 min 0.01% Brij), slides were incubated with streptavidin peroxidase solution for 30 min. Afterwards, slides were washed again (PBS, PBS, 10 min 0.01% Brij) and finally incubated for 10 min with AEC chromogen to visualize the target proteins in red. Furthermore, slides were shortly washed with dH_2O, followed by an incubated for 4 min in Hämalaun solution (MAYER) to stain the nuclei black. Next, slides were rinsed for 10 min with tap water and mounted with aquatex.

An Axioshop 2 mot plus microscope was used to document all sections. In the case of C3aR and C5aR1 IHC, the number of negative and positive cells was manually counted in at least 3 images of different sections and locations. Only the superficial zone and the upper part of the middle zone (about 0.5-0.6 mm) was analysed. The percentage of C3aR- and C5aR1-positive cells was calculated and used for statistical analysis and data presentation.

2.2.5.2 Safranin O staining

All steps were carried out at room temperature. The tissue sections were deparaffinised and rehydrated as described above (see 2.2.5.1). After the second incubation in 96% isopropyl alcohol, slides were directly placed in Hämatoxylin solution (WEIGERT) for 7 min and washed shortly in dH_2O. Nuclei were stained black by rinsing the slides for

10 min with tap water. Next, slides were washed once again with dH_2O and incubated for 1 min in Fast Green staining solution, followed by a washing step in 1% acetic acid. Sections were incubated for 10 min in Safranin O staining solution and dehydrate by washing them shortly in the following solutions: 1% acetic acid, 75% isopropyl alcohol, 96% isopropyl alcohol, 100% isopropyl alcohol, xylene. Finally, sections were mounted with Eukitt.

An Axioshop 2 mot plus microscope was used to document all sections. Nuclei are stained black, cytoplasm is stained green, and Safranin O stains sulphated glycosaminoglycans red, thus hyaline cartilage appears red.

2.2.5.3 Alizarin Red S staining

An Alizarin Red S kit (pH 4.0) was used to stain paraffin embedded sections with Alizarin Red S. The kit was carried out according to the manufacturer's instructions. All steps were carried out at room temperature. Sections were at first deparaffinised (2x 5 min xylene) and rehydrated (2 min 96% ethanol, 2 min 80% ethanol, 2 min 70% ethanol, 2 min 60% ethanol, 2 min tap water). Next, sections were stained with the provided Alizarin Red S staining solution (pH 4.0) for 5 min, followed by a washing step in acetate buffer (provided) and dehydration (2x 30 sec 96% ethanol, 30 sec 100% isopropyl alcohol, 2x 5 min xylene). In the last step, sections were mounted with Eukitt.

Alizarin Red S forms with calcium a complex, which is visible in a bright red staining. Thus, calcification appears red [18]. Axioshop 2 mot plus microscope was used to document all sections.

2.2.5.4 Von Kossa staining

All steps were carried out at room temperature. Sections were deparaffinised and rehydrated as described above (see 2.2.5.1) and transferred from dH_2O in 5% silver nitrate for 1 h. Remaining silver nitrate was removed by rinsing the slides with dH_2O.

Next, slides were incubated in 1% pyrogallol for 5 min and the staining was fixated with 5% sodium thiosulfate. Again, sections were washed with dH_2O, followed by a counterstaining with nuclear fast red solution for 10 min. Sections were shortly placed back in dH_2O, dehydrated (75% isopropyl alcohol, 96% isopropyl alcohol, 100% isopropyl alcohol, xylene), and mounted with Eukitt.

During the staining procedure, calcium ions are replaced by silver ions, which are made visible by light exposure [190]. Thus, calcification is indicated in black and nuclei are stained red. Axioshop 2 mot plus microscope was used to document all sections.

2.2.5.5 Immunocytochemistry (ICC)

The expression and localisation of C3aR and C5aR1 in primary cells was assessed by means of ICC. If not indicated otherwise, all steps were carried out at room temperature. 20,000 hAC were seeded per well on a CultureSlide. On the next day, cells were washed with PBS and fixated with 300 µL formalin for 15 minutes. In case of osteogenic differentiation, cells were washed and fixated on day 14. After fixation, cells were washed twice with PBS and incubated in 0.01% Brij for 15 min. Similar to the IHC protocol, unspecific binding was prevented by incubating cells with protein block for 30 min. Afterwards, the respective primary antibodies (C3aR: 1:400; C5aR1: 1:500) were incubated overnight (4 °C). Unbound antibodies were removed by washing twice with PBS and incubating in 0.01% Brij for 10 min. Endogenous peroxidase activity was supressed by a 30 min incubation with 3% hydrogen peroxide. After another washing step with PBS and 0.01% Brij, cells were incubated for 30 min with biotinylated goat anti-polyvalent solution, followed by the next washing step with PBS and 0.01% Brij. Subsequently, a 30 min incubation step with streptavidin peroxidase solution was performed. Again, unbound antibodies were removed with a final washing step and the target protein was visualised in red by incubating the cells for 10 min with AEC chromogen. The chambers were removed and slides were washed with dH_2O and placed for 4 min in Hämalaun solution (MAYER) to stain nuclei black. After rinsing the slides with tap water, cells were mounted with aquatex.

To evaluate the localization of the receptors further, the above-described protocol was also carried out by replacing 0.01% Brij with PBS without any detergents, which permeabilise the cell membrane. Consequently, only extracellular, membrane bound proteins were stained.

The different wells on the CultureSlide were documented using an Axioshop 2 mot plus microscope.

2.2.6 Flow cytometry analysis

To investigate the protein deposition of the anaphylatoxin receptors on the cell membrane, flow cytometry analysis was carried out. With this method, the size (forward scatter) and granularity (sideward scatter) of the cells can be measured. Simultaneously, the fluorescence of stained cells is recorded. In this thesis, fluorescence antibody's binding C3aR or C5aR1 were used (see 2.1.7).

At first, primary cells (hAC, BM-MSC, or CSPC) were detached with either trypsin/EDTA (7 min, 37°C) or 5 mM EDTA solution (30 min, room temperature) and suspended in PBS. After centrifugation (180*g*, 10 min), cells were washed once with PBS, resuspended in PBS, and at least 2 x 10^5 cells were used for each individual staining. The staining was perfomed in a V-bottom 96-well plate in a total volume of 100 µL PBS and 5 µL C3aR-FITC and 5 µL C5aR1-APC antibody was added. As species-matching isotype control, 5 µL mIgG2b-FITC and 5 µL mIgG2a-APC was added. After an incubation of 30 min on ice in the dark, staining solution was removed after centrifugation (500*g*, 11 min), following a washing step with PBS. Finally, stained cells were resuspended in 1:10 diluted BD CellFix and transferred in a 5 mL round-bottom tube. At least 3 x 10^4 cells were analysed on a BD FACSCalibur Flow Cytometer. The measurement and subsequent analysis were performed with a BD CellQuest Pro software. Percentage of C3aR- or C5aR1-positive cells was determined and only 1% isotype control-positive cells were accepted.

Furthermore, it was tested if C3aR and C5aR1 are also localised intracellularly. For this purpose, hAC were detached with 5 mM EDTA solution. After centrifugation (180*g*, 10 min), cells were resuspended in formalin and fixated for 15 min. Formalin was removed after centrifugation (180*g*, 10 min), following a washing step with PBS. Next, cells were permeabilised for 10 min with PBS containing 0.5% Tween-20 and stained and analysed as described above.

2.2.7 Preparation of cartilage conditioned medium

Culture medium of cartilage explants isolated from macroscopically intact and highly degenerated tissue was collected and used for a C3 or C5 cleavage assay (see 2.2.9). At first, the explants were cultured in 400 µL SFM for 24 h on a 48-well plate. The conditioned medium was collected and stored at -80 °C. Next, highly degenerated explants were discarded. Macroscopically intact explants were traumatised (see 2.2.2) and cultured in 400 µL SFM. The conditioned medium was collected after 24 h. Subsequently, cartilage explants were cultured further in SFM till 7 days after traumatization. Medium was changed at day 4 and day 6 and conditioned medium was once more collected on day 7.

2.2.8 Preparation of cartilage homogenizate (HG)

HG was used to mimic a post-traumatic environment *in vitro*. At first, a piece of highly degenerated cartilage (200-300 mg) was isolated, washed in PBS, and weighed. Subsequently, it was stored at -80 °C in a cryogenic vial. Homogenization was carried out with a Microdismembrator S as described before (see 2.2.4.1). In this case, pulverised cartilage was directly suspended in sterile PBS to reach a concentration of 100 mg/mL.

2.2.9 C3 and C5 cleavage assay

To evaluate under which conditions C3 and C5 are cleaved in the respective anaphylatoxins C3a and C5a, a cleavage assay was carried out according to Ignatius et al. 2011 [84]. 6,000 hAC (passage 1, 2, or 3) were seeded on a 96-well plate. On the next day, medium was removed and hAC were washed with PBS. Cells were stimulated in a total volume of 110 µL SFM with 20 µg/mL C3, 20 µg/mL C5, and/or 2 µL HG (1.8 mg/mL). Additionally, instead of SFM, cartilage conditioned medium was used (see 2.2.7) to investigate, if proteins are expressed and released in the supernatant that favour C3 or C5 cleavage. As a control, the experiment was also performed in wells without cells to verify, that hAC are involved in C3a or C5a generation. This control was also necessary to determine if C3a and C5a are generated due to components in the cartilage conditioned medium.

After an incubation time of 4 h in a 37 °C cell culture incubator, the resulting supernatants were collected in a Protein LoBind Tube and centrifuged at 800*g* for 5 min to remove cell debris. Next, supernatant was transferred in a new Protein LoBind Tube and stored till further analysis (see 2.2.10.1) at -80 °C.

2.2.10 Enzyme-linked immunosorbent assay (ELISA)

2.2.10.1 C3a- and C5a-ELISA

The amount of C3a and C5a was analysed by means of C3a- or C5a-ELISA according to the manufacturer's instructions. All steps were carried out at room temperature. Previously stored supernatants (see 2.2.9) were thawed on ice. In the meantime, the provided microwell plate (coated with either a monoclonal antibody to human C3a or C5a) was washed three times with the provided Wash Buffer and excessive wash buffer was removed by inverting the plate against clean paper towels. Next, 50 µL of sample diluent was added to every well and a two-fold serial dilution of the respective standard was prepared (C3a: 20 ng/mL, 10 ng/mL, 5 ng/mL, 2.5 ng/mL, 1.25 ng/mL, 0.625 ng/mL, 0.313 ng/mL; C5a: 5 ng/mL, 2.5 ng/mL, 1.25 ng/mL, 0.625 ng/mL,

0.313 ng/mL, 0.156 ng/mL, 0.078 ng/mL). 50 µL of the samples was added, following a 2 h incubation on a microplate shaker. Next, the solutions were discarded and wells were washed eight times with Wash Buffer. Afterwards, 100 µL of the provided Biotin-conjugated anti-C3a/C5a antibody was added to every well and the plate was incubated for another hour on a microplate shaker. Again, the wells were emptied, washed with Wash Buffer, and 100 µL of the provided Streptavidin-HRP antibody was added. Subsequently, the plate was incubated for 1 h on a microplate shaker. After the last washing step, 100 µL TMB substrate solution (provided) was added and incubated for 15 to 30 min. HRP metabolises the substrate and thus, a change of colour is visible, which is proportional to the amount if bound Streptavidin-HRP antibody to the target protein. Colour development was monitored and 100 µL stop solution (provided) was added to all wells when at least one well reached an optical density of 0.9-0.95 at 650 nm, measured with a multimode microplate reader Infinite M200 Pro. After addition of the stop solution, the absorbance at 450 nm was measured. With the help of the software Magellan, a standard curve was generated and the C3a/C5a concentration of each individual sample was calculated.

2.2.10.2 IL-6-ELISA

The protein level of IL-6 was determined by means of an IL-6-ELISA according to the manufacturer's instructions. If not indicated otherwise, all steps were carried out at room temperature. In the first step, 100 µL of the capture antibody diluted in Coating Buffer (both provided) was added in each well of the provided 96-well plate and incubated shaking overnight at 4 °C. On the next day, wells were washed three times with Wash Buffer and excessive wash buffer was removed by inverting the plate against clean paper towels. To block wells, 200 µL of provided ELISA/ELISPOT Diluent was added and incubated for 1 h on a microplate shaker. Wells were washed once and a two-fold serial dilution of the standard was prepared (200 pg/mL, 100 pg/mL, 50 pg/mL, 25 pg/mL, 12.5 pg/mL, 6.25 pg/mL, 3.125 pg/mL, 1.565 pg/mL). Next, 100 µL of the thawed supernatants of cartilage explants (see 2.2.2) were added and incubated for

2 h on a microplate shaker. Afterwards, wells were washed five times with Wash Buffer and 100 µL of diluted Detection Antibody (provided) was added to all wells. After 1 h of incubation, wells were washed once again five times with Wash Buffer and 100 µL of diluted Streptavidin-HRP (provided) was added to all wells. 30 minutes later, in the final washing step the wells were washed eight times and provided TMB solution (100 µL/well) was incubated for 15 min. Subsequently, 100 µL stop solution was added to all wells. A multimode microplate reader Infinite M200 Pro was used to measure the absorbance at 450 nm. With the help of the software Magellan, a standard curve was generated and the IL-6 concentration of each individual sample was calculated.

2.2.11 Statistical analysis

At least three biological replicates were carried out for each experiment and statistical analysis was performed using GraphPad Prism Version 10. Normally distributed data (according to Shapiro-Wilk test) was analysed with an unpaired t test, one-way ANOVA, mixed-effects analysis, or Pearson correlation to test statistical significance. Not normally distributed data was analysed with a Kruskal-Wallis test or unpaired Mann-Whitney test. A p-value smaller than 0.05 was considered as statistically significant.

3 Results

3.1 Generation of C3a and C5a by hAC

Previous studies indicated that the complement system is involved in OA progression [187, 196]. So far, it is not known whether hAC, as the main cell type in articular cartilage, are actively involved in complement activation. In the first paragraph of this thesis, it was tested if hAC express C3 and C5 and under which conditions hAC cleave C3 and C5 in the respective anaphylatoxins C3a and C5a.

C3 and C5 gene expression was analysed in macroscopically intact (OARSI grade ≤ 1) and highly degenerated (OARSI grade ≥ 3) human cartilage. To illustrate the different grades, exemplary Safranin O staining is shown in **Figure 3 A**. OARSI grad 0 and 1 was assigned when the surface was intact and the cartilage possessed an overall intact morphology concerning cellularity and proteoglycan content. OARSI grade 3 or higher was reached when vertical fissures were visible in the superficial zone, cells were mainly found in clusters, and proteoglycan content was reduced. Gene expression analysis indicated that *C3* and *C5* are expressed in human articular cartilage (**Figure 3 B**). However, no difference between macroscopically intact or highly degenerated cartilage tissue was observed.

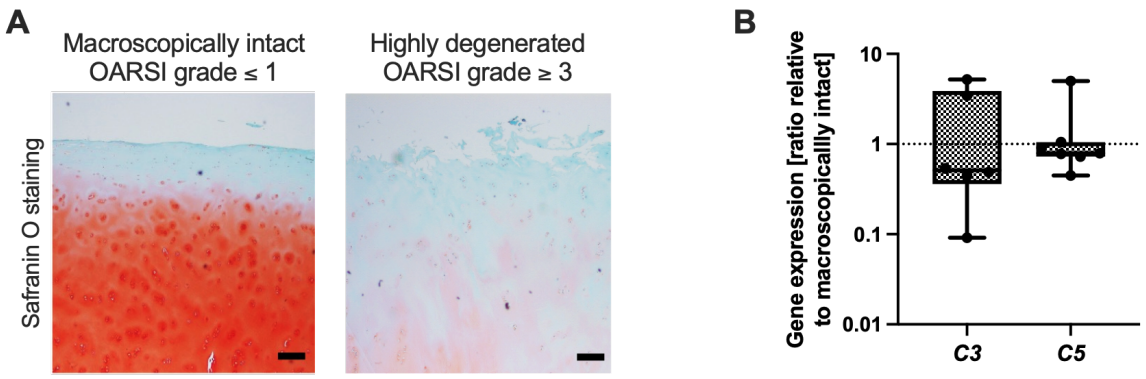

Figure 3: Gene expression of C3 and C5 in human articular cartilage. (A) Exemplary images of macroscopically intact (OARSI grade ≤ 1) and highly degenerated (OARSI grade ≥ 3) cartilage tissue, stained with Safranin O. Scale bars represent 200 μm. **(B)** Gene expression of *C3* and *C5* in highly degenerated tissue, normalised to macroscopically intact cartilage; n ≥ 6. Box plot shows median with minimum to maximum whiskers. Each datapoint represents an independent biological replicate. Images in (A) were published in Ruths et al. 2024 [182]. Licensed under CC BY 4.0, https://creativecommons.org/licenses/by/4.0/.

Next, the ability of hAC to cleave C3 or C5 was tested. These experiments (**Figure 4** and **Figure 5**) were carried out by the student Jana Hengge, but planed, supervised, and evaluated by me. At first, hAC were cultured in SFM in presence of 20 μg C3, 20 μg C5, and/or 1.8 mg/mL HG. The same set-up was carried out in wells without cells (see 2.2.9). After 4 h, supernatants were collected and either a C3a- (**Figure 4 A**) or C5a-ELISA (**Figure 4 B**) was performed. In case of C3a, only low concentrations were detected, when no supplements (median: 0.46 ng/mL) were added. Similar amounts of C3a were detected when C3 was added, regardless of the presence (median: 1.47 ng/mL) or absence (median: 1.41 ng/mL) of hAC. When HG (median: 5.35 ng/mL, $p < 0.0001$) was supplemented together with C3 to the cells, a significant increase of C3a was observed. Additionally, a significant difference between wells without cells and with cells was observed in the presence of HG ($p < 0.0001$).

Similar results were observed when C5 was added, but no C5a was detected in the supernatants of hAC when no C5 was supplemented. Sole addition of C5 resulted in a significant higher C5a concentration ($p = 0.026$) in wells with cells (median: 4.17 ng/mL) compared to wells without cells (median: 3.02 ng/mL). The same was true when C5 + HG ($p = 0.0035$; median with cells: 5.04 ng/mL; median without cells: 3.94 ng/mL) was

added. In presence of hAC, significant more C5 was cleaved, when C5 and HG was supplemented, compared to the sole addition of C5 (p = 0.026).

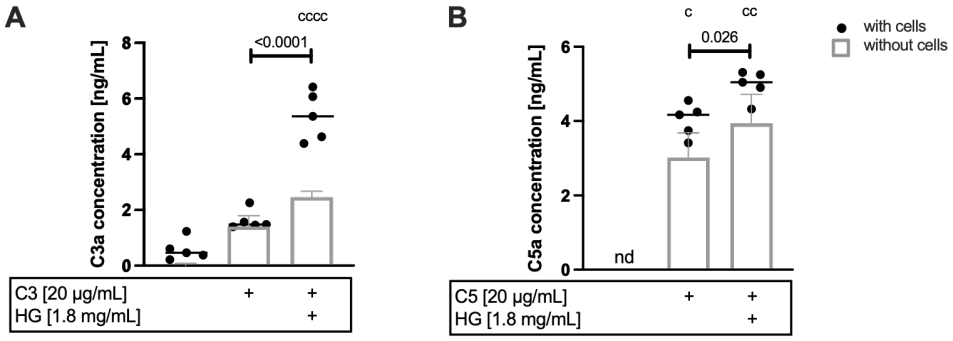

Figure 4: Cleavage of C3 and C5 by hAC. hAC were stimulated for 4 h with 20 µg/mL C3, 20 µg/mL C5, and/or 1.8 mg/mL cartilage homogenizate (HG). Each datapoint represents an independent biological replicate; n = 5. Median values are shown. Wells without cells served as control, indicated by a bar graph with median and range; n = 3. Collected supernatants were used for **(A)** C3a- or **(B)** C5a-ELISA, nd = not detected. One-way ANOVA (A: Šidák´s correction; B: Holm-Šidák´s correction); with cells vs. without cells: $^{C}p < 0.05$, $^{CC}p < 0.01$, $^{CCCC}p < 0.0001$.

The cleavage of C3 and C5 was also tested in a post-traumatic and OA environment. Macroscopically intact and highly degenerated cartilage tissue was cultured in SFM, which was collected after 24 h. Also, supernatant of traumatised explants was harvested 24 h and 7 days after trauma. This cartilage conditioned medium was added to wells with or without hAC together with either 20 µg C3 or 20 µg C5 (see 2.2.9). After an incubation of 4 h, supernatants were collected and used for an C3a- (**Figure 5 A**) or C5a-ELISA (**Figure 5 B**). In both cases, no differences were observed. Neither between the stimulations nor between wells with and without cells. The measured C5a concentrations was similar to the concentration, when only C5 was added. However, the C3a concentration was much higher (median ranged from 36 to 43 ng/mL) compared to the previously analysed samples. Also, cartilage conditioned medium was directly analysed without 4 h of cultivation and even higher C3a concentrations were detected.

In summary, these results indicate that hAC express the complement components C3 and C5 and can cleave them in the corresponding anaphylatoxins C3a and C5a. The cleavage was enhanced when a posttraumatic environment was mimicked by HG. Furthermore, C3a was found in relatively high concentrations in the supernatant of hAC and cartilage explants. Traumatization of the explants had no effect on the C3a or C5a concentration found in the cartilage conditioned medium.

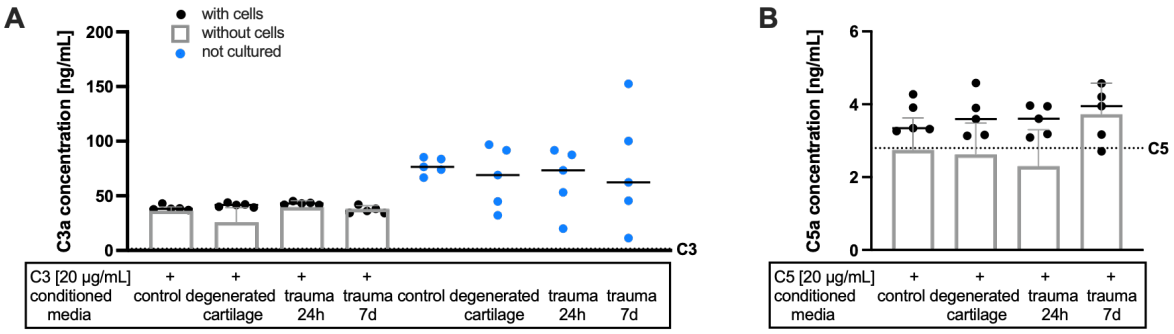

Figure 5: Results of cleavage assay after incubation of hAC with cartilage conditioned media. (A) C3a- and **(B)** C5a-ELISA. hAC were stimulated for 4 h with either 20 µg/mL C3 or 20 µg/mL C5 in cartilage conditioned media; n = 5. Median values are shown. Media derived from unimpacted controls, degenerated explants, and impacted (0.59 J) explants (24 h and 7 d after traumatization). Wells without cells served as control, indicated by a bar graph with median and range; n = 3. Blue dots indicate cartilage conditioned medium without further cultivation; n = 5. Median values are shown. Each datapoint represents an independent biological replicate.

3.2 Pro-osteogenic effects of C3a and C5a

In the first part of this thesis, it was shown that hAC are involved in the generation of the anaphylatoxins C3a and C5a, especially in a post-traumatic environment. However, so far it is unclear if and how the anaphylatoxins contribute to the degeneration of cartilage and thus play a role in OA pathogenesis. Previous studies indicated that calcification of blood vessels is associated with anaphylatoxins and the respective anaphylatoxin receptors C3aR and C5aR1 [89, 133, 144, 225]. Furthermore, cartilage calcification is associated with cartilage degeneration and is considered as a hallmark of OA [80]. Because of this, it was investigated if anaphylatoxins influence

mineralisation during osteogenic differentiation and how the anaphylatoxin receptors are expressed during osteogenic differentiation of hAC.

Osteogenic differentiation was performed in monolayer and hAC were cultured in ODM, supplemented with 50 or 1,000 ng/mL C3a, 50 ng/mL C5a, 10 μM SB290175, and/or 10 μM PMX53 (see 2.2.3.1). Cells cultured in BM served as undifferentiated, negative control. Successful osteogenic differentiation was evaluated on mRNA level after 7 and 14 days of differentiation. Gene expression analysis showed that the hypertrophic markers *ALPL* and *RUNX2* (**Figure 6 A, B**) were significantly upregulated after 7 (*ALPL*: $p = 0.017$; *RUNX2*: $p = 0.0008$) and 14 days (*ALPL*: $p = 0.049$; *RUNX2*: $p = 0.0045$), compared to undifferentiated control. Additionally, differentiation was evaluated by Alizarin Red S staining after 21 days (**Figure 6 C**). Quantification of Alizarin Red S staining confirmed successful osteogenic differentiation as well (**Figure 6 D**). Furthermore, when 1,000 ng/mL C3a ($p = 0.032$) or 50 ng/mL C5a ($p = 0.049$) was supplemented, a higher amount of Alizarin Red S was detected, indicating that calcium deposition during osteogenic differentiation increased (**Figure 6 C, D, E**). Simultaneous addition of either the C3aR inhibitor SB290175 or the C5aR1 inhibitor PMX53 reversed this effect, respectively. Moreover, PMX53 alone did also reduce the overall mineralisation during osteogenic differentiation compared to untreated control.

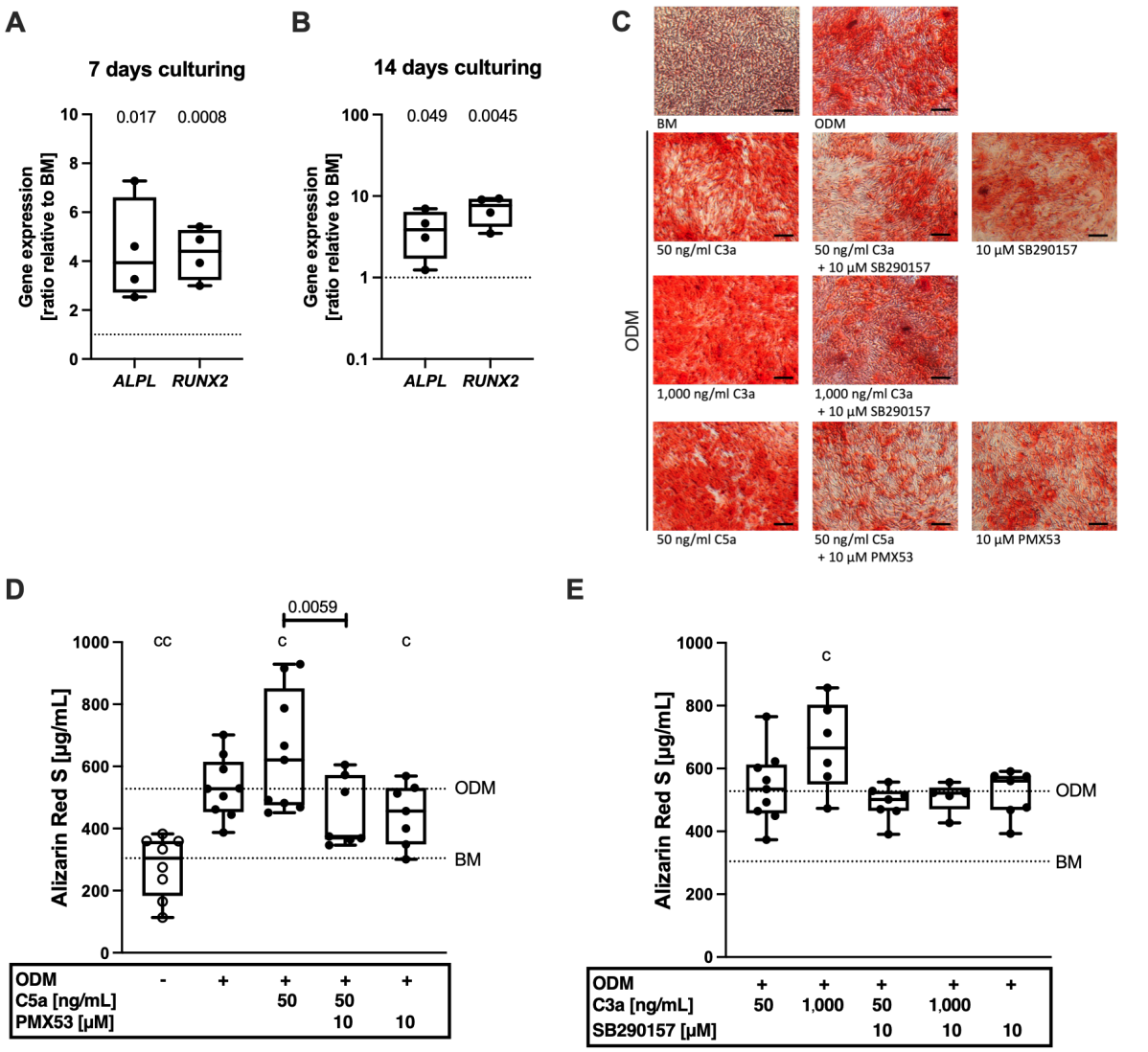

Figure 6: Evaluation of osteogenic differentiation of hAC. Cells were cultured in monolayer either in basal medium (BM) as negative control or in osteogenic differentiation medium (ODM) to induce osteogenic differentiation. Gene expression of *ALPL* and *RUNX2* was analysed via qRT-PCR after **(A)** 7 and **(B)** 14 days of osteogenic differentiation, normalised to undifferentiated cells cultured in BM; n = 4. Box plots show median with minimum to maximum whiskers. Unpaired two-tailed t test. **(C)** Exemplary images of osteogenic differentiated cells stained with Alizarin Red S. Calcification appears in red and scale bars represent 100 µm. **(D)** and **(E)** Alizarin Red S staining was carried out and quantified 21 days after osteogenic differentiation. 50 or 1,000 ng/mL C3a, 50 ng/mL C5a, 10 µM SB290157, and/or 10 µM PMX53 was added to ODM; n ≥ 5. Box plots show median with minimum to maximum whiskers. Mixed-effects analysis (D: Holm-Šidák´s correction; E: Šidák´s correction); multiple comparison vs. ODM: $^{C}p < 0.05$, $^{CC}p < 0.01$. Each datapoint represents an independent biological replicate. Figure has been modified from Ruths et al. 2024 [182]. Licensed under CC BY 4.0, https://creativecommons.org/licenses/by/4.0/.

Next, expression of both anaphylatoxin receptors was investigated during osteogenic differentiation. On mRNA level, expression of *C3AR* was significantly increased after 14 days ($p = 0.029$), while *C5AR1* expression was significantly induced after 7 ($p = 0.0012$) and 14 days ($p = 0.041$) of osteogenic differentiation (**Figure 7 A, B**). To verify this exemplarily on protein level, hAC were seeded on a CultureSlide and cultured in either BM or ODM for 14 days. Subsequently, an ICC staining was carried out with either an C3aR or C5aR1 antibody. As shown in **Figure 7 C**, cells cultured in BM had a low staining intensity for both receptors on the cell surface, indicated by a light red colour. Osteogenic differentiated hAC had in turn a high staining intensity. This was true for both receptors.

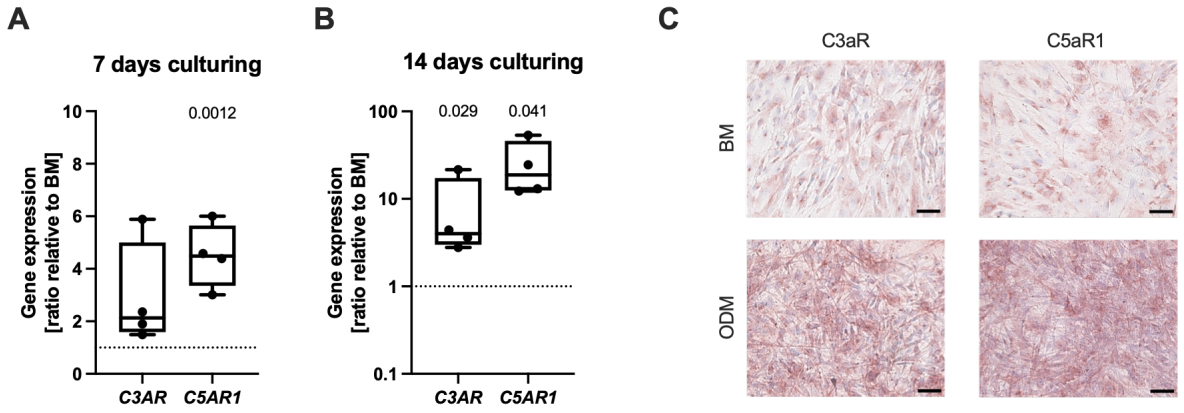

Figure 7: Gene and protein expression of C3aR and C5aR1 during osteogenic differentiation of hAC. mRNA levels of *C3AR* and *C5AR1* after osteogenic differentiation with osteogenic differentiation medium (ODM) for **(A)** 7 or **(B)** 14 days, normalised to basal medium (BM); n = 4. Box plots show median with minimum to maximum whiskers. Unpaired two-tailed t test, for *C3AR* (14 days): Mann-Whitney test. Each datapoint represents an independent biological replicate. **(C)** Exemplary images of hAC cultured in either BM or ODM for 14 days and following C3aR- and C5aR1-ICC. Scale bars represent 100 µm. Figure has been modified from Ruths et al. 2024 [182]. Licensed under CC BY 4.0, https://creativecommons.org/licenses/by/4.0/.

Additionally, gene expression of *ALPL*, *RUNX2*, *C3AR*, and *C5AR1* was analysed in osteogenic differentiated hAC in presence of anaphylatoxins and/or anaphylatoxin receptor inhibitors. However, neither expression of the hypertrophic markers, nor expression of the anaphylatoxin receptors were altered after 7 or 14 days of osteogenic differentiation (**Figure 8**).

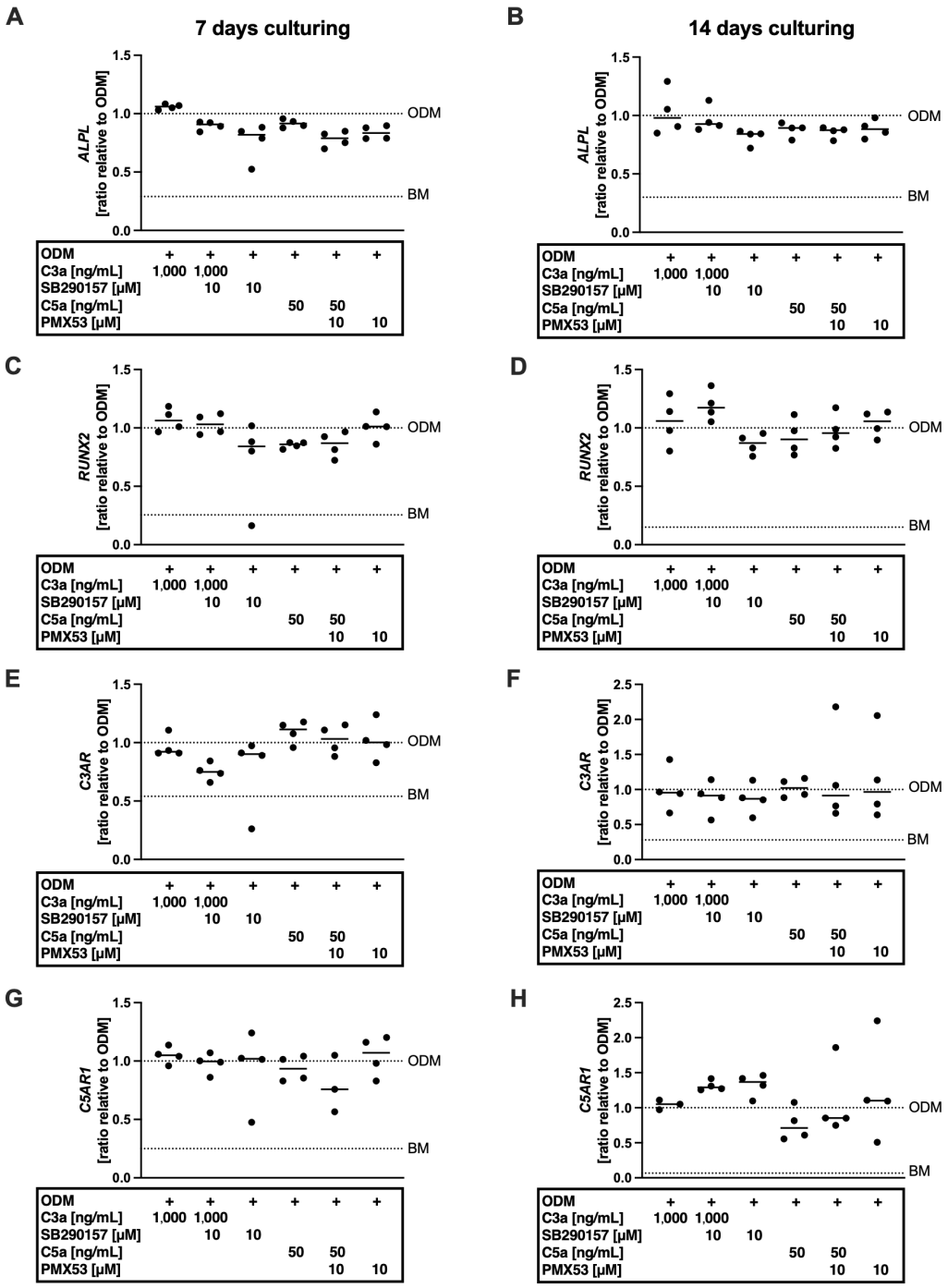

Figure 8: Gene expression of osteogenic differentiated hAC. hAC were cultured for **(A, C, E, and G)** 7 or **(B, D, F, and H)** 14 days in osteogenic differentiation medium (ODM), supplemented with 50 or 1,000 ng/mL C3a, 50 ng/mL C5a, 10 µM SB290157, and/or 10 µM PMX53. mRNA levels of **(A, B)** *ALPL*, **(C, D)** *RUNX2*, **(E, F)** *C3AR*, and **(G, H)** *C5AR1* were normalised to ODM; n = 4. Median values are shown. BM = basal medium. Each datapoint represents an independent biological replicate. Figure has been modified from Ruths et al. 2024 [182]. Licensed under CC BY 4.0, https://creativecommons.org/licenses/by/4.0/.

Furthermore, it was evaluated if pro-osteogenic effects can be observed in cartilage-embedded hAC which are cultured *ex vivo* in the presence of either C3a or C5a. Cartilage explants, isolated from macroscopically intact human cartilage, were stimulated in SFM for 4 days with either 1,000 ng/mL C3a or 50 ng/mL C5a *ex vivo*. Gene expressions analysis revealed that *RUNX2* and *ALPL* were induced by anaphylatoxin exposition, but statistical significance was missed (**Figure 9 A, B**). The fibrocartilage and bone matrix marker *COL1A1* [114] was upregulated by 1,000 ng/mL C3a (**Figure 9 C**). However, *COL10A1* and *SP7*, both hypertrophic markers, were not affected by the presence of anaphylatoxins (**Figure 9 D, E**).

Overall, this data indicates that not only anaphylatoxins, but also the corresponding receptors, might be involved in mineralisation processes.

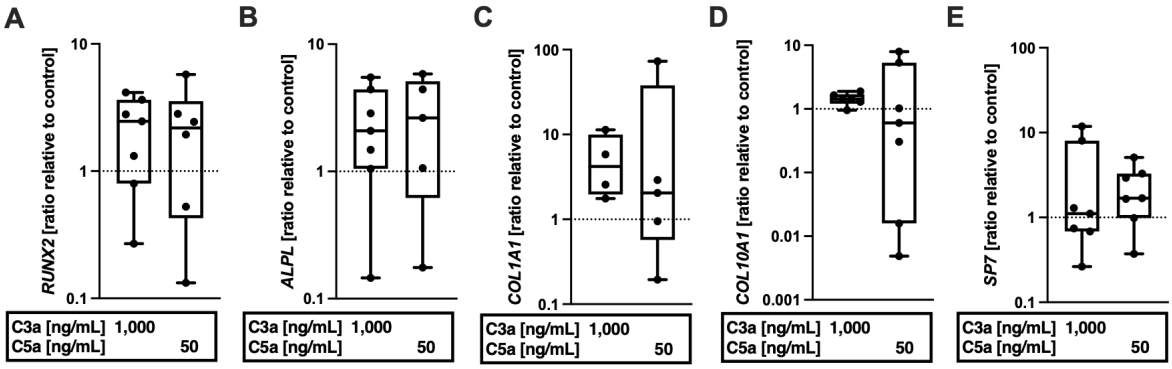

Figure 9: Gene expression of human cartilage explants. Explants were cultured *ex vivo* in serum free medium for 4 days and 1,000 ng/mL C3a or 50 ng/mL C5a were added as indicated. mRNA levels of **(A)** *RUNX2*, **(B)** *ALPL,* **(C)** *COL1A1,* **(D)** *COL10A1,* and **(E)** *SP7* were normalised to untreated control; n ≥ 4. Box plots show median with minimum to maximum whiskers. Each datapoint represents an independent biological replicate. Figure has been modified from Ruths et al. 2024 [182]. Licensed under CC BY 4.0, https://creativecommons.org/licenses/by/4.0/.

3.3 Influence of C3a and C5a on chondrogenic differentiation of hAC

Next, it was investigated if the inflammatory peptides C3a and C5a influence the regeneration potential of hAC und thus affect the chondrogenic phenotype. Therefore, a chondrogenic differentiation was carried out (see 2.2.3.2). hAC were cultured in a 3D-

pellet culture in either BM as negative control or chondrogenic differentiation medium (CDM). After 28 days, resulting cell pellets were embedded in paraffin and differentiation was evaluated based on Safranin O staining (**Figure 10 A**) and collagen type II IHC (**Figure 10 B**) and an overall score was calculated (**Figure 10 C, D**). The additives C5a, SB290175, and PMX53 did not alter the overall score. However, 50 ng/mL C3a had a positive effect on the chondrogenic differentiation, while 1,000 ng/mL decreased the overall score significantly ($p = 0.0073$). Since it is known, that inflammation interferes with chondrogenesis [214], mRNA levels of the cytokines *CXCL1*, *IL6*, and *IL8* were analysed in cartilage explants stimulated with either 1,000 ng/mL C3a or 50 ng/mL C5a (**Figure 11 A-C**). *CXCL1* expression was neither affected by C3a nor C5a stimulation. Both, *IL8* ($p = 0.0009$) and *IL6* ($p = 0.0069$), were upregulated in presence of C3a. On protein level, IL-6 was upregulated after C3a stimulation by trend (**Figure 11 D**). C5a had no significant effect on *IL8* or *IL6* expression.

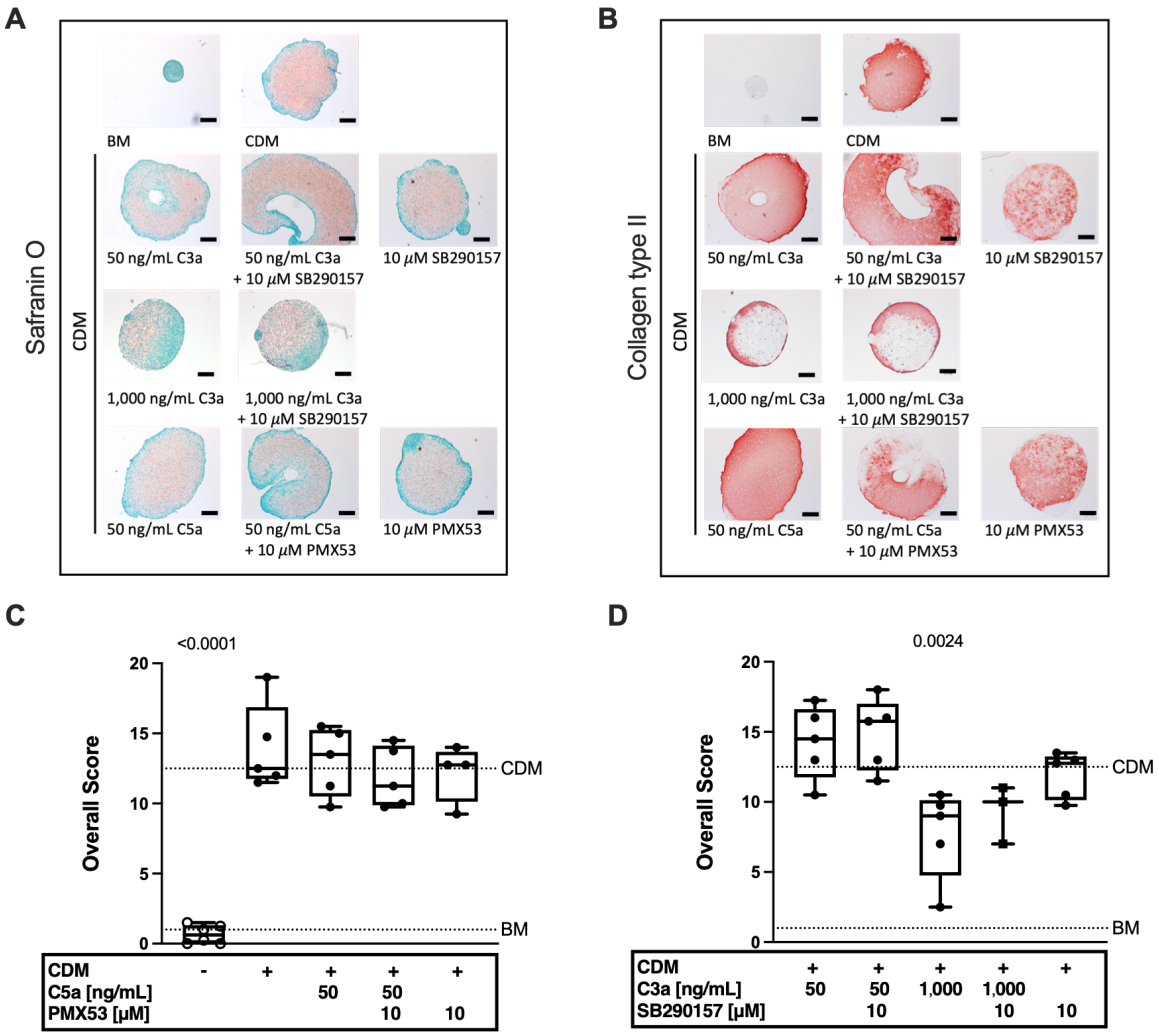

Figure 10: Assessment of chondrogenic differentiation of hAC. For differentiation, cells were cultured in a pellet in chondrogenic differentiation medium (CDM) in presence of 50 or 1,000 ng/mL C3a, 50 ng/mL C5a, 10 µM SB290157, and/or 10 µM PMX53 for 28 days. Cell pellets cultured in basal medium (BM) served as negative control. Neo-cartilage formation was assessed by pellet size (diameter), collagen type II/Safranin O staining intensity, matrix production and cell morphology. **(A)** Exemplary images of Safranin O-stained cell pellets. Cytoplasm is stained green and sulphated glycosaminoglycans are stained red, indicating cartilage production. **(B)** Exemplary images of collagen type II-stained cell pellets via IHC. Positive staining is indicated in red. Scale bars represent 200 µm. The resulting overall score is visualised in **(C)** and **(D)**; n ≥ 3. Box plots show median with minimum to maximum whiskers. One-way ANOVA, Dunnett´s correction, multiple correction vs. CDM. Each datapoint represents an independent biological replicate. Figure has been modified from Ruths et al. 2024 [182]. Licensed under CC BY 4.0, https://creativecommons.org/licenses/by/4.0/.

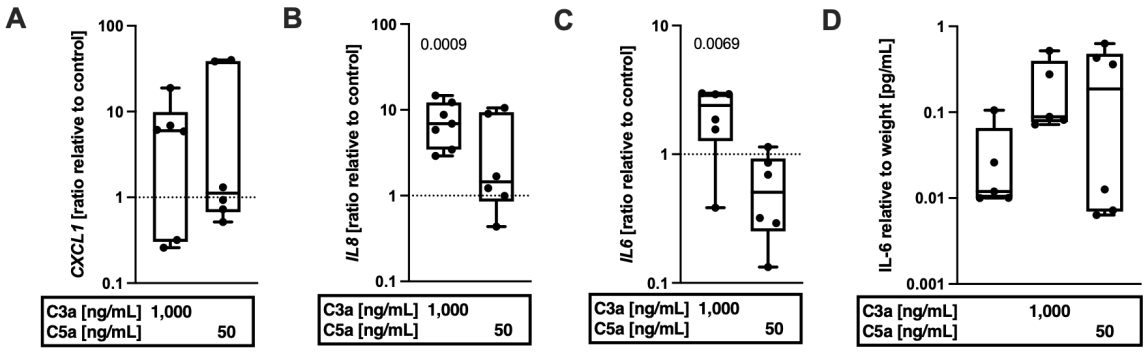

Figure 11: Gene and protein expression of human cartilage explants. Cartilage explants were cultured *ex vivo* in serum free medium for 4 days in presence of either 1,000 ng/mLC3a or 50 ng/mL C5a. Gene expression of **(A)** *CXCL1*, **(B)** *IL8*, and **(C)** *IL6* was evaluated via qRT-PCR. mRNA levels were normalised to untreated control; n ≥ 6. Box plots show median with minimum to maximum whiskers. One-way ANOVA, Šidák´s correction. **(D)** IL-6 levels of supernatants were evaluated via ELISA, n ≥ 5. Box plot shows median with minimum to maximum whiskers. Each datapoint represents an independent biological replicate. Figure has been modified from Ruths et al. 2024 [182]. Licensed under CC BY 4.0, https://creativecommons.org/licenses/by/4.0/.

It was also analysed whether the cell pellets show characteristics of cartilage calcification or of a hypertrophic phenotype after chondrogenic differentiation. Alizarin Red S staining revealed that none of the pellets were mineralised (**Figure 12 A**) and collagen type X IHC was found negative (**Figure 12 B**). The growth zone of a foetal knee served as positive control of collagen type X (**Figure 12 C**). In contrast to the osteogenic differentiation, both anaphylatoxin receptors were not detected in the cell pellets (**Figure 12 D, E**). The IgG control was also found negative (**Figure 12 F**).

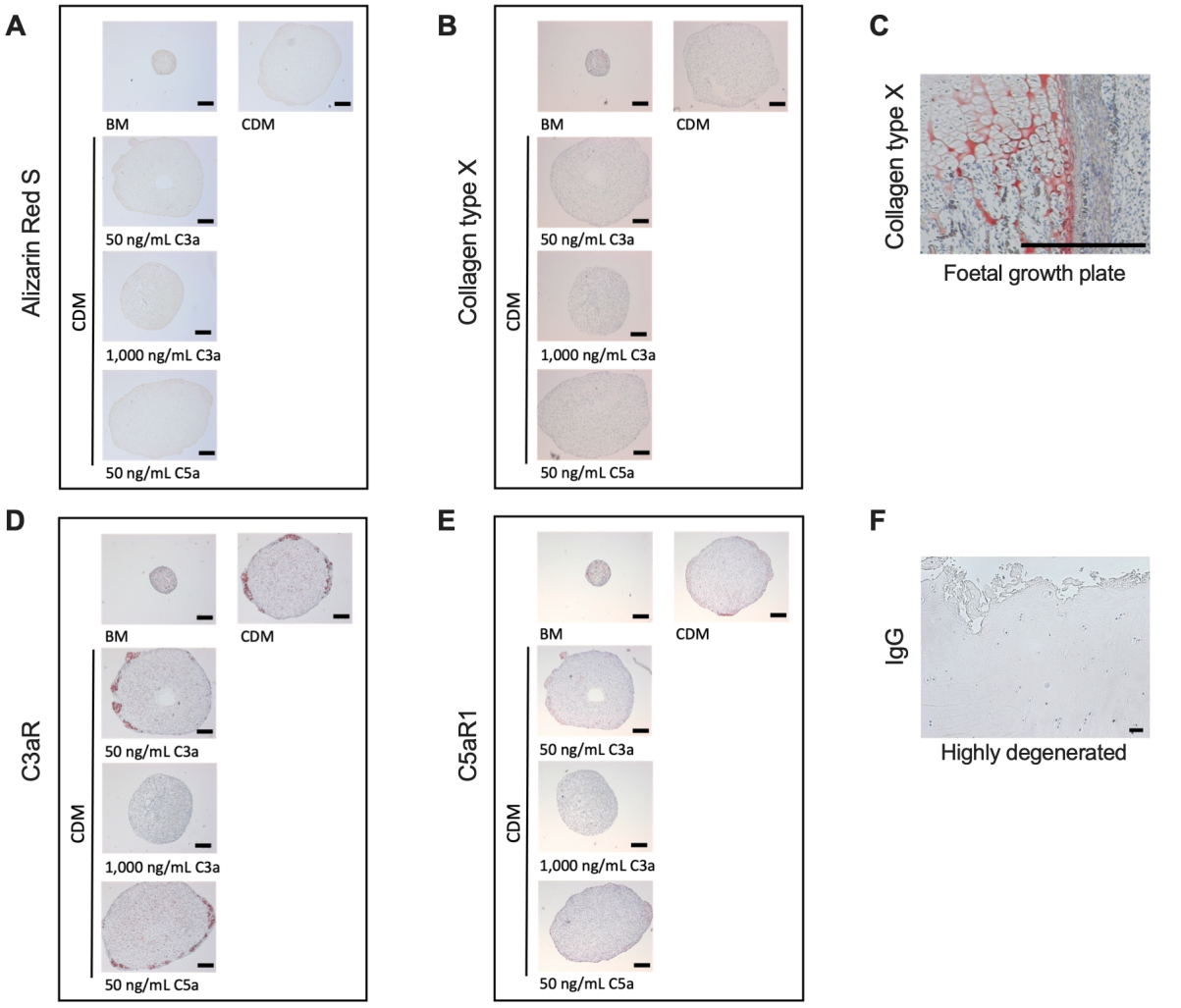

Figure 12: Histology of cell pellets after chondrogenic differentiation of hAC. Cells were cultured for 28 days in basal medium (BM) as negative control or in chondrogenic differentiation medium (CDM) supplemented with 50 or 1,000 ng/mL C3a, 50 ng/mL C5a, 10 µM SB290157, and/or 10 µM PMX53. Light microscope images of **(A)** Alizarin Red S-stained cells pellets and **(B, C)** IHC of collagen type X, (**D)** C3aR, and **(E)** C5aR1. An **(F)** IgG control was included. Scale bars represent 200 µm. Figure has been modified from Ruths et al. 2024 [182]. Licensed under CC BY 4.0, https://creativecommons.org/licenses/by/4.0/.

3.4 Trans-differentiation of hAC

Usage of primary hAC *in vitro* has various limitations. One is that hAC lose their chondrogenic phenotype in 2D-culture quite fast. They change from a polygonal, cobblestone to a flattened, elongated morphology and dedifferentiated hAC express

mainly collagen type I instead of collagen type II [15, 138, 218]. Consequently, hAC previously used in the osteogenic (see 3.2) and chondrogenic differentiation (see 3.3) in passage 3 or higher can be considered as dedifferentiated. In the following experiment, hAC were at first re-differentiated towards a chondrogenic phenotype by cultivate them in CDM for 7 days. Subsequently, medium was replaced by ODM (+ BMP-2) to evaluate whether the osteogenic differentiation is in this set-up altered by the addition of anaphylatoxins or anaphylatoxin receptor inhibitors (see 2.2.3.3). The experimental scheme is depicted in **Figure 13 A**. Chondrogenic differentiation was confirmed by means of Alcian blue staining (**Figure 13 B**). In this experiment, chondrogenic differentiation was not affected by the stimulation with C3a, C5a, SB290157, or PMX53. In contrast to the sole osteogenic differentiation, calcification during osteogenic differentiation, assessed by Alizarin Red S staining, after chondrogenic differentiation was not influenced by the presence of anaphylatoxins or receptor inhibitors. This was true when additives were supplemented only during osteogenic differentiation (**Figure 13 C**) and when they were additionally supplemented during chondrogenic differentiation (**Figure 13 D**). To evaluate, if these observed discrepancies are due to the preceding chondrogenic differentiation, a modified osteogenic differentiation protocol was applied (see 2.2.3.1), which was based on the trans-differentiation protocol. In this case, hAC were cultured the first 7 days in BM, which was replaced by ODM (+ BMP-2) for the following 10 days (**Figure 14 A**). The culture time in ODM had to be increased to achieve a successful osteogenic differentiation. (**Figure 14 B**). In this case, 50 ng/mL C5a increased ($p = 0.031$) and 10 μM PMX53 ($p = 0.0045$) reduced the mineralisation during osteogenic differentiation significantly.

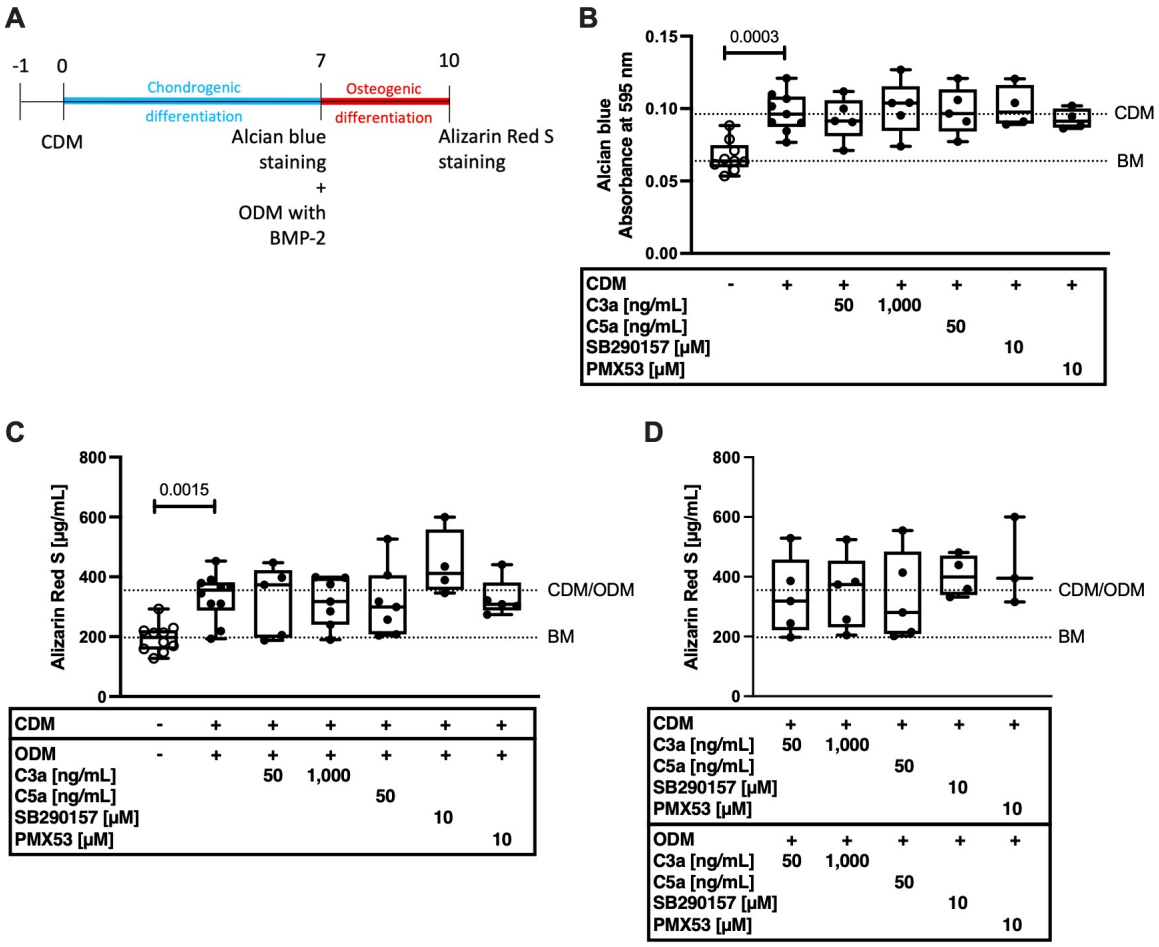

Figure 13: Evaluation of trans-differentiation of hAC. hAC were cultured in monolayer for 7 days in chondrogenic differentiation medium (CDM), followed by 3 days incubation in osteogenic differentiation medium (ODM) supplemented with 100 ng/mL BMP-2. 50 or 1,000 ng/mL C3a, 50 ng/mL C5a, 10 µM SB290157, and 10 µM PMX was added as indicated. Cells cultured in basal medium (BM) served as negative control. **(A)** Scheme of trans-differentiation protocol. **(B)** Chondrogenic differentiation was assessed by Alcian blue staining; n ≥ 4. Box plot shows median with minimum to maximum whiskers. Mixed-effects analysis, Dunnett´s correction. **(C)** and **(D)** osteogenic differentiation was assessed by means of Alizarin Red S staining; n ≥ 3. Box plots show median with minimum to maximum whiskers. Mixed-effects analysis, Dunnett´s correction. Each datapoint represents an independent biological replicate. Figure has been modified from Ruths et al. 2024 [182]. Licensed under CC BY 4.0, https://creativecommons.org/licenses/by/4.0/.

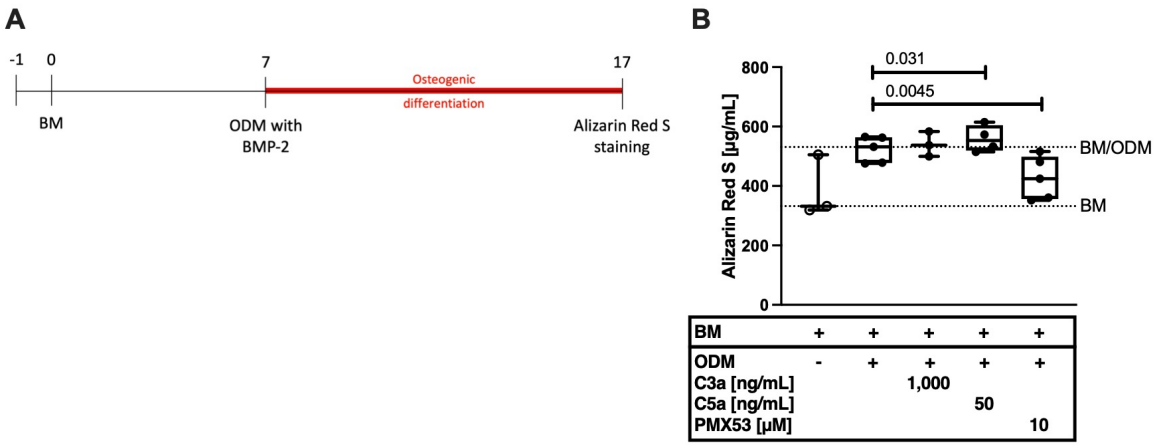

Figure 14: Assessment of osteogenic differentiation with modified protocol. hAC were cultured in monolayer for 7 days in basal medium (BM), followed by 10 days in osteogenic differentiation medium (ODM) supplemented with 100 ng/mL BMP-2. 1,000 ng/mL C3a, 50 ng/mL C5a, and 10 µM PMX53 was added as indicated. **(A)** Scheme of modified differentiation protocol. **(B)** Quantification of Alizarin Red S staining; n ≥ 3. Box plot shows median with minimum to maximum whiskers. Mixed-effects analysis, Holm-Šidák´s correction. Each datapoint represents an independent biological replicate. Figure has been modified from Ruths et al. 2024 [182]. Licensed under CC BY 4.0, https://creativecommons.org/licenses/by/4.0/.

Another difference of the trans-differentiation and the previously carried out osteogenic differentiation (see 3.2) is the addition of 100 ng/mL BMP-2 into ODM. BMP-2 is known to be a pro-hypertrophic growth factor and induces differentiation of MSC into hypertrophic chondrocytes [3, 203]. Thus, it is feasible that the pro-osteogenic effects of BMP-2 are very strong and the inductive effects of C3a and C5a vanish in comparison. To exclude this, trans-differentiation and the modified osteogenic differentiation were carried out without addition of BMP-2 (**Figure 15 A, B**). However, similar results were observed. With a preceding chondrogenic differentiation, addition of 1,000 ng/mL C3a, 50 ng/mL C5a, or 10 µM PMX53 did not alter the osteogenic differentiation (**Figure 15 C**). Without a preceding chondrogenic differentiation, a positive trend was found for C5a and a negative trend for PMX53 (**Figure 15 D**).

These findings suggest that dedifferentiation, resulting from hAC cultivation, leads to a more sensitive response to anaphylatoxins regarding mineralisation processes during osteogenic differentiation.

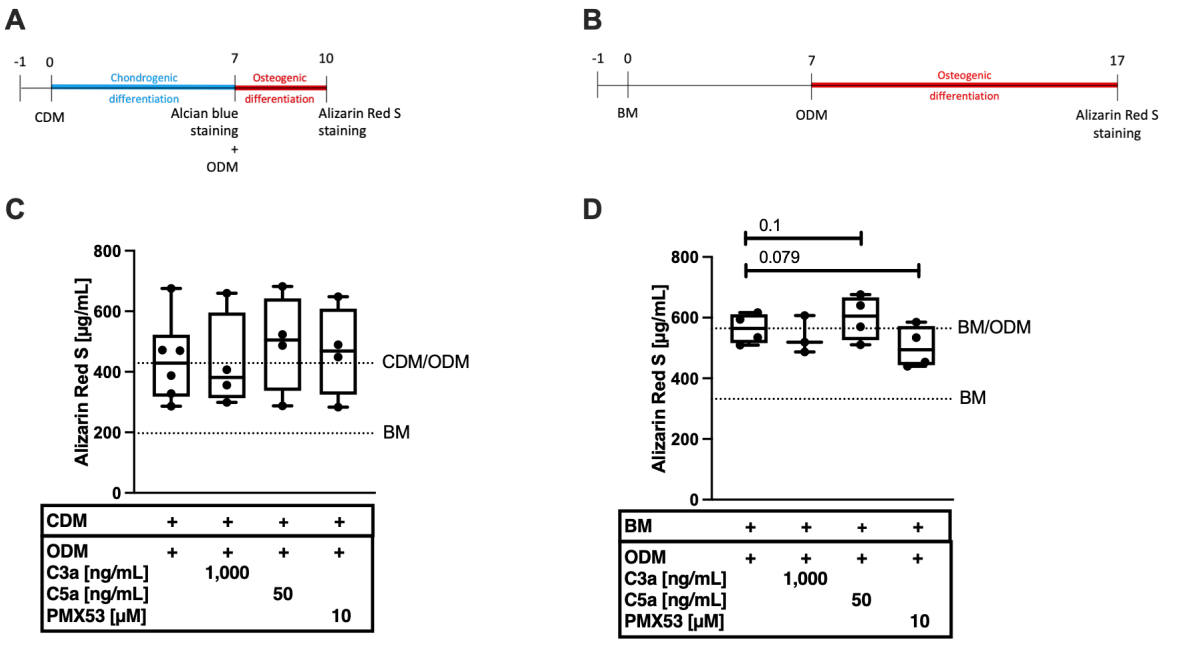

Figure 15: (Trans-)differentiation of hAC without addition of BMP-2 during osteogenic differentiation. (A) Scheme of trans-differentiation protocol. hAC were cultured in monolayer for 7 days in chondrogenic differentiation medium (CDM), followed by 3 days incubation in osteogenic differentiation medium (ODM). 1,000 ng/mL C3a, 50 ng/mL C5a, and 10 µM PMX was added as indicated. **(B)** Scheme of modified differentiation protocol. hAC were cultured for 7 days in basal medium (BM) and subsequently cultured for 10 days in ODM. **(C)** Quantification of Alizarin Red S staining after trans-differentiation at day 10; n ≥ 4. Box plot shows median with minimum to maximum whiskers. **(D)** Quantification of Alizarin Red S staining at day 17; n ≥ 3. Box plot shows median with minimum to maximum whiskers. Mixed-effects analysis, Dunnett´s correction. Each datapoint represents an independent biological replicate.

3.5 Impact of anaphylatoxins on osteogenic differentiation of stem cells

Previous research provided evidence that hAC are not the only cell type found in hyaline cartilage. Another cell population called CSPC are the cartilage tissue's own stem cells [217]. Furthermore, it is stated that BM-MSC migrate from the subchondral bone through breaks of the tidemark into OA cartilage tissue [52, 93]. Thus, both cell types might contribute to cartilage calcification. An osteogenic differentiation was performed in monolayer with isolated CSPC and BM-MSC for 21 days. ODM was supplemented with 500 ng/mL C3a, 50 ng/mL C5a, 10 µM SB290175, and/or 10 µM

PMX5. Afterwards, cells were stained with Alizarin Red S (**Figure 16 A, B**). Osteogenic differentiation was confirmed for both cell types (**Figure 16 C, D**), but differentiation was more efficient in BM-MSC (median: 800 µg/mL Alizarin Red S) compared to CSPC (median: 492 µg/mL Alizarin Red S) and hAC (median: 504 µg/mL Alizarin Red S) (**Figure 6**). However, addition of anaphylatoxins had no influence on the Alizarin Red S staining intensity.

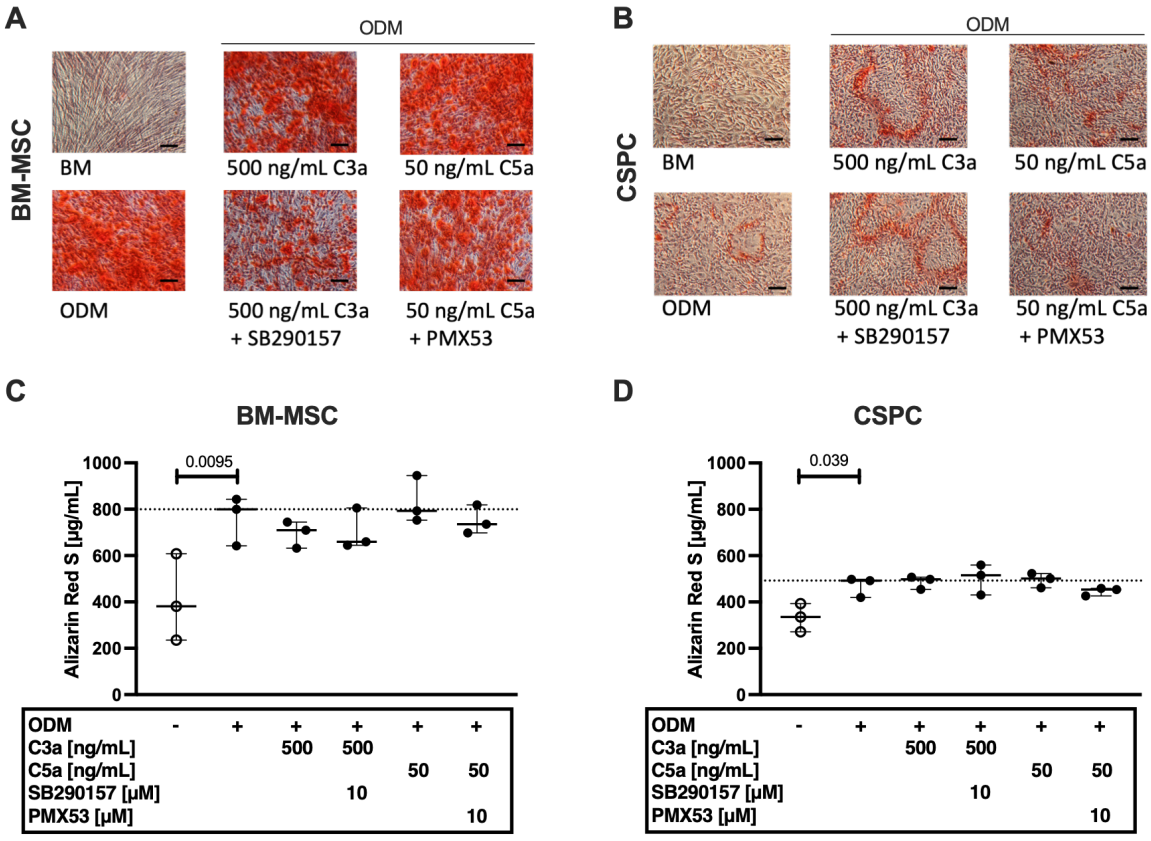

Figure 16: Osteogenic differentiation of BM-MSC and CSPC. Cells were cultured in monolayer in osteogenic differentiation medium (ODM) for 21 days. ODM was supplemented with 500 ng/mL C3a, 50 ng/mL C5a, 10 µM SB290157, and/or 10 µM PMX. As negative control, BM-MSC and CSPC were cultured in basal medium (BM). Exemplary images of osteogenic differentiated **(A)** BM-MSC and **(B)** CSPC stained with Alizarin Red S. Calcification appears in red and scale bars represent 100 µm. Osteogenic differentiation of **(C)** BM-MSC and **(D)** CSPC was assessed by Alizarin Red S staining; n = 3. Median values with 95% confidence intervals are shown. One-way ANOVA, Šidák´s correction. Each datapoint represents an independent biological replicate. Figure has been modified from Ruths et al. 2024 [182]. Licensed under CC BY 4.0, https://creativecommons.org/licenses/by/4.0/.

3.6 Expression of C3aR and C5aR1 in cartilage tissue and isolated hAC, BM-MSC, and CSPC

Next, anaphylatoxin receptors C3aR and C5aR1 were further investigated to unravel their potential role in OA progression, especially their role in top-down calcification of hyaline cartilage. At first, macroscopically intact and highly degenerated human cartilage was compared and elevated mRNA levels of both genes (*C3AR*: p = 0.043; *C5AR1*: p = 0.044) were found in degenerated cartilage tissue (**Figure 17 A**). This was confirmed on protein level (**Figure 17 B-E**). Significant more cells were positively stained for C3aR (p = 0.0006) and C5aR1 (p = 0.0004) in the analysed regions of highly degenerated cartilage tissue compared to intact tissue. In macroscopically intact human cartilage tissue, about 4.9% (C3aR) and 15.4% (C5aR1) of the cells were positively stained. In degenerated tissue, about 77,5% (C3aR) and 46,15% (C5aR1). An association between the age of the donors and the percentage of positive cells was not detected (**Figure 17 F**).

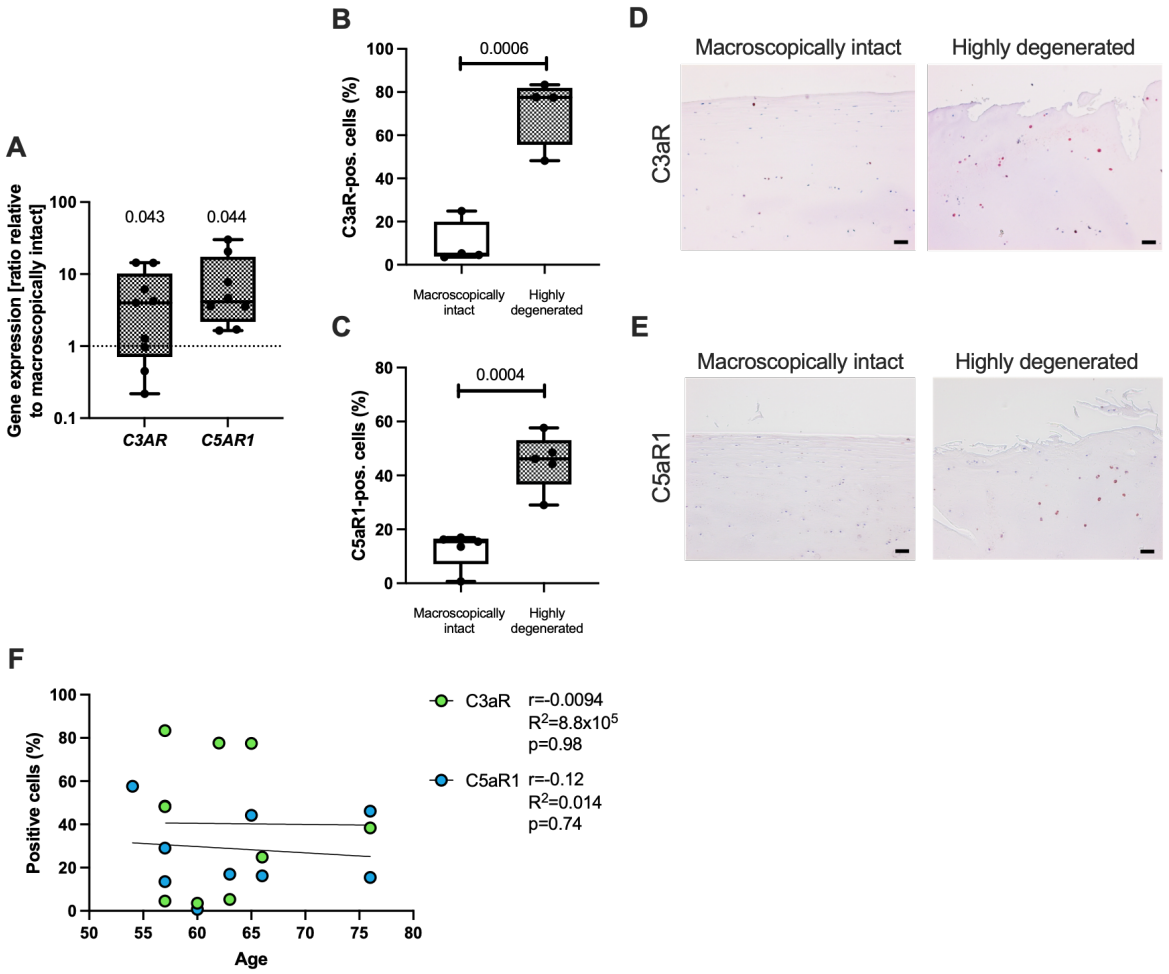

Figure 17: Gene and protein expression of C3aR and C5aR1 in human articular cartilage tissue. (A) mRNA level of *C3AR* and *C5AR1* in highly degenerated cartilage tissue (OARSI grade ≥ 3). Normalised to macroscopically intact cartilage tissue (OARSI grade ≤ 1); n ≥ 8. Box plot shows median with minimum to maximum whiskers. Unpaired two-tailed t test. Quantified IHC staining of **(B)** C3aR and **(C)** C5aR1 in the superficial zone and the upper part of the middle zone (about 0.5-0.6 mm) of human cartilage tissue; C3aR: n = 4; C5aR1: n = 5. Box plots show median with minimum to maximum whiskers. Unpaired two-tailed t test. Exemplary images of **(D)** C3aR and **(E)** C5aR1 IHC of human cartilage. Positive cells are indicated in red. Scale bars represent 50 μm. **(F)** Pearson correlation analysis (with 95% confidence intervals) of age of the donors and percentage of C3aR- and C5aR1-positive cells. Each datapoint represents an independent biological replicate. Figure has been modified from Ruths et al. 2024 [182]. Licensed under CC BY 4.0, https://creativecommons.org/licenses/by/4.0/.

To clarify, if the responsiveness towards anaphylatoxin treatment is due to a different expression profile of the corresponding receptors in BM-MSC, CSPC or hAC, the percentage of C3aR- and C5aR1-positive cells was analysed via flow cytometry *in vitro*. Prior flow cytometry analysis, cells are detached either with trypsin/EDTA or 5 mM EDTA alone (**Figure 18 A**). This was carried out to exclude that the protease trypsin digests the anaphylatoxin receptors. Depending on the cell type and analysed receptor, 3- to 5-fold more cells were positively stained when detached with 5 mM EDTA solution. Consequently, EDTA solution was used for further flow cytometric analysis. Next, the amount of C3aR- and C5aR1-positive BM-MSC, CSPC and hAC was analysed in similar passages (**Figure 18 B**). Overall, significant more BM-MSC were positive for C3aR (vs. CSPC: p = 0.0004; vs. hAC: p < 0.0001) and C5aR1 (vs. CSPC: p = 0.0007; vs. hAC: p < 0.0001), compared to cartilage-derived cells.

A

	C3aR-pos. cells (%)		C5aR1-pos. cells (%)	
	Trypsin/ EDTA	EDTA	Trypsin/ EDTA	EDTA
hAC	3.5	14.0	8.4	22.4
BM-MSC	5.1	25.4	16.5	66.1

B

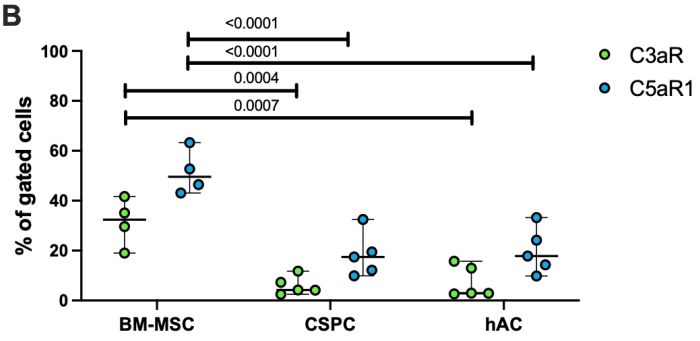

Figure 18: Analysis of C3aR and C5aR1 expression of BM-MSC, CSPC, and hAC by means of flow cytometry. (A) Percentage of cells which were found positive for the anaphylatoxin receptors when detached either with trypsin/EDTA or 5 mM EDTA solution; n = 1. **(B)** C3aR and C5aR1 expression on the cell surface of BM-MSC, CSPC or hAC in comparable passages, cultured in the respective medium and detached with 5 mM EDTA solution; n ≥ 4. Median values with 95% confidence intervals are shown. One-way ANOVA, Šidák´s correction. Each datapoint represents an independent biological replicate. Figure has been modified from Ruths et al. 2024 [182]. Licensed under CC BY 4.0, https://creativecommons.org/licenses/by/4.0/.

Furthermore, expression of C3aR and C5aR1 was investigated in hAC in more detail *in vitro*. On mRNA level, *C3AR* gene expression did not differ between passage 1 to 5 (**Figure 19 A**). In case of *C5AR1* gene expression, a negative association (p = 0.004) between passage number and *C5AR1* expression was observed (**Figure 19 B**). In contrast to the gene expression of *C3AR*, flow cytometry analysis revealed that hAC in

passage 0 expressed C3aR more frequently on the cell surface (**Figure 19 C**), compared to cells in passage 2 ($p = 0.012$) and passage 4 ($p = 0.0001$). The same was true for C5aR1 (**Figure 19 D**). The percentage of C5aR1-positive cells declined during cultivation (passage 0 vs. passage 2: $p = 0.0099$; passage 0 vs. passage 4: $p = 0.0026$).

To evaluate if both receptors are found intracellularly, hAC were permeabilised with 0.5% Tween-20 prior to the flow cytometry staining. In this case, almost all hAC were found positive for C3aR and C5aR1, respectively (**Figure 19 E, F**). This was observed independent of the passage. Additionally, this was confirmed with hAC stained via ICC in adherence (**Figure 19 G**).

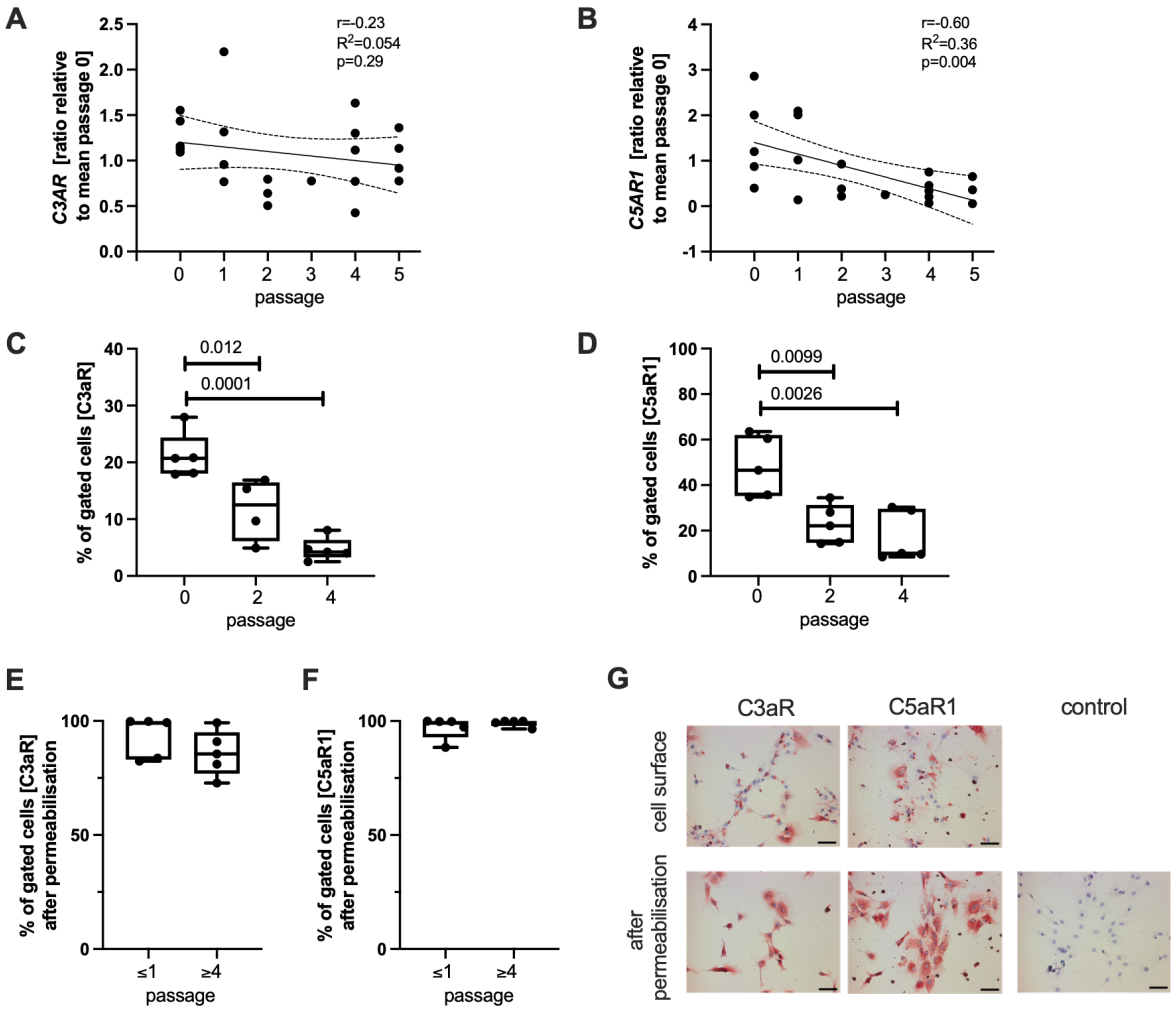

Figure 19: Gene and protein expression of C3aR and C5aR1 of isolated hAC. Gene expression of **(A)** *C3AR* and **(B)** *C5AR1* was correlated with the passage number. mRNA expression was normalised to mean ΔCt value of passage 0; n = 21. Donors were measured at various passages. Pearson correlation analysis (with 95% confidence intervals). Flow cytometry analysis of **(C)** C3aR and **(D)** C5aR1 expression on the cell surface of hAC in passage 0, 2, and 4, cultured in chondrocyte BM and detached with 5 mM EDTA solution; n ≥ 4. Box plots show median with minimum to maximum whiskers. One-way ANOVA, Tukey´s correction. Presence of intracellular **(E)** C3aR and **(F)** C5aR1, analysed via flow cytometry. hAC were cultured in chondrocyte BM, detached with 5 mM EDTA and permeabilised with 0.5% Tween-20 prior staining; n = 5. Box plots show median with minimum to maximum whiskers. Each datapoint represents an independent biological replicate. **(G)** Representative images of C3aR and C5aR1 stained hAC by means of ICC. Cells were partially permeabilised with 0.01% Brij. Scale bars represent 50 μm. Figure has been modified from Ruths et al. 2024 [182]. Licensed under CC BY 4.0, https://creativecommons.org/licenses/by/4.0/.

3.7 Association of C3aR and C5aR1 expression and calcification processes

In the beginning of this thesis, it was shown that the anaphylatoxin receptors C3aR and C5aR1 are upregulated during osteogenic differentiation (see 3.2). Furthermore, flow cytometry revealed that many BM-MSC were positive for both receptors on the cell surface (see 3.6) and osteogenic differentiation was comparable stronger (see 3.5) than differentiation of cartilage derived cells (see 3.2), expressing the receptors to a lesser extent (see 3.6). Thus, in this paragraph, a connection between C3aR and C5aR1 expression and cartilage calcification was investigated in more detail *in vitro* and *ex vivo*. At first, the percentage of C3aR- and C5aR1-positive hAC of each individual donor was determined by means of flow cytometry. Simultaneously, the donors were used for an osteogenic differentiation. Calcification was assessed after 21 days by Alizarin Red S staining and the detected amount of Alizarin Red S was correlated with determined percentage of C3aR or C5aR1-positive cells (**Figure 20 A, B**). In both cases, a positive association between receptor expression and Alizarin Red S staining intensity after osteogenic differentiation was found. This is also nicely shown by the exemplary images of Alizarin Red S-stained cells together with the corresponding percentage of C3aR and C5aR1-positive hAC (**Figure 20 C**). Next, clinical samples (OARSI grade 0-4) were used for an Alizarin Red S staining and von Kossa staining to evaluate mineralisation within the upper part of the cartilage tissue (about 0.5 – 0.6 mm). These staining were used to establish a calcification score as shown in **Figure 20 D** (0 = no staining, 1 = weak staining, 2 = frequent staining). Also, this data demonstrated a positive association between cartilage calcification and the protein expression of C3aR ($p = 0.006$) and C5aR1 ($p = 0.013$), determined by IHC (**Figure 20 E, F**).

Overall, these results imply that higher expression of C3aR and C5aR1 is associated with an increased mineralisation during osteogenic differentiation and in cartilage tissue.

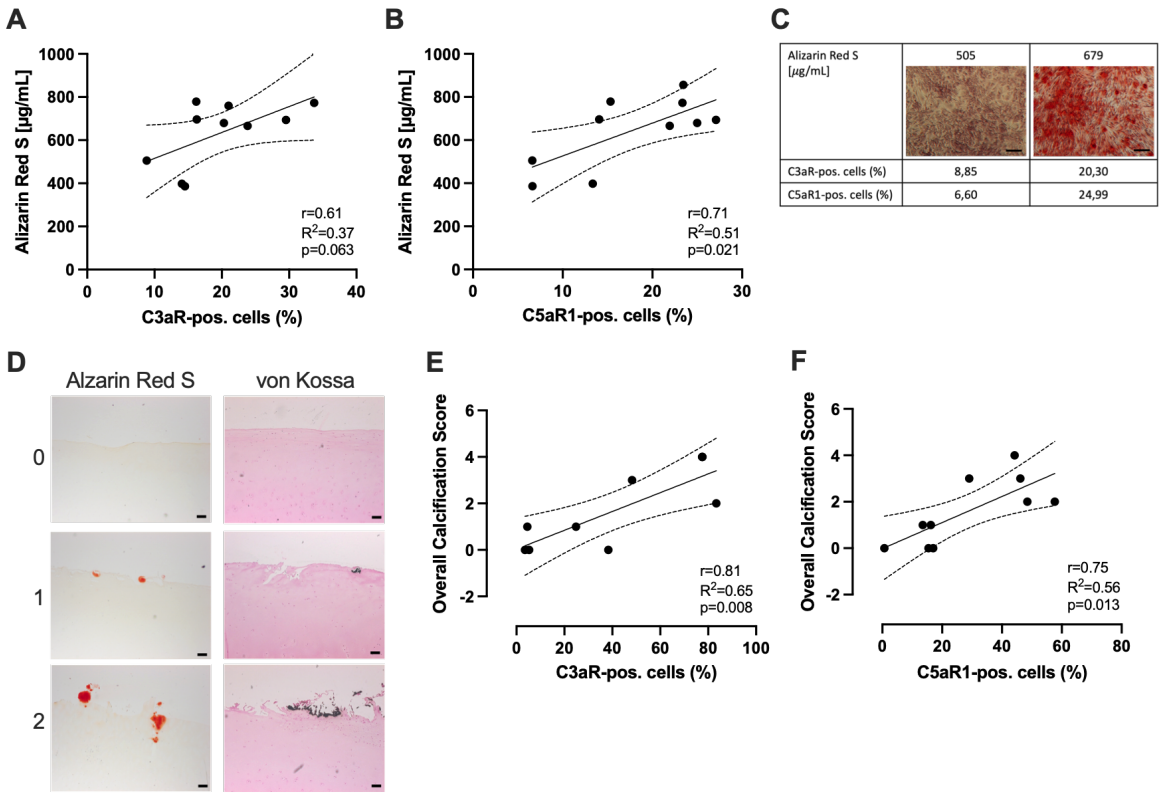

Figure 20: Correlation of C3aR and C5aR1 expression and mineralisation. Anaphylatoxin receptor expression on the surface of hAC was analysed by means of flow cytometry. Simultaneously, an osteogenic differentiation was carried out with the same donors by incubating hAC in monolayer for 21 days in osteogenic differentiation medium. Calcification during osteogenic differentiation was evaluated via Alizarin Red S staining. Resulting Alizarin Red S values were correlated with the percentage of **(A)** C3aR- and **(B)** C5aR1-positve cells; n = 10. Pearson correlation analysis (with 95% confidence intervals). **(C)** Representative images of Alizarin Red S-stained hAC with corresponding Alizarin Red S values and number of C3aR- and C5aR1-positive cells. Calcification is indicated in red. Scale bars represent 100 µm. **(D)** Representative images of human cartilage explants, stained with either Alizarin Red S (calcification in red) or von Kossa (calcification in black). Mineralisation was scored in the upper part of the cartilage tissue (0.5 – 0.6 mm) the following: 0 = no staining, 1 = weak staining, 2 = frequent staining. Scale bars represent 50 µm. Calculated overall calcification score was correlated with the **(E)** C3aR and **(F)** C5aR1 expression, assessed by IHC; n ≥ 9. Pearson correlation analysis (with 95% confidence intervals). Each datapoint represents an independent biological replicate. Figure has been modified from Ruths et al. 2024 [182]. Licensed under CC BY 4.0, https://creativecommons.org/licenses/by/4.0/.

3.8 Influence of BMP-2 on C3aR and C5aR1 expression

As previously mentioned, BMP-2 (encoded by *BMP2*) is a pro-hypertrophic growth factor which is expressed in chondrocytes located in calcified cartilage [3]. Therefore, it was tested if BMP-2 modifies the expression of C3aR and C5aR1 during osteogenic differentiation. Gene expression analysis revealed that *BMP2* is upregulated ($p = 0.054$) in degenerated cartilage tissue compared to intact tissue (**Figure 21 A**). Also, 14 days after induction of osteogenic differentiation, *BMP2* was stronger expressed compared to undifferentiated control (**Figure 21 B**). Furthermore, the addition of 100 ng/mL BMP-2 during osteogenic differentiation of hAC did not alter the mRNA level of *C3AR* (**Figure 21 C**, **D**). However, *C5AR1* was significantly upregulated in presence of 100 ng/mL BMP-2 after 14 days of osteogenic differentiation ($p = 0.047$). This was confirmed on protein level by means of C5aR1 IHC in isolated cartilage explants, which were cultured for 21 days *ex vivo* in BM or ODM in presence or absence of 100 ng/mL BMP-2 (**Figure 21 E**, **F**).

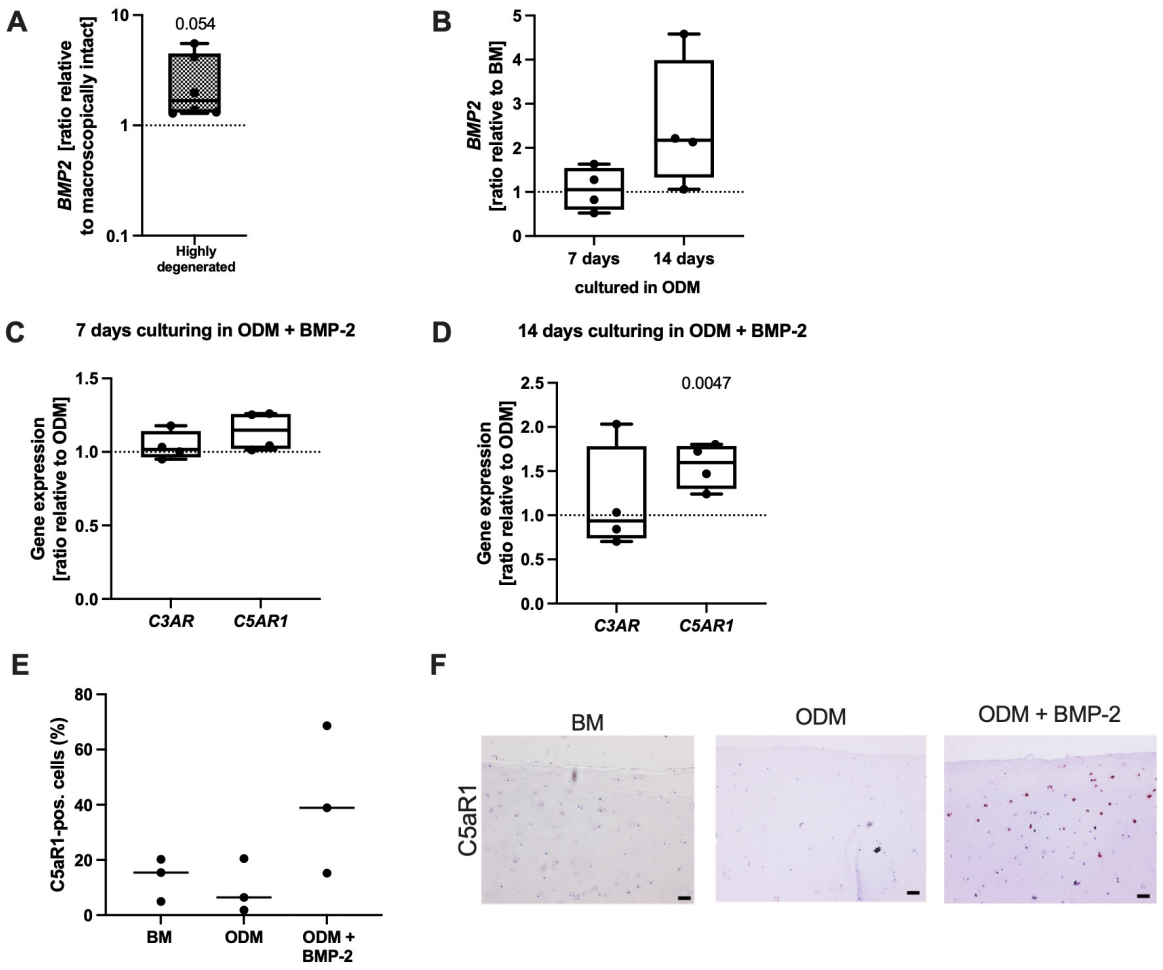

Figure 21: Expression of *BMP2, C3AR*, and *C5AR1* expression in various experimental set-ups. (A) mRNA level of *BMP2* in highly degenerated cartilage tissue (OARSI grade ≥ 3). Normalised to macroscopically intact tissue (OARSI grade ≤ 1); n = 6. Box plot shows median with minimum to maximum whiskers. Unpaired two-tailed t test. **(B)** Gene expression of *BMP2* after 7 and 14 days of osteogenic differentiation with osteogenic differentiation medium (ODM). Normalised to basal medium (BM); n = 4. Box plot shows median with minimum to maximum whiskers. mRNA level of C3aR and C5aR1 after **(C)** 7 and **(D)** 14 days of osteogenic differentiation in presence of 100 ng/mL BMP-2. Relative to hAC cultured in ODM; n = 4. Box plots show median with minimum to maximum whiskers. Unpaired two-tailed t test. **(E)** Quantified IHC staining of C5aR1 in human cartilage tissue, cultured in BM or ODM in presence or absence of 100 ng/mL BMP-2; n = 3. Median values are shown. Each datapoint represents an independent biological replicate. **(F)** Exemplary images of C5aR1 IHC of human cartilage. Scale bars represent 50 μm. Figure has been modified from Ruths et al. 2024 [182]. Licensed under CC BY 4.0, https://creativecommons.org/licenses/by/4.0/.

3.9 Traumatic impact alters expression of complement associated proteins

It was previously reviewed that the *in vitro* induced shift of chondrocytes towards a dedifferentiated fibroblast-like phenotype is also observed *in situ* in OA cartilage [24]. A pathological trigger causing this shift might be mechanical stress and cartilage trauma [122, 176]. Therefore, it was tested if and how a traumatic impact (0.59 J) on human cartilage explants alters the expression of C3, C5, C3aR, and C5aR1 *ex vivo* (**Figure 22 A**, **B**). On mRNA level, only *C3* was significantly downregulated 4 days after traumatization ($p = 0.02$). Furthermore, the percentage of C3aR- (**Figure 22 C**) and C5aR1-positive (**Figure 22 D**) cells was determined via IHC. For both receptors, a slight upregulation 24 h after traumatization was observed. However, 7 and 14 days after trauma, the percentage of positive cells was back to the level of unimpacted control.

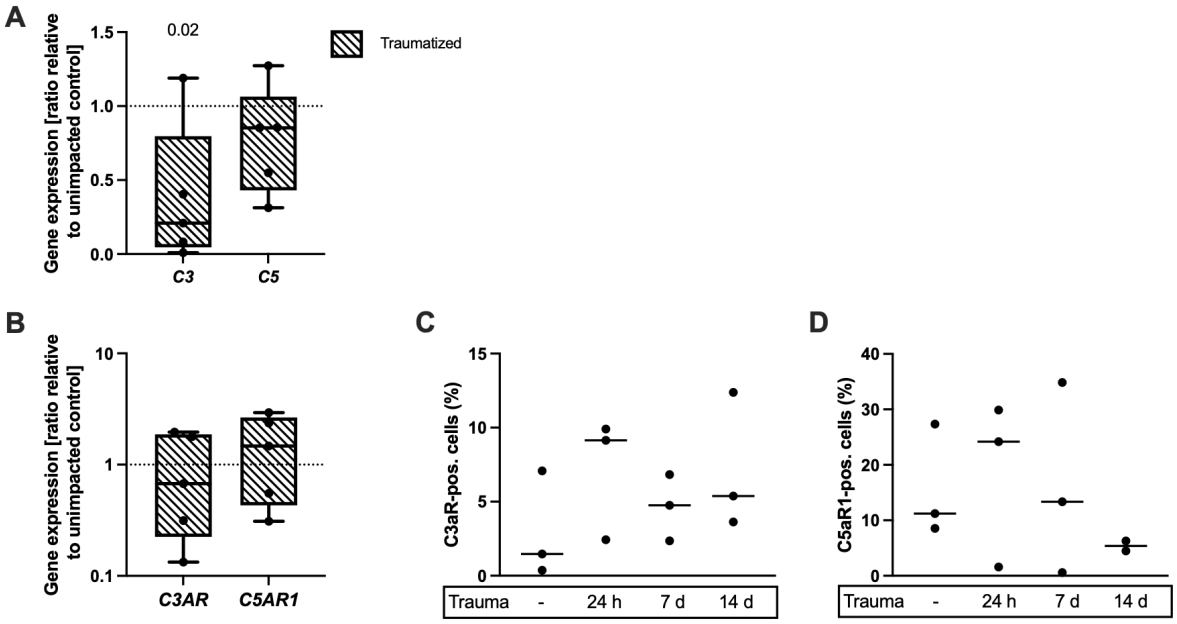

Figure 22: Expression of *C3*, *C5*, C3aR, and C5aR1 in human cartilage explants after *ex vivo* traumatic impact (0.59 J). Gene expression of **(A)** *C3*, *C5*, **(B)** *C3AR*, and *C5AR1* 4 days after traumatization. Normalised to unimpacted cartilage tissue; n = 4. Box plots show median with minimum to maximum whiskers. Unpaired two-tailed t test. Quantification of **(C)** C3aR- and **(D)** C5aR1 IHC of unimpacted control and 24 h, 7 days, and 14 days after traumatization; n = 3. Median values are shown. Each datapoint represents an independent biological replicate.

Furthermore, impacted cartilage explants were treated 4 days with 1,000 ng/mL C3a or 50 ng/mL C5a and gene expression of multiple genes, associated with hypertrophy or inflammation, were analysed. *RUNX2* ($p = 0.045$) and *ALPL* ($p < 0.0001$) were both significantly upregulated after traumatization and subsequent treatment with C3a (**Figure 23 A, B**). However, expression of *COL1A1* and *COL10A1* remained mainly unaffected by trauma and anaphylatoxin exposition (**Figure 23 C, D**). *SP7* was significantly enhanced by traumatization alone ($p = 0.0038$) and in combination with C3a ($p = 0.013$) (**Figure 23 E**). Furthermore, *CXCL1* was induced by trauma in combination with C3a ($p = 0.0079$) or C5a ($p = 0.027$) (**Figure 23 F**). Increased mRNA levels of *IL8* were found after traumatic impact alone ($p = 0.0009$) and in combination with C3a ($p = 0.0039$) or C5a ($p = 0.0082$) (**Figure 23 G**). *IL6* was only enhanced after traumatization ($p = 0.017$) (**Figure 23 H**). However, on protein level, IL-6 was significantly upregulated after trauma alone ($p = 0.0049$) and when additionally stimulated with C3a ($p = 0.01$) (**Figure 23 I**). A positive trend was observed for traumatization and treatment with C5a.

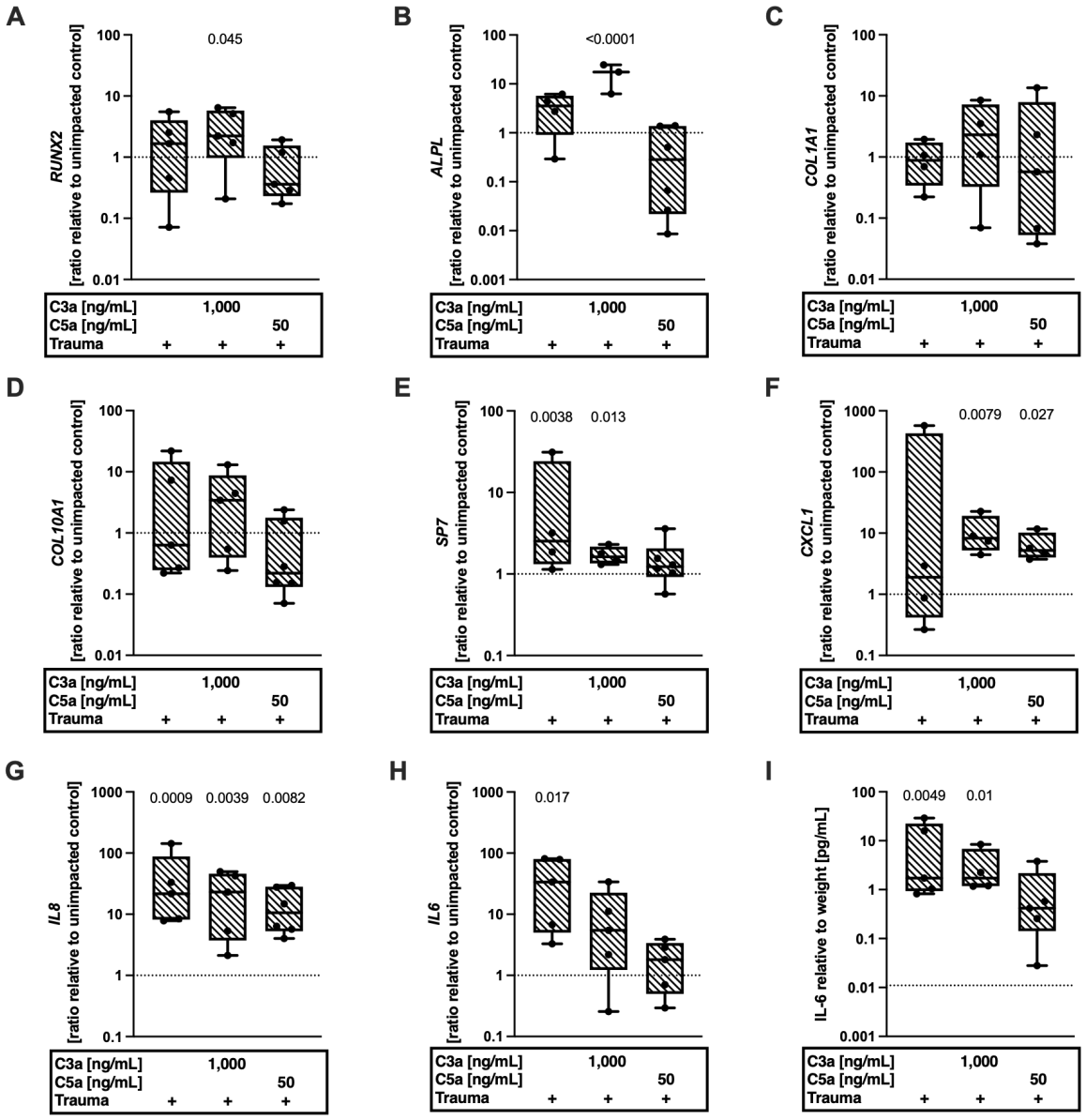

Figure 23: Gene and protein expression of impacted (0.59 J) human cartilage explants. Explants were cultured *ex vivo* after traumatization in serum free medium for 4 days and 1,000 ng/mL C3a or 50 ng/mL C5a were added as indicated. Expression of genes associated with hypertrophic changes (**(A)** *RUNX2*, **(B)** *ALPL*, **(C)** *COL1A1,* **(D)** *COL10A1,* **(E)** *SP7*) and inflammation (**(F)** *CXCL1*, **(G)** *IL8*, **(H)** *IL6*) was determined by qRT-PCR. Normalised to unimpacted and untreated control; n ≥ 3. Box plots show median with minimum to maximum whiskers. One-way ANOVA (A: Dunnet´s correction; B, H: Holm-Šidák´s correction); Kruskal-Wallis (E, F, G: Dunn´s correction). **(I)** IL-6 levels of the supernatants were evaluated via ELISA, n ≥ 4. Box plot shows median with minimum to maximum whiskers. Kruskal-Wallis, Dunn´s correction. Each datapoint represents an independent biological replicate.

3.10 Expression of complement regulatory proteins in hAC

The experiments of the previous paragraphs indicate a crucial role of the complement system in cartilage calcification and thus in the pathogenesis of OA. However, somatic cells express various complement regulatory proteins such as CD35, CD46, CD55, and CD59, which impair the complement cascade at different points to reduce complement activation (see 1.3). Previous studies showed that hAC express CD46, CD55, and CD59 [192]. However, expression of CD35 was not at all or only at a very low level detected in hAC. CD35 expression was also analysed in the process of this thesis and all tested hAC were found negative. Furthermore, elevated mRNA levels of *CD46* and *CD55* were found in highly degenerated cartilage tissue, compared to macroscopically intact cartilage (**Figure 24 A**). This was also previously shown for CD59 [176]. During cultivation of hAC, gene expression of *CD55* decreased with every passage (**Figure 24 C**), while gene expression of *CD46* and *CD59* was not influenced (**Figure 24 B, D**).

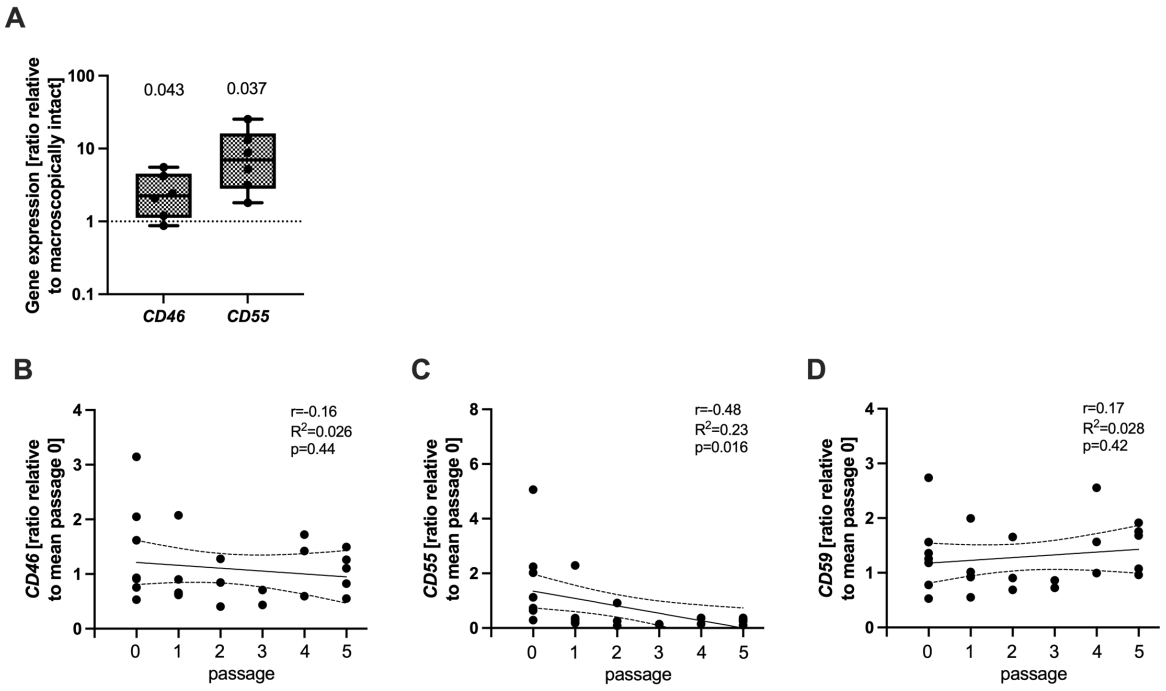

Figure 24: Gene expression in human articular tissue and isolated hAC. (A) mRNA level of *CD46* and *CD55* in highly degenerated cartilage tissue (OARSI grade ≥ 3). Normalised to macroscopically intact cartilage tissue (OARSI grade ≤ 1); n = 6. Box plot shows median with minimum to maximum whiskers. Unpaired two-tailed t test. Gene expression of **(B)** *CD46*, **(C)** *CD55*, and **(D)** CD59 was correlated with the passage number. mRNA expression was normalised to mean ΔCt value of passage 0; n = 25. Donors were measured at various passages. Pearson correlation analysis (with 95% confidence intervals).

4 Discussion

The degenerative joint disease OA impairs the quality of life of affected people severely. 48% of all women and 31% of all men over the age of 65 years are in Germany diagnosed with OA [108, 179]. Treatment of OA is quite challenging due to the complex structure and hypocellular nature of hyaline cartilage. Until now, no adequate OA therapy exist which reliably restores or maintains the function and structure of hyaline cartilage tissue. Previous studies indicated that the complement system plays an essential role in OA progression [187, 196]. However, there is a lack of information regarding the pathological processes in which the complement system is involved and contributes to cartilage degeneration. At first, I investigated whether hAC are involved in the generation of C3a and C5a. Furthermore, studies dealing with either fracture healing or vascular calcification indicated a potential role of the complement system, especially of the anaphylatoxins C3a and C5a and the corresponding receptors C3aR and C5aR1, in mineralisation processes [83, 84, 89, 133, 144, 225]. Therefore, I explored whether the anaphylatoxins and their corresponding receptors are involved in the mineralisation of hyaline cartilage, which is an established hallmark of OA [17, 234]. Additionally, I examined the expression of complement associated proteins in cartilage tissue and hAC.

4.1 Generation of C3a and C5a by hAC

In the first part of this thesis, I evaluated the expression of C3 and C5 in hyaline cartilage and whether hAC are involved in the cleavage of C3 and C5 in the respective anaphylatoxins C3a and C5a. Assirelli et al. 2020 showed that C3 is expressed in cartilage tissue of OA patients. However, they did not test the expression in cartilage derived from healthy individuals [9]. In this study, I could show that *C3* and *C5* are expressed on mRNA level in a similar amount in macroscopically intact and highly degenerated cartilage tissue. At least for C3, an increased expression would have been expected as Bradley et al. 1996 and Xu et al. 2024 reported that C3 is upregulated on protein level in presence of IL-1β [22, 232]. The cytokine IL-1β is enhanced in cartilage

tissue derived from OA patients [183] and IL-1β exposition is an established *in vitro* model to study OA mechanisms [2, 88]. As the human cartilage tissue derived from OA patients undergoing knee replacement surgery, it cannot be excluded that also macroscopically intact tissue was exposed to IL-1β. Thus, C3 expression is in this case similar in macroscopically intact and highly degenerated cartilage tissue.

In line with Xu et al. 2024, I detected C3a in the medium of *in vitro* cultured hAC and *ex vivo* cultured cartilage explants [232]. The authors reported additionally that they could not detect C5 on protein level in the culture medium of human primary chondrocytes. Accordingly, I did not observe C5a in the supernatant of *in vitro* cultured hAC. Furthermore, a cleavage assay was carried out which was based on Ignatius et al. 2011 [84]. The authors showed that osteoblasts and osteoclasts were able to cleave C5 while C3 cleavage was not found. However, my results indicate that hAC can cleave purified human C3 and C5, especially in the presence of HG, which was supplemented to mimic a posttraumatic environment. This goes along with the observation of Schmal et al. 2014 who measured elevated C3a and C5a levels intra-articular in individuals with an acute ankle dislocation fracture [189]. Furthermore, Wang et al. 2011 reported enhanced C3a-desArg concentrations in the synovial fluid of patients with early-stage OA [223]. However, the incubation of hAC with C3 or C5 and cartilage conditioned medium collected from traumatised or highly degenerated cartilage tissue had no influence on the cleavage. Particularly in the media collected after traumatisation, an increased cleavage of both complement components was expected as DAMPs and proteases are released which might activate the complement system [168, 172, 175]. It cannot be ruled out that the concentration of released DAMPs and proteases was too low to induce the cleavage of C3 or C5.

Overall, these results indicate that the complement system is constantly activated in cartilage tissue, as the C3a levels were comparable high in the supernatant of *ex vivo* cultured cartilage explants. Presumably, the alternative pathway is permanently active at a low level. This is supported by Assirelli et al. 2020 as they found a high C3 and factor B expression and a low C4 expression in cartilage tissue [9]. Under physiological conditions, the complement cascade does not proceed further with the cleavage of C5,

as no C5a was found. This might be due to the expression of complement regulatory proteins such as CD46, CD55, and CD59 on hAC [192]. However, under pathological conditions, further triggers (e.g., accumulation of DAMPs derived from degraded ECM components or apoptotic and necrotic cells) might additionally activate the complement system via the lectin pathway, classical pathway [96, 129, 151, 175, 196], or by complement independent enzymes (see 1.3) [28, 70, 76, 119]. Furthermore, transcripts encoding for C5 were enhanced in osteoarthritic synovial membranes compared to healthy ones [223]. This indicates that the synovial membrane and not cartilage tissue is the more relevant source of C5 in regards of OA pathogenesis. Consequently, activation exceeds the intercepting control mechanism, C5 is cleaved, and the complement cascade continues. In line with this, Wang et al. 2011 could show in a mouse model (PTOA induced by medial meniscectomy) that C5-deficient mice exhibited reduced cartilage degeneration [223]. On the contrary, C3-deficient mice were not protected. The authors suggested that in the absence of C3, other proteases such as thrombin cleave C5 to allow the complement cascade to proceed [75]. To test which proteases are involved and thus which complement pathway is potentially activated, it would be advisable to repeat the cleavage assay in the presence of various protease inhibitors. For example, specific inhibitors of the proteases C1r and C1s (classical pathway), MASPs (lectin pathway), C2 (classical and lectin pathway), Factor B and Factor D (alternative pathway), and CatD, CatL, thrombin, and plasmin (complement independent enzymes) [58, 78].

4.2 Influence of C3a and C5a on osteogenic and chondrogenic differentiation

In the previous part of this thesis, I provided evidence that hAC are involved in the cleavage of C3 and C5 in the respective anaphylatoxins. It is described that C3a and C5a play a role in nociceptor activation and sensitization and thus might contribute to OA-associated pain [87, 113, 167]. Apart from this, further research dealing with anaphylatoxins and OA is scarce. In other fields, C3a and C5a are described in the

context of matrix mineralisation. Nagaraj et al. 2015 found in middle aged women an association between C3 serum levels and aortic calcification as well as coronary calcification [144]. The authors did not find an association between C4 and arterial calcification. In case of C5, a study from 2020 reported that C5 plasma levels positively correlated with coronary calcification [133]. In line with this, C5 expression was predominantly found in the hypertrophic zone of the growth plate [5]. Focusing on the anaphylatoxins, enhanced C3a plasma levels were associated with severe abdominal aortic calcification in haemodialysis patients [225]. They also showed that both C3a and C5a plasma levels correlate with the concentration of C-reactive protein, analysed in the serum. C-reactive protein is a common clinical parameter and used mainly as an inflammatory marker [202]. Furthermore, high levels of C-reactive protein were found to be associated with vascular calcification in aorta and hand arteries [86]. In line with this, my data indicated that both 1,000 ng/mL C3a and 50 ng/mL C5a enhanced the matrix calcification during *in vitro* osteogenic differentiation of hAC. Apart from vascular calcification, a recent study provided evidence, that C5a is involved in tooth regeneration. Liu et al. 2021 showed that 400 ng/mL C5a amplified the mineralisation of human dental pulp mesenchymal stem cells [121]. Interestingly, addition of 50 ng/mL C5a had no effect. Accordingly, I could show that 50 ng/mL C5a did not influence the matrix mineralisation during osteogenesis of CSPC or BM-MSC. This implies that different cell types respond differently to C5a and the concentration is crucial for the anticipated effect. It would be interesting to test various C5a concentrations during the osteogenic differentiation of hAC, CSPC, and BM-MSC to determine if the stem cells do not contribute to cartilage calcification due to anaphylatoxin exposition. However, it is debatable whether higher C5a concentrations exceed pathophysiological concentrations found in the knee joint.

To confirm a successful osteogenic differentiation not only based on the calcium deposition, gene expression of the hypertrophic markers *RUNX2* and *ALPL* was analysed. Both are known to be expressed in osteogenic differentiated cells and are often referred to as osteogenesis-associated genes. [140, 194, 238]. I could show that both genes were upregulated in differentiated cells compared to undifferentiated cells.

However, addition of neither C3a nor C5a did influence the expression of *RUNX2* or *ALPL*. Previous studies showed that expression of these markers varies a lot depending on the cell type, the cultivation medium, and the cultivation method (e.g., 2D monolayer, 3D microcarrier) [74, 140, 152, 194, 238]. Osteogenesis is a complex process and especially the time point of analysis is crucial to observe effects on mRNA level. *RUNX2* and *ALPL* are both considered as early osteogenic differentiation markers [194, 238]. Thus, 7 and 14 days might overall be a too late time point to detect effects of the anaphylatoxins during osteogenic differentiation. This would also explain, why *RUNX2* and *ALPL* were upregulated by trend after 4 days when cartilage explants were cultured *ex vivo* in presence of C3a or C5a.

Apart from mineralisation processes, anaphylatoxins, especially C3a, are described to contribute to regenerative processes. *In vivo* studies showed that topical application of C3 or C5 improved early wound healing in rats [197-199] and C3 and C5 expression was found in the regenerating limbs of newts [37, 91]. Furthermore, Mastellos et al. 2001 and Strey et al. 2003 provided evidence that C3a as well as C5a are essential for liver regeneration [134, 204]. Impaired liver regeneration was observed in C5-deficient mice and hepatocyte regeneration could be restored by injection of either C5 or C5a [134]. Accordingly, single reconstruction with C3a and/or C5a prevented in $C3^{-/-}C5^{-/-}$ mice liver failure and resulted in reduced tissue damage [204]. C3a is also associated with retina regeneration [67]. In line with this, I could observe a positive trend of 50 ng/mL C3a on the chondrogenic differentiation. As I previously suggested that the alternative pathway is constantly active in cartilage tissue (see 4.1), generated C3a might promote cartilage anabolism and thus is involved in maintaining the integrity of cartilage tissue. However, higher concentrations of 1,000 ng/mL C3a impaired chondrogenic differentiation. In this case, the pro-inflammatory effects of C3a might be predominant which diminish chondrogenesis [214]. In line with this, 1,000 ng/mL C3a induced an upregulation of *IL6* and *IL8* in cartilage tissue *ex vivo*.

Next, I carried out a trans-differentiation with hAC which is an established model to investigate endochondral ossification [211]. This *in vitro* assay represents the processes occurring *in vivo* during cartilage calcification more accurate than sole

osteogenic differentiation. One limitation of the previously performed osteogenic differentiation is the usage of expanded, dedifferentiated hAC. During trans-differentiation, hAC were first re-differentiated towards a chondrogenic phenotype and subsequently underwent an osteogenic differentiation. In this experiment, chondrogenic differentiation was evaluated after 7 days by means of Alcian blue staining. However, no influence of C3a was observed. This might be due to the shorter cultivation time and/or due to the 2D, not 3D, cultivation. Furthermore, mineralisation during subsequent osteogenic differentiation (3 days) was not altered by C3a or C5a. To examine this in more detail, a modified osteogenic differentiation protocol was applied (7 days BM, 10 days ODM), which was based on the trans-differentiation timeline. Again, C5a had an inductive effect on mineralisation during osteogenic differentiation which implies that only differentiated hAC are responsive to C5a during osteogenic differentiation. However, I cannot exclude, that the cultivation time in presence of anaphylatoxins plays a significant role, since osteogenic differentiation had to be extended from 3 to 10 days. In contrast to the ATDC5 cells used in Tschaffon et al. 2022, supplementation of BMP-2 was not required for a successful osteogenic differentiation after chondrogenic differentiation [211]. Furthermore, addition of BMP-2 increased the inductive effect of C5a. The potential role of BMP-2 in cartilage calcification due to anaphylatoxin exposition will be addressed in 4.3.

Overall, my results indicate that hAC with a chondrogenic phenotype, in contrast to dedifferentiated hAC, are not responsive to anaphylatoxins during osteogenic differentiation. In line with this, during chondrogenic differentiation, neither C3a nor C5a induced hypertrophic alterations of hAC or matrix mineralisation. I assume that multiple stimuli or triggers are needed to make hAC susceptible to anaphylatoxins in the context of cartilage calcification. Previous studies described that hAC lose their chondrogenic phenotype during OA progression and one feasible inducer might be cartilage trauma [24, 122, 176]. This will be discussed in more detail in 4.4.

4.3 Expression of C3aR and C5aR1 and association with calcification processes

In the context of mineralisation processes, not only the anaphylatoxins C3a and C5a are frequently mentioned, but also the corresponding receptors C3aR and C5aR1. Kalbasi Anaraki et al. 2014 observed a link between C5aR1 expression and vascular calcification in mice [89]. Furthermore, the C5a-C5aR1 axis is associated with matrix mineralisation in the context of bone fracture healing. Endochondral ossification observed in the callus during fracture healing can be compared to molecular mechanism taking place during cartilage calcification [25, 224, 234]. Ignatius et al. 2011 detected in rats that C5aR1 was expressed in the fracture callus of bone forming osteoblasts [83]. Further studies of the same authors indicated that a balanced C5aR1 expression is important for a flawless bone fracture healing. They showed in mice that global knockdown of C5aR1 as well as osteoblast-specific C5aR1 overexpression impaired fracture healing [16, 97]. Additionally, an upregulation of C3aR and C5aR1 was observed in BM-MSC differentiating into osteoblasts [83, 84, 89]. I observed similar results in osteogenic differentiated hAC and could show that the amplified mineralisation during osteogenic differentiation due to anaphylatoxin stimulation could be reversed by C3aR or C5aR1 inhibition, respectively. This indicates that pro-osteogenic effects of C3a and C5a are mediated by their respective receptors. In case of C5aR1, even inhibition alone reduced the calcification during osteogenic differentiation. These are first indications that C5aR1 is actively involved in the differentiation processes and might serve as a marker for osteogenic differentiated cells. In chondrogenic differentiated cells, expression of C3aR or C5aR1 was not detected and inhibition of the receptors did not alter the differentiation. Therefore, I suspect that the anaphylatoxin receptors play no or only a minor role during chondrogenic differentiation processes.

To unravel the potential involvement of C3aR and C5aR1 in cartilage mineralisation further, I analysed their expression in human hyaline cartilage tissue. I focused only on the superficial zone and upper part of the middle zone (about 0.5-0.6 mm) since Wang et al. 2023 described a top-down calcification of cartilage at the joint surface [224].

Furthermore, complement components are rather large (e.g., C3a has a molecular mass of 9 kDa [81] and C5a of 11 kDa [42]) and penetrate the cartilage matrix only to a certain degree [22, 109, 132]. I could show that both receptors are more frequently expressed in highly degenerated cartilage tissue as compared to macroscopically intact tissue. I could exclude that the increased expression is due to the age of the donors. It is likely that C3aR and C5aR1 are upregulated as a consequence of the chronic inflammation during OA progression. It is known that both receptors are induced in the presence of pro-inflammatory cytokines such as IL-6, IFN-γ, and IL-1β [60, 156, 166]. *In vitro* experiments with hAC revealed that TNF and IL-1β increased the expression of C3aR and C5aR1 [153, 192]. Furthermore, Wang et al. 2023 observed in the context of top-down calcification spherical mineral particles at the surface of OA cartilage tissue [224]. By means of Alizarin Red S staining and von Kossa staining, I could also observe mineralisation at the surface in the clinical samples of hyaline cartilage and established a score to quantify the mineralisation in the upper part of the cartilage tissue (about 0.5 – 0.6 mm). In cooperation with Julia Marzi and Katja Schenke-Layland (University of Tübingen), the specificity of the calcification staining was validated by RAMAN spectroscopy analysis [182]. Additionally, a positive association was found between the determined calcification score and the number of cells positively stained for either C3aR or C5aR. This was also true in primary hAC. In donors with a low expression of the receptors on the cell surface, a low Alizarin Red S staining intensity was measured after osteogenic differentiation. Higher exposition of the receptors resulted in higher Alizarin Red S values. To define this relation further, I performed fluorescence-activated cell sorting to collect two hAC populations of one donor. One population which was negative for C5aR1 and one which was positive. Unfortunately, the number of C5aR1-positive cells was rather low and the osteogenic differentiation of both populations was in general very weak and therefore inconclusive. Presumably, the procedure of cell sorting, including preparation and transportation of the cells, was too stressful for the sensitive hAC. Nevertheless, my results imply that there is a connection between the expression of anaphylatoxin receptors, a possible higher OA grade, and an increased cartilage calcification. This data is in line with my previous hypothesis that C5aR1 is actively involved in the differentiation processes and might serve as a marker for

osteogenic differentiated cells or at least indicates a cell population which is more likely to develop a hypertrophic phenotype and induce mineralisation of the surrounding tissue. Taking my last described results into account, this could also apply for C3aR.

I observed that the addition of BMP-2 during osteogenesis of hAC increased the inductive effect of C5a and reductive effect of the C5aR1 inhibitor PMX53. BMP-2 can be found in the hypertrophic zone of the growth plate and promotes a hypertrophic phenotype of hAC [25, 149]. I could validate the observation from Nakase et al. 2003 that BMP-2 is upregulated in OA cartilage [145]. Addition of BMP-2 in turn promoted the expression of C5aR1 during osteogenic differentiation. This is another indication that C5aR can be associated with a hypertrophic phenotype of hAC and might explain why BMP-2 amplified the effects of C5a and PMX53 during the osteogenic differentiation of cultured hAC, since there is more C5aR1. It would be interesting to test the influence of other BMPs on the C3aR and C5aR1 expression as well. Potential candidates would be BMP-4, BMP-6, BMP-7 and BMP-9. BMP-6 and BMP-9 are like BMP-2 involved in bone formation [162] and BMP-4 is associated with a hypertrophic differentiation [203]. Furthermore, BMP-4, BMP-6, and BMP-7 are expressed in the hypertrophic zone of the growth plate [4, 149].

Furthermore, I analysed the expression of C3aR and C5aR1 in hAC, CSPC, and BM-MSC *in vitro*. In line with my previous results, for BM-MSC, which had an intense mineralisation after osteogenic differentiation, a high number C3aR- and C5aR1-positive cells was detected. In contrast, hAC and CSPC expressed both receptors on a lower level and Alizarin Red S staining after osteogenic differentiation was weaker. Interestingly, in the case of BM-MSC, the higher expression of the receptors was not accompanied by an amplified matrix mineralisation during osteogenic differentiation in the presence of anaphylatoxins. In conclusion, higher C3aR or C5aR1 expression indicates cells which undergo osteogenic differentiation more thoroughly but is not necessarily associated with a higher responsiveness to C3a or C5a, respectively. As discussed in 4.2, the pro-osteogenic effects of anaphylatoxins depend on the cell type.

Several studies, including this thesis, proved evidence that C3a, C5a, C3aR, and C5aR1 are involved in mineralisation processes. However, the underlying molecular processes are to the present day unknown. Kalbasi Anaraki et al. 2014 indicated, that NF-κB signaling is involved [89]. In the case of vascular calcification, it is described that systemic inflammation, endoplasmic reticulum stress, ECM remodelling, oxidative stress, and cell apoptosis promote mineralisation [120]. For example, C5a-C5aR1 signalling is associated with endoplasmic reticulum stress in neutrophils [73] and C3a-C3aR signalling induced endoplasmic reticulum stress in mice and retinal pigment epithelium cells [103]. Furthermore, ROS production was observed in polymorphonuclear leucocytes mediated by C5a-C5aR1 signalling [12] and in human eosinophils mediated by both C3a-C3aR and C5a-C5aR1 signalling, respectively [48]. All of the mentioned aspects are in general also relevant in OA pathogenesis (see 1.2.1). Thus, further studies are necessary, to unravel in which pathways and molecular processes the anaphylatoxins and corresponding receptors are involved and thereby potentially promote cartilage calcification. Feasible experiments could be the inhibition of NF-kB signaling or application of antioxidative therapy and/or monitoring of NF-kB signaling and ROS production during osteogenic differentiation in presence of C3a or C5a.

Schulze-Tanzil et al. 2012 showed that *C3AR* and *C5AR1* are expressed in freshly isolated and cultured hAC [192]. By trend, cultured hAC expressed the receptors to a lesser extent. I could confirm this observation on protein level on the cell surface. The authors suggested that this might be due to the phenotypic shift of cultured hAC. I showed previously that cultured, dedifferentiated hAC are more responsive to anaphylatoxin treatment during osteogenic differentiation, however, these hAC express C3aR and C5aR1 on a lower level. This is in line with my previous assumption that the expression of the anaphylatoxin receptors, at least when only the location on the cell surface is considered, does not go along with a higher responsiveness to anaphylatoxins during osteogenic differentiation. Furthermore, additional experiments revealed that both receptors are still present in hAC, however, not located on the cell surface but rather found intracellularly. Internalisation of both receptors after stimulation

with their respective ligands is described for immune cells [69, 124, 193] and MSC [84, 191]. It is feasible that bovine C3a and C5a, contained in FBS, bind to the receptors and cause internalisation. Another explanation might be that the enzyme trypsin, used to detach the cells during passaging, digested the receptors on the cell surface. As the gene expression during cultivation decreases, progressively fewer receptors are synthesised to replace the digested ones. Either way, only the intracellular receptors are still present after multiple passages. The non-canonical role of anaphylatoxins receptors located intracellularly is up to the present day not clear. It is known that C3 can be cleaved intracellular by the protease CatL in immune cells as well as in somatic cells such as epithelial cells, endothelial cells, and fibroblasts [54, 119]. In the case of T cells, Liszewski et al. 2013 showed that intracellular C3a binding to intracellular C3aR is required for cell survival [119]. Upon the activation of the T cell receptor, intracellular C3aR is transported to the cell surface to promote production of pro-inflammatory cytokines. Thus, signalling of G-protein-coupled receptors differs depending on the localisation of the receptors, as it has been shown in Irannejad et al. 2013 [85] and reviewed in Tóth et al. 2024 [210]. Furthermore, Arbore et al. 2016 demonstrated that T cells also have an intracellular C5 system, which is like the intracellular C3 system involved in T cell activation [6]. In general, the intracellular complement system is rather newly emerged and so far, poorly studied. An involvement in cell proliferation, survival, and metabolism is described in immune but also nonimmune cells [7, 55, 104]. Considering the current limited availability of studies addressing the intracellular complement system in hAC, I could only speculate about its role. However, it is very likely that the intracellular complement system is involved in various processes and further research is required.

4.4 Expression of complement associated proteins

Next, I evaluated the effects of cartilage trauma on the expression of *C3*, *C5*, *C3aR*, and *C5aR1*. Except from *C3*, which was downregulated, none of the genes were affected 4 days after traumatization. This implies that the expression of these

complement associated proteins in cartilage tissue is no relevant regulatory factor in the first days after cartilage trauma. However, I did not test the mRNA expression levels directly after trauma (e.g., after 4 h). It seems to be more crucial if the complement system is in general activated (e.g., by DAMPs) and if anaphylatoxins are generated. Indeed, I could show that the addition of HG amplified the cleavage of C3 and C5 by hAC (see 4.1). In line with this, C3a, C5a, and sTCC were found in elevated levels in the synovial fluid after acute ankle dislocation fracture [189]. Furthermore, Struglics et al. 2016 reported high C3bBbP and sTCC levels in the synovial fluid after an acute knee injury (0-83 days after injury), which was not detected in the group with an old knee injury (1-37 years after injury) [205]. At least several years after injury, the reduced complement activation could be explained by an enhanced expression of the complement regulatory protein *CD59* which was found in elevated levels in cartilage tissue derived from osteoarthritic joints [176]. Accordingly, I detected elevated mRNA levels of *CD46* and *CD55* in highly degenerated cartilage tissue compared to macroscopically intact cartilage.

So far, my results indicated that only dedifferentiated hAC are responsive to anaphylatoxins during osteogenic differentiation and I previously stated in 4.2 that hAC lose their chondrogenic phenotype during OA progression and one feasible inducer might be cartilage trauma [24, 122, 176]. In line with this, C3a stimulation in combination with trauma induced the expression of the hypertrophic markers *RUNX2*, *ALPL*, and *SP7*. Unexpectedly, C5a did not alter the expression of the hypertrophic markers in traumatized cartilage explants. This was not due to a reduced expression of C5aR1, as it was unaffected by trauma. Presumably, trauma alone does not lead after 4 days to the phenotypical shift required to be responsive to C5a regarding mineralisation processes, at least if only the analysed genes were taken into account. Additionally, the time point of analysis of the hypertrophic markers might be too late to observe effects of C5a. Furthermore, in traumatized cartilage explants stimulated with C3a, an upregulation of pro-inflammatory cytokines was observed on mRNA (*CXCL1* and *IL8*) and protein (IL-6) level. This underlines my previous assumption that C3a impairs

chondrogenesis and thus the regeneration of hyaline cartilage, due to its pro-inflammatory properties (see 4.2).

Overall, this implies that after an acute knee injury, the complement system should be immediately addressed to prevent the excessive generation of anaphylatoxins and TCC deposition at an early state. Especially TCC deposition is associated with detrimental effects in musculoskeletal diseases such as intervertebral disc degeneration [100, 206, 207] and OA [176]. Furthermore, absence of TCC in C6-deficient rabbits partially protected them from OA progression in an injury-induced OA model [177]. A feasible approach might be local application of peptides of the compstatin family (binds C3 and prevents its cleavage; approved for the treatment of paroxysmal nocturnal hemoglobinuria) [107, 135] and of Ravulizumab (binds C5 and prevents its cleavage; approved for the treatment of atypical haemolytic uremic syndrome) [195, 226]. Furthermore, I observed in degenerated cartilage tissue an enhanced expression of C3aR and C5aR1. Both receptors were associated with cartilage mineralisation and a hypertrophic phenotype (see 4.3). Inhibition of C3aR and C5aR1 might be advisable in OA and PTOA treatment to reduce cartilage calcification, consequent cartilage degeneration and thus attenuate OA progression. For both receptors, no inhibitor has been approved in clinical trials yet. However, SB290157 and PMX53 were successfully used in various animal models [59, 101, 229].

Finally, I would like to add that complement components are not only involved in calcification processes but also contribute to matrix degradation of mineralised tissue such as calcified cartilage by osteoclasts [143, 181]. C3a and C5a induced osteoclastogenesis [84] and knockdown of C5aR1 lead to a decreased number of osteoclasts during fracture healing [97]. Furthermore, Luntzer et al. associated C3, C5a, and C5aR1 with an increased destruction of dental mineralised tissue leading to tooth resorption [127]. Therefore, targeting the complement system or especially the anaphylatoxin receptors might have many beneficial effects. C3aR or C5aR1 inhibition counteracts cartilage calcification and might also reduce subsequent resorption of the mineralised cartilage by osteoclasts.

4.5 Limitations of the study

One limitation of the study is the origin of the human cartilage tissue. Although it was classified in macroscopically intact (OARSI grade ≤ 1) and highly degenerated (OARSI grade ≥ 3) cartilage tissue and differences were observed in Safranin O staining, it cannot be ruled out that the macroscopically intact tissue was affected by OA on a molecular level. Nevertheless, the human material should also be considered as a strength. The described effects were observed in at least three independent human donors for each experiment. Thus, it is very likely that the drawn conclusions can be directly applied in humans. There is no species-specific effect, as often described for animal experiments where the findings are not always transferable to humans.

Another limitation of the study is that the disease OA is not only affecting the hyaline cartilage tissue but is considered as a whole joint disease [125, 165]. Especially the synovium is crucially involved in the pathomechanisms of OA and is a source of complement components as well as pro-inflammatory cytokines [9, 141, 186]. Additionally, the biomechanics which occur in the OA joint are not considered *in vitro* [40, 185]. Furthermore, cartilage calcification is a rather slow process which can hardly be reconstructed and monitored *in vitro*. To include these aspects, it would be interesting to carry out *in vivo* experiments with mice who lack either C3, C5, C3aR, or C5aR1. This would clarify whether C3a, C5a, C3aR, and C5aR1 play a pivotal role in age- or trauma-related OA and elucidate if plausible protective effects are mediated by a reduced cartilage calcification. Taken the literature and my data into account, C5aR1 is the most promising target. Therefore, an *in vivo* experiment with C5aR1$^{-/-}$ mice is scheduled for the near future. By destabilizing the medial meniscus, PTOA will be induced and cartilage calcification will be analysed after 12 weeks.

5 Summary

Within this thesis, I investigated the role of the complement system in osteoarthritis (OA) progression. I focused mainly on the anaphylatoxins C3a and C5a and their respective receptors C3aR and C5aR1 and whether they are involved in cartilage calcification. The mineralisation of hyaline cartilage tissue is an established hallmark of OA and associated with cartilage degeneration [17, 234].

In the first part of this thesis, I could show that human articular chondrocytes (hAC) express the complement components C3 and C5 and can cleave them in the corresponding anaphylatoxins C3a and C5a. Enhanced levels of both anaphylatoxins were detected in a posttraumatic environment, mimicked by cartilage homogenizate (HG). In general, C3a was found in relatively high concentrations in the supernatant of hAC and cartilage explants. Next, I investigate which role the generated anaphylatoxins might have during OA progression and observed that mineralisation was amplified during osteogenesis of hAC in the presence of C3a and C5a, mediated by C3aR or C5aR1, respectively. However, this effect was only observed in cultured and therefore dedifferentiated hAC. A preceding chondrogenic differentiation caused that the anaphylatoxins did not alter the mineralisation during osteogenic differentiation of hAC. This indicates that hAC with a chondrogenic phenotype are not responsive to anaphylatoxins concerning mineralisation processes. In line with this, neither C3a nor C5a induced hypertrophic alterations of hAC or matrix mineralisation during chondrogenic differentiation. Regardless of this, C3a influenced the chondrogenic differentiation in a concentration depending manner. A low concentration promoted chondrogenesis while a high concentration induced the expression of pro-inflammatory cytokines and impaired chondrogenic differentiation.

Furthermore, I observed that C3aR and C5aR1 were predominantly found in highly degenerated cartilage tissue. Additionally, both anaphylatoxin receptors were upregulated during osteogenic differentiation and their expression on hAC was positively associated with matrix mineralisation during osteogenic differentiation as well as cartilage calcification of native tissue. Interestingly, the expression level of the

receptors did not necessarily influence the responsiveness towards anaphylatoxins during osteogenic differentiation. Nevertheless, my data indicate that C3aR and especially C5aR1 are actively involved in osteogenic differentiation and induction of a hypertrophic phenotype. Future studies have to elucidate the molecular process further and are required to define their role in cartilage calcification in more detail.

Overall, I provided first evidence that anaphylatoxins and the corresponding receptors are involved in cartilage calcification. Targeting C3aR and C5aR1 might be a future approach to reduce mineralisation of cartilage tissue and consequent cartilage degradation. Additionally, the findings of my thesis are not only relevant in the context of OA but might also contribute to find a treatment for other diseases, associated with anaphylatoxin-related mineralisation of tissues such as atherosclerosis, which is often accompanied by vascular calcification.

6 List of references

1. Acosta JC, Banito A, Wuestefeld T, Georgilis A, Janich P, Morton JP, Athineos D, Kang TW, Lasitschka F, Andrulis M, Pascual G, Morris KJ, Khan S, Jin H, Dharmalingam G, Snijders AP, Carroll T, Capper D, Pritchard C, Inman GJ, Longerich T, Sansom OJ, Benitah SA, Zender L, Gil J: A complex secretory program orchestrated by the inflammasome controls paracrine senescence. Nat Cell Biol 15: 978-990 (2013)
2. Allas L, Rochoux Q, Leclercq S, Boumediene K, Bauge C: Development of a simple osteoarthritis model useful to predict in vitro the anti-hypertrophic action of drugs. Lab Invest 100: 64-71 (2020)
3. Anderson HC, Hodges PT, Aguilera XM, Missana L, Moylan PE: Bone morphogenetic protein (BMP) localization in developing human and rat growth plate, metaphysis, epiphysis, and articular cartilage. J Histochem Cytochem 48: 1493-1502 (2000)
4. Andersson C, Wenander CS, Usher PA, Hebsgaard JB, Sondergaard BC, Rono B, Mackay C, Friedrichsen B, Chang C, Tang R, Hornum L: Rapid-onset clinical and mechanistic effects of anti-C5aR treatment in the mouse collagen-induced arthritis model. Clin Exp Immunol 177: 219-233 (2014)
5. Andrades JA, Nimni ME, Becerra J, Eisenstein R, Davis M, Sorgente N: Complement proteins are present in developing endochondral bone and may mediate cartilage cell death and vascularization. Exp Cell Res 227: 208-213 (1996)
6. Arbore G, West EE, Spolski R, Robertson AAB, Klos A, Rheinheimer C, Dutow P, Woodruff TM, Yu ZX, O'Neill LA, Coll RC, Sher A, Leonard WJ, Kohl J, Monk P, Cooper MA, Arno M, Afzali B, Lachmann HJ, Cope AP, Mayer-Barber KD, Kemper C: T helper 1 immunity requires complement-driven NLRP3 inflammasome activity in CD4(+) T cells. Science 352: (2016)
7. Arbore G, Kemper C, Kolev M: Intracellular complement - the complosome - in immune cell regulation. Mol Immunol 89: 2-9 (2017)
8. Armiento AR, Alini M, Stoddart MJ: Articular fibrocartilage - Why does hyaline cartilage fail to repair? Adv Drug Deliv Rev 146: 289-305 (2019)
9. Assirelli E, Pulsatelli L, Dolzani P, Mariani E, Lisignoli G, Addimanda O, Meliconi R: Complement Expression and Activation in Osteoarthritis Joint Compartments. Front Immunol 11: (2020)
10. Baddam P, Bayona-Rodriguez F, Campbell SM, El-Hakim H, Graf D: Properties of the Nasal Cartilage, from Development to Adulthood: A Scoping Review. Cartilage 13: (2022)
11. Banda NK, Hyatt S, Antonioli AH, White JT, Glogowska M, Takahashi K, Merkel TJ, Stahl GL, Mueller-Ortiz S, Wetsel R, Arend WP, Holers VM: Role of C3a receptors, C5a receptors, and complement protein C6 deficiency in collagen antibody-induced arthritis in mice. J Immunol 188: 1469-1478 (2012)
12. Barrett CD, Hsu AT, Ellson CD, B YM, Kong YW, Greenwood JD, Dhara S, Neal MD, Sperry JL, Park MS, Cohen MJ, Zuckerbraun BS, Yaffe MB: Blood clotting and traumatic injury with shock mediates complement-dependent neutrophil priming for extracellular ROS, ROS-dependent organ injury and coagulopathy. Clin Exp Immunol 194: 103-117 (2018)

13. Bartok B, Firestein GS: Fibroblast-like synoviocytes: key effector cells in rheumatoid arthritis. Immunol Rev 233: 233-255 (2010)

14. Bensa A, Albanese J, Boffa A, Previtali D, Filardo G: Intra-articular corticosteroid injections provide a clinically relevant benefit compared to placebo only at short-term follow-up in patients with knee osteoarthritis: A systematic review and meta-analysis. Knee Surg Sports Traumatol Arthrosc 32: 311-322 (2024)

15. Benya PD, Padilla SR, Nimni ME: Independent regulation of collagen types by chondrocytes during the loss of differentiated function in culture. Cell 15: 1313-1321 (1978)

16. Bergdolt S, Kovtun A, Hagele Y, Liedert A, Schinke T, Amling M, Huber-Lang M, Ignatius A: Osteoblast-specific overexpression of complement receptor C5aR1 impairs fracture healing. PLoS One 12: (2017)

17. Bernabei I, So A, Busso N, Nasi S: Cartilage calcification in osteoarthritis: mechanisms and clinical relevance. Nat Rev Rheumatol 19: 10-27 (2023)

18. Bernar A, Gebetsberger JV, Bauer M, Streif W, Schirmer M: Optimization of the Alizarin Red S Assay by Enhancing Mineralization of Osteoblasts. Int J Mol Sci 24: (2022)

19. Bijlsma JW, Berenbaum F, Lafeber FP: Osteoarthritis: an update with relevance for clinical practice. Lancet 377: 2115-2126 (2011)

20. Bohlson SS, Garred P, Kemper C, Tenner AJ: Complement Nomenclature-Deconvoluted. Front Immunol 10: (2019)

21. Bokisch VA, Muller-Eberhard HJ: Anaphylatoxin inactivator of human plasma: its isolation and characterization as a carboxypeptidase. J Clin Invest 49: 2427-2436 (1970)

22. Bradley K, North J, Saunders D, Schwaeble W, Jeziorska M, Woolley DE, Whaley K: Synthesis of classical pathway complement components by chondrocytes. Immunology 88: 648-656 (1996)

23. Castrogiovanni P, Di Rosa M, Ravalli S, Castorina A, Guglielmino C, Imbesi R, Vecchio M, Drago F, Szychlinska MA, Musumeci G: Moderate Physical Activity as a Prevention Method for Knee Osteoarthritis and the Role of Synoviocytes as Biological Key. Int J Mol Sci 20: (2019)

24. Charlier E, Deroyer C, Ciregia F, Malaise O, Neuville S, Plener Z, Malaise M, de Seny D: Chondrocyte dedifferentiation and osteoarthritis (OA). Biochem Pharmacol 165: 49-65 (2019)

25. Chawla S, Mainardi A, Majumder N, Donges L, Kumar B, Occhetta P, Martin I, Egloff C, Ghosh S, Bandyopadhyay A, Barbero A: Chondrocyte Hypertrophy in Osteoarthritis: Mechanistic Studies and Models for the Identification of New Therapeutic Strategies. Cells 11: (2022)

26. Cheng TH, Zeng J, Dehghani A, Dimaculangan D, Zhang M, Maheshwari AV: Complement C3-alpha and C3-beta Levels in Synovial Fluid But Not in Blood Correlate With the Severity of Osteoarthritis Research Society International Histopathological Grades in Primary Knee Osteoarthritis. J Arthroplasty 37: 1541-1548 (2022)

27. Claes L, Recknagel S, Ignatius A: Fracture healing under healthy and inflammatory conditions. Nat Rev Rheumatol 8: 133-143 (2012)

28. Clark A, Weymann A, Hartman E, Turmelle Y, Carroll M, Thurman JM, Holers VM, Hourcade DE, Rudnick DA: Evidence for non-traditional activation of complement factor C3 during murine liver regeneration. Mol Immunol 45: 3125-3132 (2008)

29. Coppe JP, Desprez PY, Krtolica A, Campisi J: The senescence-associated secretory phenotype: the dark side of tumor suppression. Annu Rev Pathol 5: 99-118 (2010)

30. Coulthard LG, Woodruff TM: Is the complement activation product C3a a proinflammatory molecule? Re-evaluating the evidence and the myth. J Immunol 194: 3542-3548 (2015)

31. Couves EC, Gardner S, Voisin TB, Bickel JK, Stansfeld PJ, Tate EW, Bubeck D: Structural basis for membrane attack complex inhibition by CD59. Nat Commun 14: (2023)

32. Crofford LJ: Use of NSAIDs in treating patients with arthritis. Arthritis Res Ther 15: (2013)

33. Darling EM, Athanasiou KA: Rapid phenotypic changes in passaged articular chondrocyte subpopulations. J Orthop Res 23: 425-432 (2005)

34. Darwiche H, Barsoum WK, Klika A, Krebs VE, Molloy R: Retrospective analysis of infection rate after early reoperation in total hip arthroplasty. Clin Orthop Relat Res 468: 2392-2396 (2010)

35. Davies RL, Kuiper NJ: Regenerative Medicine: A Review of the Evolution of Autologous Chondrocyte Implantation (ACI) Therapy. Bioengineering 6: (2019)

36. De Nanteuil G, Portevin B, Benoist A: Disease-modifying anti-osteoarthritic drugs: current therapies and new prospects around protease inhibition. Farmaco 56: 107-112 (2001)

37. Del Rio-Tsonis K, Tsonis PA, Zarkadis IK, Tsagas AG, Lambris JD: Expression of the third component of complement, C3, in regenerating limb blastema cells of urodeles. J Immunol 161: 6819-6824 (1998)

38. Derwich M, Mitus-Kenig M, Pawlowska E: Mechanisms of Action and Efficacy of Hyaluronic Acid, Corticosteroids and Platelet-Rich Plasma in the Treatment of Temporomandibular Joint Osteoarthritis-A Systematic Review. Int J Mol Sci 22: (2021)

39. Di Martino A, Di Matteo B, Papio T, Tentoni F, Selleri F, Cenacchi A, Kon E, Filardo G: Platelet-Rich Plasma Versus Hyaluronic Acid Injections for the Treatment of Knee Osteoarthritis: Results at 5 Years of a Double-Blind, Randomized Controlled Trial. Am J Sports Med 47: 347-354 (2019)

40. Diamond LE, Grant T, Uhlrich SD: Osteoarthritis year in review 2023: Biomechanics. Osteoarthritis Cartilage 32: 138-147 (2024)

41. Dieterich JD, Fields AC, Moucha CS: Short term outcomes of revision total knee arthroplasty. J Arthroplasty 29: 2163-2166 (2014)

42. DiScipio RG: The conversion of human complement component C5 into fragment C5b by the alternative-pathway C5 convertase. Biochem J 199: 497-504 (1981)

43. Ea HK, Chobaz V, Nguyen C, Nasi S, van Lent P, Daudon M, Dessombz A, Bazin D, McCarthy G, Jolles-Haeberli B, Ives A, Van Linthoudt D, So A, Liote F, Busso N: Pathogenic role of basic calcium phosphate crystals in destructive arthropathies. PLoS One 8: (2013)

44. Edouard P, Rannou F, Coudeyre E: Animal evidence for hyaluronic acid efficacy in knee trauma injuries. Review of animal-model studies. Phys Ther Sport 14: 116-123 (2013)

45. Ehrengruber MU, Geiser T, Deranleau DA: Activation of human neutrophils by C3a and C5A. Comparison of the effects on shape changes, chemotaxis, secretion, and respiratory burst. FEBS Lett 346: 181-184 (1994)

46. Ekdahl KN, Mohlin C, Adler A, Aman A, Manivel VA, Sandholm K, Huber-Lang M, Fromell K, Nilsson B: Is generation of C3(H(2)O) necessary for activation of the alternative pathway in real life? Mol Immunol 114: 353-361 (2019)

47. el-Lati SG, Dahinden CA, Church MK: Complement peptides C3a- and C5a-induced mediator release from dissociated human skin mast cells. J Invest Dermatol 102: 803-806 (1994)

48. Elsner J, Oppermann M, Czech W, Dobos G, Schopf E, Norgauer J, Kapp A: C3a activates reactive oxygen radical species production and intracellular calcium transients in human eosinophils. Eur J Immunol 24: 518-522 (1994)

49. Eschweiler J, Horn N, Rath B, Betsch M, Baroncini A, Tingart M, Migliorini F: The Biomechanics of Cartilage-An Overview. Life 11: (2021)

50. Fearon DT, Austen KF: Properdin: binding to C3b and stabilization of the C3b-dependent C3 convertase. J Exp Med 142: 856-863 (1975)

51. Ferguson VL, Bushby AJ, Boyde A: Nanomechanical properties and mineral concentration in articular calcified cartilage and subchondral bone. J Anat 203: 191-202 (2003)

52. Fickert S, Fiedler J, Brenner RE: Identification of subpopulations with characteristics of mesenchymal progenitor cells from human osteoarthritic cartilage using triple staining for cell surface markers. Arthritis Res Ther 6: R422-432 (2004)

53. Flood J: The role of acetaminophen in the treatment of osteoarthritis. Am J Manag Care 16: 48-54 (2010)

54. Freeley S, Cardone J, Gunther SC, West EE, Reinheckel T, Watts C, Kemper C, Kolev MV: Asparaginyl Endopeptidase (Legumain) Supports Human Th1 Induction via Cathepsin L-Mediated Intracellular C3 Activation. Front Immunol 9: (2018)

55. Friscic J, Bottcher M, Reinwald C, Bruns H, Wirth B, Popp SJ, Walker KI, Ackermann JA, Chen X, Turner J, Zhu H, Seyler L, Euler M, Kirchner P, Kruger R, Ekici AB, Major T, Aust O, Weidner D, Fischer A, Andes FT, Stanojevic Z, Trajkovic V, Herrmann M, Korb-Pap A, Wank I, Hess A, Winter J, Wixler V, Distler J, Steiner G, Kiener HP, Frey B, Kling L, Raza K, Frey S, Kleyer A, Bauerle T, Hughes TR, Gruneboom A, Steffen U, Kronke G, Croft AP, Filer A, Kohl J, Klein K, Buckley CD, Schett G, Mougiakakos D, Hoffmann MH: The complement system drives local inflammatory tissue priming by metabolic reprogramming of synovial fibroblasts. Immunity 54: 1002-1021 (2021)

56. Fuerst M, Bertrand J, Lammers L, Dreier R, Echtermeyer F, Nitschke Y, Rutsch F, Schafer FK, Niggemeyer O, Steinhagen J, Lohmann CH, Pap T, Ruther W: Calcification of articular cartilage in human osteoarthritis. Arthritis Rheum 60: 2694-2703 (2009)

57. Gal P, Dobo J, Zavodszky P, Sim RB: Early complement proteases: C1r, C1s and MASPs. A structural insight into activation and functions. Mol Immunol 46: 2745-2752 (2009)

58. Gal P, Dobo J, Beinrohr L, Pal G, Zavodszky P: Inhibition of the serine proteases of the complement system. Adv Exp Med Biol 735: 23-40 (2013)

59. Gao S, Cui Z, Zhao MH: Complement C3a and C3a Receptor Activation Mediates Podocyte Injuries in the Mechanism of Primary Membranous Nephropathy. J Am Soc Nephrol 33: 1742-1756 (2022)

60. Gasque P, Singhrao SK, Neal JW, Wang P, Sayah S, Fontaine M, Morgan BP: The receptor for complement anaphylatoxin C3a is expressed by myeloid cells and nonmyeloid cells in inflamed human central nervous system: analysis in multiple sclerosis and bacterial meningitis. J Immunol 160: 3543-3554 (1998)

61. Gerstenfeld LC, Cullinane DM, Barnes GL, Graves DT, Einhorn TA: Fracture healing as a post-natal developmental process: molecular, spatial, and temporal aspects of its regulation. J Cell Biochem 88: 873-884 (2003)

62. Goldring MB: The role of the chondrocyte in osteoarthritis. Arthritis Rheum 43: 1916-1926 (2000)

63. Grillet B, Pereira RVS, Van Damme J, Abu El-Asrar A, Proost P, Opdenakker G: Matrix metalloproteinases in arthritis: towards precision medicine. Nat Rev Rheumatol 19: 363-377 (2023)

64. Hadzic E, Beier F: Emerging therapeutic targets for osteoarthritis. Expert Opinion on Therapeutic Targets 27: 111-120 (2023)

65. Hamilton DF, Howie CR, Burnett R, Simpson AH, Patton JT: Dealing with the predicted increase in demand for revision total knee arthroplasty: challenges, risks and opportunities. Bone Joint J 97-B: 723-728 (2015)

66. Hartmann K, Henz BM, Kruger-Krasagakes S, Kohl J, Burger R, Guhl S, Haase I, Lippert U, Zuberbier T: C3a and C5a stimulate chemotaxis of human mast cells. Blood 89: 2863-2870 (1997)

67. Haynes T, Luz-Madrigal A, Reis ES, Echeverri Ruiz NP, Grajales-Esquivel E, Tzekou A, Tsonis PA, Lambris JD, Del Rio-Tsonis K: Complement anaphylatoxin C3a is a potent inducer of embryonic chick retina regeneration. Nat Commun 4: (2013)

68. Hengartner NE, Fiedler J, Schrezenmeier H, Huber-Lang M, Brenner RE: Crucial role of IL1beta and C3a in the in vitro-response of multipotent mesenchymal stromal cells to inflammatory mediators of polytrauma. PLoS One 10: (2015)

69. Herrmann JB, Muenstermann M, Strobel L, Schubert-Unkmeir A, Woodruff TM, Gray-Owen SD, Klos A, Johswich KO: Complement C5a Receptor 1 Exacerbates the Pathophysiology of N. meningitidis Sepsis and Is a Potential Target for Disease Treatment. mBio 9: (2018)

70. Heurich M, McCluskey G: Complement and coagulation crosstalk - Factor H in the spotlight. Immunobiology 228: (2023)

71. Hojo H: Emerging RUNX2-Mediated Gene Regulatory Mechanisms Consisting of Multi-Layered Regulatory Networks in Skeletal Development. Int J Mol Sci 24: (2023)

72. Hu Q, Ecker M: Overview of MMP-13 as a Promising Target for the Treatment of Osteoarthritis. Int J Mol Sci 22: (2021)

73. Hu R, Chen ZF, Yan J, Li QF, Huang Y, Xu H, Zhang XP, Jiang H: Endoplasmic Reticulum Stress of Neutrophils Is Required for Ischemia/Reperfusion-Induced Acute Lung Injury. J Immunol 195: 4802-4809 (2015)

74. Huang W, Yang S, Shao J, Li YP: Signaling and transcriptional regulation in osteoblast commitment and differentiation. Front Biosci 12: 3068-3092 (2007)

75. Huber-Lang M, Sarma JV, Zetoune FS, Rittirsch D, Neff TA, McGuire SR, Lambris JD, Warner RL, Flierl MA, Hoesel LM, Gebhard F, Younger JG, Drouin SM, Wetsel RA, Ward PA: Generation of C5a in the absence of C3: a new complement activation pathway. Nat Med 12: 682-687 (2006)

76. Huber-Lang M, Denk S, Fulda S, Erler E, Kalbitz M, Weckbach S, Schneider EM, Weiss M, Kanse SM, Perl M: Cathepsin D is released after severe tissue trauma in vivo and is capable of generating C5a in vitro. Mol Immunol 50: 60-65 (2012)

77. Huber-Lang M, Kovtun A, Ignatius A: The role of complement in trauma and fracture healing. Semin Immunol 25: 73-78 (2013)

78. Huber-Lang M, Ekdahl KN, Wiegner R, Fromell K, Nilsson B: Auxiliary activation of the complement system and its importance for the pathophysiology of clinical conditions. Semin Immunopathol 40: 87-102 (2018)

79. Huber-Lang MS, Ignatius A, Kohl J, Mannes M, Braun CK: Complement in trauma-Traumatised complement? Br J Pharmacol 178: 2863-2879 (2021)

80. Hubert J, Beil FT, Rolvien T, Butscheidt S, Hischke S, Puschel K, Frosch S, Mussawy H, Ries C, Hawellek T: Cartilage calcification is associated with histological degeneration of the knee joint: a highly prevalent, age-independent systemic process. Osteoarthritis Cartilage 28: 1351-1361 (2020)

81. Hugli TE: Human anaphylatoxin (C3a) from the third component of complement. Primary structure. J Biol Chem 250: 8293-8301 (1975)

82. Hunter DJ, March L, Chew M: Osteoarthritis in 2020 and beyond: a Lancet Commission. Lancet 396: 1711-1712 (2020)

83. Ignatius A, Ehrnthaller C, Brenner RE, Kreja L, Schoengraf P, Lisson P, Blakytny R, Recknagel S, Claes L, Gebhard F, Lambris JD, Huber-Lang M: The anaphylatoxin receptor C5aR is present during fracture healing in rats and mediates osteoblast migration in vitro. J Trauma 71: 952-960 (2011)

84. Ignatius A, Schoengraf P, Kreja L, Liedert A, Recknagel S, Kandert S, Brenner RE, Schneider M, Lambris JD, Huber-Lang M: Complement C3a and C5a modulate osteoclast formation and inflammatory response of osteoblasts in synergism with IL-1beta. J Cell Biochem 112: 2594-2605 (2011)

85. Irannejad R, Tomshine JC, Tomshine JR, Chevalier M, Mahoney JP, Steyaert J, Rasmussen SG, Sunahara RK, El-Samad H, Huang B, von Zastrow M: Conformational biosensors reveal GPCR signalling from endosomes. Nature 495: 534-538 (2013)

86. Ishimura E, Okuno S, Kitatani K, Maekawa K, Izumotani T, Yamakawa T, Jono S, Shoji T, Shioi A, Inaba M, Massry SG, Nishizawa Y: C-reactive protein is a significant predictor of vascular calcification of both aorta and hand arteries. Semin Nephrol 24: 408-412 (2004)

87. Jang JH, Clark DJ, Li X, Yorek MS, Usachev YM, Brennan TJ: Nociceptive sensitization by complement C5a and C3a in mouse. Pain 148: 343-352 (2010)

88. Jenei-Lanzl Z, Meurer A, Zaucke F: Interleukin-1beta signaling in osteoarthritis - chondrocytes in focus. Cell Signal 53: 212-223 (2019)

89. Kalbasi Anaraki P, Patecki M, Larmann J, Tkachuk S, Jurk K, Haller H, Theilmeier G, Dumler I: Urokinase receptor mediates osteogenic differentiation of mesenchymal stem cells and vascular calcification via the complement C5a receptor. Stem Cells Dev 23: 352-362 (2014)

90. Kijowski R: Risks and Benefits of Intra-articular Corticosteroid Injection for Treatment of Osteoarthritis: What Radiologists and Patients Need to Know. Radiology 293: 664-665 (2019)

91. Kimura Y, Madhavan M, Call MK, Santiago W, Tsonis PA, Lambris JD, Del Rio-Tsonis K: Expression of complement 3 and complement 5 in newt limb and lens regeneration. J Immunol 170: 2331-2339 (2003)

92. Klos A, Tenner AJ, Johswich KO, Ager RR, Reis ES, Kohl J: The role of the anaphylatoxins in health and disease. Mol Immunol 46: 2753-2766 (2009)

93. Koelling S, Kruegel J, Irmer M, Path JR, Sadowski B, Miro X, Miosge N: Migratory chondrogenic progenitor cells from repair tissue during the later stages of human osteoarthritis. Cell Stem Cell 4: 324-335 (2009)

94. Kolasinski SL, Neogi T, Hochberg MC, Oatis C, Guyatt G, Block J, Callahan L, Copenhaver C, Dodge C, Felson D, Gellar K, Harvey WF, Hawker G, Herzig E, Kwoh CK, Nelson AE, Samuels J, Scanzello C, White D, Wise B, Altman RD, DiRenzo D, Fontanarosa J, Giradi G, Ishimori M, Misra D, Shah AA, Shmagel AK, Thoma LM, Turgunbaev M, Turner AS, Reston J: 2019 American College of Rheumatology/Arthritis Foundation Guideline for the Management of Osteoarthritis of the Hand, Hip, and Knee. Arthritis Rheumatol 72: 220-233 (2020)

95. Kon E, Filardo G, Di Matteo B, Perdisa F, Marcacci M: Matrix assisted autologous chondrocyte transplantation for cartilage treatment: A systematic review. Bone Joint Res 2: 18-25 (2013)

96. Korb LC, Ahearn JM: C1q binds directly and specifically to surface blebs of apoptotic human keratinocytes: complement deficiency and systemic lupus erythematosus revisited. J Immunol 158: 4525-4528 (1997)

97. Kovtun A, Bergdolt S, Hagele Y, Matthes R, Lambris JD, Huber-Lang M, Ignatius A: Complement receptors C5aR1 and C5aR2 act differentially during the early immune response after bone fracture but are similarly involved in bone repair. Sci Rep 7: (2017)

98. Krishnan Y, Grodzinsky AJ: Cartilage diseases. Matrix Biol 71-72: 51-69 (2018)

99. Krisinger MJ, Goebeler V, Lu Z, Meixner SC, Myles T, Pryzdial EL, Conway EM: Thrombin generates previously unidentified C5 products that support the terminal complement activation pathway. Blood 120: 1717-1725 (2012)

100. Kuhn A, Riegger J, Teixeira GQ, Huber-Lang M, Lambris JD, Neidlinger-Wilke C, Brenner RE: Terminal Complement Activation Is Induced by Factors Released from Endplate Tissue of Disc Degeneration Patients and Stimulates Expression of Catabolic Enzymes in Annulus Fibrosus Cells. Cells 12: (2023)

101. Kumar V, Lee JD, Clark RJ, Noakes PG, Taylor SM, Woodruff TM: Preclinical Pharmacokinetics of Complement C5a Receptor Antagonists PMX53 and PMX205 in Mice. ACS Omega 5: 2345-2354 (2020)

102. Kumari R, Jat P: Mechanisms of Cellular Senescence: Cell Cycle Arrest and Senescence Associated Secretory Phenotype. Front Cell Dev Biol 9: (2021)

103. Kunchithapautham K, Atkinson C, Rohrer B: Smoke exposure causes endoplasmic reticulum stress and lipid accumulation in retinal pigment epithelium through oxidative stress and complement activation. J Biol Chem 289: 14534-14546 (2014)

104. Kunz N, Kemper C: Complement Has Brains-Do Intracellular Complement and Immunometabolism Cooperate in Tissue Homeostasis and Behavior? Front Immunol 12: (2021)

105. Lachmann PJ: The amplification loop of the complement pathways. Adv Immunol 104: 115-149 (2009)

106. Laine L, White WB, Rostom A, Hochberg M: COX-2 selective inhibitors in the treatment of osteoarthritis. Semin Arthritis Rheum 38: 165-187 (2008)

107. Lamers C, Mastellos DC, Ricklin D, Lambris JD: Compstatins: the dawn of clinical C3-targeted complement inhibition. Trends Pharmacol Sci 43: 629-640 (2022)

108. Lange C, Jentsch F, Allen J, Hoebel J, Kratz AL, von der Lippe E, Muters S, Schmich P, Thelen J, Wetzstein M, Fuchs J, Ziese T: Data Resource Profile: German Health Update (GEDA)-the health interview survey for adults in Germany. Int J Epidemiol 44: 442-450 (2015)

109. Lee JI, Sato M, Ushida K, Mochida J: Measurement of diffusion in articular cartilage using fluorescence correlation spectroscopy. BMC Biotechnol 11: (2011)

110. Lefebvre V, Smits P: Transcriptional control of chondrocyte fate and differentiation. Birth Defects Res C Embryo Today 75: 200-212 (2005)

111. Lepetsos P, Papavassiliou AG: ROS/oxidative stress signaling in osteoarthritis. Biochim Biophys Acta 1862: 576-591 (2016)

112. Leung LL, Morser J: Plasmin as a complement C5 convertase. EBioMedicine 5: 20-21 (2016)

113. Levine JD, Gooding J, Donatoni P, Borden L, Goetzl EJ: The role of the polymorphonuclear leukocyte in hyperalgesia. J Neurosci 5: 3025-3029 (1985)

114. Li J, Jiang H, Lv Z, Sun Z, Cheng C, Tan G, Wang M, Liu A, Sun H, Guo H, Chen F, Liu Z, Fei Y, Liu Y, Wu R, Xu X, Yan W, Jiang Q, Shi D: Articular fibrocartilage-targeted therapy by microtubule stabilization. Sci Adv 8: (2022)

115. Li S, Cao P, Chen T, Ding C: Latest insights in disease-modifying osteoarthritis drugs development. Ther Adv Musculoskelet Dis 15: (2023)

116. Li XX, Lee JD, Kemper C, Woodruff TM: The Complement Receptor C5aR2: A Powerful Modulator of Innate and Adaptive Immunity. J Immunol 202: 3339-3348 (2019)

117. Liodakis E, Bergeron SG, Zukor DJ, Huk OL, Epure LM, Antoniou J: Perioperative Complications and Length of Stay After Revision Total Hip and Knee Arthroplasties: An Analysis of the NSQIP Database. J Arthroplasty 30: 1868-1871 (2015)

118. Liszewski MK, Post TW, Atkinson JP: Membrane cofactor protein (MCP or CD46): newest member of the regulators of complement activation gene cluster. Annu Rev Immunol 9: 431-455 (1991)

119. Liszewski MK, Kolev M, Le Friec G, Leung M, Bertram PG, Fara AF, Subias M, Pickering MC, Drouet C, Meri S, Arstila TP, Pekkarinen PT, Ma M, Cope A, Reinheckel T, Rodriguez de Cordoba S, Afzali B, Atkinson JP, Kemper C: Intracellular complement activation sustains T cell homeostasis and mediates effector differentiation. Immunity 39: 1143-1157 (2013)

120. Liu A, Luo P, Huang H: New insight of complement system in the process of vascular calcification. J Cell Mol Med 27: 1168-1178 (2023)

121. Liu J, Wei X, Hu J, Tan X, Kang X, Gao L, Li N, Shi X, Yuan M, Hu W, Liu M: Different concentrations of C5a affect human dental pulp mesenchymal stem cells differentiation. BMC Oral Health 21: (2021)

122. Liu Q, Hu X, Zhang X, Duan X, Yang P, Zhao F, Ao Y: Effects of mechanical stress on chondrocyte phenotype and chondrocyte extracellular matrix expression. Sci Rep 6: (2016)

123. Liu Y, Zhang Z, Li T, Xu H, Zhang H: Senescence in osteoarthritis: from mechanism to potential treatment. Arthritis Res Ther 24: (2022)

124. Lo MW, Amarilla AA, Lee JD, Albornoz EA, Modhiran N, Clark RJ, Ferro V, Chhabra M, Khromykh AA, Watterson D, Woodruff TM: SARS-CoV-2 triggers complement activation through interactions with heparan sulfate. Clin Transl Immunology 11: (2022)

125. Loeser RF, Goldring SR, Scanzello CR, Goldring MB: Osteoarthritis: a disease of the joint as an organ. Arthritis Rheum 64: 1697-1707 (2012)

126. Lohmander LS, Englund PM, Dahl LL, Roos EM: The long-term consequence of anterior cruciate ligament and meniscus injuries: osteoarthritis. Am J Sports Med 35: 1756-1769 (2007)

127. Luntzer K, Lackner I, Weber B, Modinger Y, Ignatius A, Gebhard F, Mihaljevic SY, Haffner-Luntzer M, Kalbitz M: Increased Presence of Complement Factors and Mast Cells in Alveolar Bone and Tooth Resorption. Int J Mol Sci 22: (2021)

128. Mackie EJ, Ahmed YA, Tatarczuch L, Chen KS, Mirams M: Endochondral ossification: How cartilage is converted into bone in the developing skeleton. Int J Biochem Cell Biol 40: 46-62 (2008)

129. Mannes M, Schmidt CQ, Nilsson B, Ekdahl KN, Huber-Lang M: Complement as driver of systemic inflammation and organ failure in trauma, burn, and sepsis. Semin Immunopathol 43: 773-788 (2021)

130. Mao L, Wu W, Wang M, Guo J, Li H, Zhang S, Xu J, Zou J: Targeted treatment for osteoarthritis: drugs and delivery system. Drug Deliv 28: 1861-1876 (2021)

131. Marc C. Hochberg MGC, Sylvia I. Watkins-Castillo. The Burden of Musculoskeletal Diseases in the United States: US Bone and Joint Initiative; [cited 2024 March 28]. Available from: https://www.boneandjointburden.org/fourth-edition/iiib10/osteoarthritis.

132. Maroudas A, Bullough P, Swanson SA, Freeman MA: The permeability of articular cartilage. J Bone Joint Surg Br 50: 166-177 (1968)

133. Martinez-Lopez D, Roldan-Montero R, Garcia-Marques F, Nunez E, Jorge I, Camafeita E, Minguez P, Rodriguez de Cordoba S, Lopez-Melgar B, Lara-Pezzi E, Fernandez-Ortiz A, Ibanez B, Valdivielso JM, Fuster V, Michel JB, Blanco-Colio LM, Vazquez J, Martin-Ventura JL: Complement C5 Protein as a Marker of Subclinical Atherosclerosis. J Am Coll Cardiol 75: 1926-1941 (2020)

134. Mastellos D, Papadimitriou JC, Franchini S, Tsonis PA, Lambris JD: A novel role of complement: mice deficient in the fifth component of complement (C5) exhibit impaired liver regeneration. J Immunol 166: 2479-2486 (2001)

135. Mastellos DC, Ricklin D, Sfyroera G, Sahu A: From discovery to approval: A brief history of the compstatin family of complement C3 inhibitors. Clin Immunol 235: (2022)

136. Matsushita T, Tokura T, Okimura K, Sano S, Nishida K, Nagai K, Hoshino Y: Surgical treatment of cartilage lesions in the knee: A narrative review. Journal of Joint Surgery and Research 1: 70-79 (2023)

137. Matthews KW, Mueller-Ortiz SL, Wetsel RA: Carboxypeptidase N: a pleiotropic regulator of inflammation. Mol Immunol 40: 785-793 (2004)

138. Mayne R, Vail MS, Mayne PM, Miller EJ: Changes in type of collagen synthesized as clones of chick chondrocytes grow and eventually lose division capacity. Proc Natl Acad Sci U S A 73: 1674-1678 (1976)

139. Meyer F, Dittmann A, Kornak U, Herbster M, Pap T, Lohmann CH, Bertrand J: Chondrocytes From Osteoarthritic and Chondrocalcinosis Cartilage Represent Different Phenotypes. Front Cell Dev Biol 9: (2021)

140. Mollentze J, Durandt C, Pepper MS: An In Vitro and In Vivo Comparison of Osteogenic Differentiation of Human Mesenchymal Stromal/Stem Cells. Stem Cells Int 2021: (2021)

141. Molnar V, Matisic V, Kodvanj I, Bjelica R, Jelec Z, Hudetz D, Rod E, Cukelj F, Vrdoljak T, Vidovic D, Staresinic M, Sabalic S, Dobricic B, Petrovic T, Anticevic D, Boric I, Kosir R, Zmrzljak UP, Primorac D: Cytokines and Chemokines Involved in Osteoarthritis Pathogenesis. Int J Mol Sci 22: (2021)

142. Morgan BP: Complement membrane attack on nucleated cells: resistance, recovery and non-lethal effects. Biochem J 264: 1-14 (1989)

143. Muthu S, Korpershoek JV, Novais EJ, Tawy GF, Hollander AP, Martin I: Failure of cartilage regeneration: emerging hypotheses and related therapeutic strategies. Nat Rev Rheumatol 19: 403-416 (2023)

144. Nagaraj N, Matthews KA, Shields KJ, Barinas-Mitchell E, Budoff MJ, El Khoudary SR: Complement proteins and arterial calcification in middle aged women: Cross-sectional effect of cardiovascular fat. The SWAN Cardiovascular Fat Ancillary Study. Atherosclerosis 243: 533-539 (2015)

145. Nakase T, Miyaji T, Tomita T, Kaneko M, Kuriyama K, Myoui A, Sugamoto K, Ochi T, Yoshikawa H: Localization of bone morphogenetic protein-2 in human osteoarthritic cartilage and osteophyte. Osteoarthritis Cartilage 11: 278-284 (2003)

146. Nataf S, Davoust N, Ames RS, Barnum SR: Human T cells express the C5a receptor and are chemoattracted to C5a. J Immunol 162: 4018-4023 (1999)

147. Nazempour A, Van Wie BJ: Chondrocytes, Mesenchymal Stem Cells, and Their Combination in Articular Cartilage Regenerative Medicine. Ann Biomed Eng 44: 1325-1354 (2016)

148. Nerurkar NL, Han W, Mauck RL, Elliott DM: Homologous structure-function relationships between native fibrocartilage and tissue engineered from MSC-seeded nanofibrous scaffolds. Biomaterials 32: 461-468 (2011)

149. Nilsson O, Parker EA, Hegde A, Chau M, Barnes KM, Baron J: Gradients in bone morphogenetic protein-related gene expression across the growth plate. J Endocrinol 193: 75-84 (2007)

150. O'Keefe RJ, Loveys LS, Hicks DG, Reynolds PR, Crabb ID, Puzas JE, Rosier RN: Differential regulation of type-II and type-X collagen synthesis by parathyroid hormone-related protein in chick growth-plate chondrocytes. J Orthop Res 15: 162-174 (1997)

151. Ogden CA, deCathelineau A, Hoffmann PR, Bratton D, Ghebrehiwet B, Fadok VA, Henson PM: C1q and mannose binding lectin engagement of cell surface calreticulin and CD91 initiates macropinocytosis and uptake of apoptotic cells. J Exp Med 194: 781-795 (2001)

152. Okamura K, Inagaki Y, Matsui TK, Matsubayashi M, Komeda T, Ogawa M, Mori E, Tanaka Y: RT-qPCR analyses on the osteogenic differentiation from human iPS cells: an investigation of reference genes. Sci Rep 10: (2020)

153. Onuma H, Masuko-Hongo K, Yuan G, Sakata M, Nakamura H, Kato T, Aoki H, Nishioka K: Expression of the anaphylatoxin receptor C5aR (CD88) by human articular chondrocytes. Rheumatol Int 22: 52-55 (2002)

154. Oo WM, Little C, Duong V, Hunter DJ: The Development of Disease-Modifying Therapies for Osteoarthritis (DMOADs): The Evidence to Date. Drug Des Devel Ther 15: 2921-2945 (2021)

155. Oppermann M, Gotze O: Plasma clearance of the human C5a anaphylatoxin by binding to leucocyte C5a receptors. Immunology 82: 516-521 (1994)

156. Orrem HL, Nilsson PH, Pischke SE, Kleveland O, Yndestad A, Ekholt K, Damas JK, Espevik T, Bendz B, Halvorsen B, Gregersen I, Wiseth R, Andersen GO, Ueland T, Gullestad L, Aukrust P, Barratt-Due A, Mollnes TE: IL-6 Receptor Inhibition by Tocilizumab Attenuated Expression of C5a Receptor 1 and 2 in Non-ST-Elevation Myocardial Infarction. Front Immunol 9: (2018)

157. Orsini F, De Blasio D, Zangari R, Zanier ER, De Simoni MG: Corrigendum: Versatility of the complement system in neuroinflammation, neurodegeneration, and brain homeostasis. Front Cell Neurosci 9: (2015)

158. Ottonello L, Corcione A, Tortolina G, Airoldi I, Albesiano E, Favre A, D'Agostino R, Malavasi F, Pistoia V, Dallegri F: rC5a directs the in vitro migration of human memory and naive tonsillar B lymphocytes: implications for B cell trafficking in secondary lymphoid tissues. J Immunol 162: 6510-6517 (1999)

159. Pangburn MK, Rawal N: Structure and function of complement C5 convertase enzymes. Biochem Soc Trans 30: 1006-1010 (2002)

160. Peffers MJ, McDermott B, Clegg PD, Riggs CM: Comprehensive protein profiling of synovial fluid in osteoarthritis following protein equalization. Osteoarthritis Cartilage 23: 1204-1213 (2015)

161. Pelletier JP, Martel-Pelletier J, Rannou F, Cooper C: Efficacy and safety of oral NSAIDs and analgesics in the management of osteoarthritis: Evidence from real-life setting trials and surveys. Semin Arthritis Rheum 45: 22-27 (2016)

162. Peng Y, Kang Q, Cheng H, Li X, Sun MH, Jiang W, Luu HH, Park JY, Haydon RC, He TC: Transcriptional characterization of bone morphogenetic proteins (BMPs)-mediated osteogenic signaling. J Cell Biochem 90: 1149-1165 (2003)

163. Pines M, Hurwitz S: The role of the growth plate in longitudinal bone growth. Poult Sci 70: 1806-1814 (1991)

164. Piontek T, Ciemniewska-Gorzela K, Szulc A, Naczk J, Slomczykowski M: All-arthroscopic AMIC procedure for repair of cartilage defects of the knee. Knee Surg Sports Traumatol Arthrosc 20: 922-925 (2012)

165. Poole AR: Osteoarthritis as a whole joint disease. HSS J 8: 4-6 (2012)

166. Purwar R, Wittmann M, Zwirner J, Oppermann M, Kracht M, Dittrich-Breiholz O, Gutzmer R, Werfel T: Induction of C3 and CCL2 by C3a in keratinocytes: a novel autocrine amplification loop of inflammatory skin reactions. J Immunol 177: 4444-4450 (2006)

167. Quadros AU, Cunha TM: C5a and pain development: An old molecule, a new target. Pharmacol Res 112: 58-67 (2016)

168. Relja B, Land WG: Damage-associated molecular patterns in trauma. Eur J Trauma Emerg Surg 46: 751-775 (2020)

169. Richard MJ, Driban JB, McAlindon TE: Pharmaceutical treatment of osteoarthritis. Osteoarthritis Cartilage 31: 458-466 (2023)

170. Ricklin D, Hajishengallis G, Yang K, Lambris JD: Complement: a key system for immune surveillance and homeostasis. Nat Immunol 11: 785-797 (2010)

171. Ricklin D, Reis ES, Lambris JD: Complement in disease: a defence system turning offensive. Nat Rev Nephrol 12: 383-401 (2016)

172. Riegger J, Joos H, Palm HG, Friemert B, Reichel H, Ignatius A, Brenner RE: Antioxidative therapy in an ex vivo human cartilage trauma-model: attenuation of trauma-induced cell loss and ECM-destructive enzymes by N-acetyl cysteine. Osteoarthritis Cartilage 24: 2171-2180 (2016)

173. Riegger J, Joos H, Palm HG, Friemert B, Reichel H, Ignatius A, Brenner RE: Striking a new path in reducing cartilage breakdown: combination of antioxidative therapy and chondroanabolic stimulation after blunt cartilage trauma. J Cell Mol Med 22: 77-88 (2018)

174. Riegger J, Palm HG, Brenner RE: The functional role of chondrogenic stem/progenitor cells: novel evidence for immunomodulatory properties and regenerative potential after cartilage injury. Eur Cell Mater 36: 110-127 (2018)

175. Riegger J, Brenner RE: Pathomechanisms of Posttraumatic Osteoarthritis: Chondrocyte Behavior and Fate in a Precarious Environment. Int J Mol Sci 21: (2020)

176. Riegger J, Huber-Lang M, Brenner RE: Crucial role of the terminal complement complex in chondrocyte death and hypertrophy after cartilage trauma. Osteoarthritis Cartilage 28: 685-697 (2020)

177. Riegger J, Joos H, Mohler V, Leucht F, Rading K, Kubisch C, Ignatius A, Huber-Lang M, Brenner RE: Functional Loss of Terminal Complement Complex Protects Rabbits from Injury-Induced Osteoarthritis on Structural and Cellular Level. Biomolecules 13: (2023)

178. Riegger J, Schoppa A, Ruths L, Haffner-Luntzer M, Ignatius A: Oxidative stress as a key modulator of cell fate decision in osteoarthritis and osteoporosis: a narrative review. Cell Mol Biol Lett 28: (2023)

179. Robert Koch Institute DoEaHM: German Health Update 2014/2015-EHIS (GEDA 2014/2015-EHIS). Scientific Use File first version: (2018)

180. Rodriguez-Merchan EC: The Current Role of Disease-modifying Osteoarthritis Drugs. Arch Bone Jt Surg 11: 11-22 (2023)

181. Ruocco A, Sirico A, Novelli R, Iannelli S, Van Breda SV, Kyburz D, Hasler P, Aramini A, Amendola PG: The role of C5a-C5aR1 axis in bone pathophysiology: A mini-review. Front Cell Dev Biol 10: (2022)

182. Ruths L, Huber-Lang M, Schulze-Tanzil G, Riegger J: Anaphylatoxins and their corresponding receptors as potential drivers in cartilage calcification during osteoarthritis progression. Osteoarthritis Cartilage 32: 514-525 (2024)

183. Saha N, Moldovan F, Tardif G, Pelletier JP, Cloutier JM, Martel-Pelletier J: Interleukin-1beta-converting enzyme/caspase-1 in human osteoarthritic tissues: localization and role in the maturation of interleukin-1beta and interleukin-18. Arthritis Rheum 42: 1577-1587 (1999)

184. Sakiyama H, Inaba N, Toyoguchi T, Okada Y, Matsumoto M, Moriya H, Ohtsu H: Immunolocalization of complement C1s and matrix metalloproteinase 9 (92kDa gelatinase/type IV collagenase) in the primary ossification center of the human femur. Cell Tissue Res 277: 239-245 (1994)

185. Sanchez-Adams J, Leddy HA, McNulty AL, O'Conor CJ, Guilak F: The mechanobiology of articular cartilage: bearing the burden of osteoarthritis. Curr Rheumatol Rep 16: (2014)

186. Sanchez-Lopez E, Coras R, Torres A, Lane NE, Guma M: Synovial inflammation in osteoarthritis progression. Nat Rev Rheumatol 18: 258-275 (2022)

187. Schafer N, Grassel S: Involvement of complement peptides C3a and C5a in osteoarthritis pathology. Peptides 154: (2022)

188. Schenker ML, Mauck RL, Ahn J, Mehta S: Pathogenesis and prevention of posttraumatic osteoarthritis after intra-articular fracture. J Am Acad Orthop Surg 22: 20-28 (2014)

189. Schmal H, Salzmann GM, Niemeyer P, Langenmair E, Guo R, Schneider C, Habel M, Riedemann N: Early intra-articular complement activation in ankle fractures. Biomed Res Int 2014: (2014)

190. Schneider MR: Von Kossa and his staining technique. Histochem Cell Biol 156: 523-526 (2021)

191. Schraufstatter IU, Discipio RG, Zhao M, Khaldoyanidi SK: C3a and C5a are chemotactic factors for human mesenchymal stem cells, which cause prolonged ERK1/2 phosphorylation. J Immunol 182: 3827-3836 (2009)

192. Schulze-Tanzil G, Kohl B, El Sayed K, Arens S, Ertel W, Stolzel K, John T: Anaphylatoxin receptors and complement regulatory proteins in human articular and non-articular chondrocytes: interrelation with cytokines. Cell Tissue Res 350: 465-475 (2012)

193. Settmacher B, Bock D, Saad H, Gartner S, Rheinheimer C, Kohl J, Bautsch W, Klos A: Modulation of C3a activity: internalization of the human C3a receptor and its inhibition by C5a. J Immunol 162: 7409-7416 (1999)

194. Shekaran A, Sim E, Tan KY, Chan JK, Choolani M, Reuveny S, Oh S: Enhanced in vitro osteogenic differentiation of human fetal MSCs attached to 3D microcarriers versus harvested from 2D monolayers. BMC Biotechnol 15: (2015)

195. Sheridan D, Yu ZX, Zhang Y, Patel R, Sun F, Lasaro MA, Bouchard K, Andrien B, Marozsan A, Wang Y, Tamburini P: Design and preclinical characterization of ALXN1210: A novel anti-C5 antibody with extended duration of action. PLoS One 13: (2018)

196. Silawal S, Triebel J, Bertsch T, Schulze-Tanzil G: Osteoarthritis and the Complement Cascade. Clin Med Insights Arthritis Musculoskelet Disord 11: (2018)

197. Sinno H, Malhotra M, Lutfy J, Jardin B, Winocour S, Brimo F, Beckman L, Watters K, Philip A, Williams B, Prakash S: Accelerated wound healing with topical application of complement C5. Plast Reconstr Surg 130: 523-529 (2012)

198. Sinno H, Malholtra M, Lutfy J, Jardin B, Winocour S, Brimo F, Beckman L, Watters K, Philip A, Williams B, Prakash S: Topical application of complement C3 in collagen formulation increases early wound healing. J Dermatolog Treat 24: 141-147 (2013 a)

199. Sinno H, Malhotra M, Lutfy J, Jardin B, Winocour S, Brimo F, Beckman L, Watters K, Philip A, Williams B, Prakash S: Complements c3 and c5 individually and in combination increase early wound strength in a rat model of experimental wound healing. Plast Surg Int 2013: (2013 b)

200. Song P, Cui Z, Hu L: Applications and prospects of intra-articular drug delivery system in arthritis therapeutics. J Control Release 352: 946-960 (2022)

201. Sophia Fox AJ, Bedi A, Rodeo SA: The basic science of articular cartilage: structure, composition, and function. Sports Health 1: 461-468 (2009)

202. Sproston NR, Ashworth JJ: Role of C-Reactive Protein at Sites of Inflammation and Infection. Front Immunol 9: (2018)

203. Steinert AF, Proffen B, Kunz M, Hendrich C, Ghivizzani SC, Noth U, Rethwilm A, Eulert J, Evans CH: Hypertrophy is induced during the in vitro chondrogenic differentiation of human mesenchymal stem cells by bone morphogenetic protein-2 and bone morphogenetic protein-4 gene transfer. Arthritis Res Ther 11: (2009)

204. Strey CW, Markiewski M, Mastellos D, Tudoran R, Spruce LA, Greenbaum LE, Lambris JD: The proinflammatory mediators C3a and C5a are essential for liver regeneration. J Exp Med 198: 913-923 (2003)

205. Struglics A, Okroj M, Sward P, Frobell R, Saxne T, Lohmander LS, Blom AM: The complement system is activated in synovial fluid from subjects with knee injury and from patients with osteoarthritis. Arthritis Res Ther 18: (2016)

206. Teixeira GQ, Yong Z, Kuhn A, Riegger J, Goncalves RM, Ruf M, Mauer UM, Huber-Lang M, Ignatius A, Brenner RE, Neidlinger-Wilke C: Interleukin-1beta and cathepsin D modulate formation of the terminal complement complex in cultured human disc tissue. Eur Spine J 30: 2247-2256 (2021 a)

207. Teixeira GQ, Yong Z, Goncalves RM, Kuhn A, Riegger J, Brisby H, Barreto Henriksson H, Ruf M, Nerlich A, Mauer UM, Ignatius A, Brenner RE, Neidlinger-Wilke C: Terminal complement complex formation is associated with intervertebral disc degeneration. Eur Spine J 30: 217-226 (2021 b)

208. Testa G, Giardina SMC, Culmone A, Vescio A, Turchetta M, Cannavo S, Pavone V: Intra-Articular Injections in Knee Osteoarthritis: A Review of Literature. J Funct Morphol Kinesiol 6: (2021)

209. Tichaczek-Goska D: Deficiencies and excessive human complement system activation in disorders of multifarious etiology. Adv Clin Exp Med 21: 105-114 (2012)

210. Toth AD, Turu G, Hunyady L: Functional consequences of spatial, temporal and ligand bias of G protein-coupled receptors. Nat Rev Nephrol: (2024)

211. Tschaffon MEA, Reber SO, Schoppa A, Nandi S, Cirstea IC, Aszodi A, Ignatius A, Haffner-Luntzer M: A novel in vitro assay to study chondrocyte-to-osteoblast transdifferentiation. Endocrine 75: 266-275 (2022)

212. Tsuno H, Tanaka N, Naito M, Ohashi S, Iwasawa M, Kadoguchi T, Mitomi H, Matsui T, Furukawa H, Fukui N: Analysis of proteins released from osteoarthritic cartilage by compressive loading. Sci Rep 13: (2023)

213. Ulici V, Chen AF, Cheng AWM, Tuan RS: Anatomy: Cartilage. In: McCarthy JC, Noble PC, Villar RN, (Eds.) Hip Joint Restoration: Worldwide Advances in Arthroscopy, Arthroplasty, Osteotomy and Joint Preservation Surgery. New York: Springer New York, p. 15-22. (2017)

214. van der Kraan PM: The Interaction between Joint Inflammation and Cartilage Repair. Tissue Engineering and Regenerative Medicine 16: 327-334 (2019)

215. Verma P, Dalal K: ADAMTS-4 and ADAMTS-5: key enzymes in osteoarthritis. J Cell Biochem 112: 3507-3514 (2011)

216. Vimalraj S: Alkaline phosphatase: Structure, expression and its function in bone mineralization. Gene 754: (2020)

217. Vinod E, Boopalan P, Sathishkumar S: Reserve or Resident Progenitors in Cartilage? Comparative Analysis of Chondrocytes versus Chondroprogenitors and Their Role in Cartilage Repair. Cartilage 9: 171-182 (2018)

218. Von Der Mark K, Gauss V, Von Der Mark H, Müller P: Relationship between cell shape and type of collagen synthesised as chondrocytes lose their cartilage phenotype in culture. Nature 267: 531-532 (1977)

219. Wakitani S, Mitsuoka T, Nakamura N, Toritsuka Y, Nakamura Y, Horibe S: Autologous bone marrow stromal cell transplantation for repair of full-thickness articular cartilage defects in human patellae: two case reports. Cell Transplant 13: 595-600 (2004)

220. Waldstein W, Perino G, Gilbert SL, Maher SA, Windhager R, Boettner F: OARSI osteoarthritis cartilage histopathology assessment system: A biomechanical evaluation in the human knee. J Orthop Res 34: 135-140 (2016)

221. Wang B, Han J, Elisseeff JH, Demaria M: The senescence-associated secretory phenotype and its physiological and pathological implications. Nat Rev Mol Cell Biol: (2024)

222. Wang L, Jie Q, Yang L: Chondrocytes-osteoblast transition in endochondral ossification. Annals of Joint 2: (2017)

223. Wang Q, Rozelle AL, Lepus CM, Scanzello CR, Song JJ, Larsen DM, Crish JF, Bebek G, Ritter SY, Lindstrom TM, Hwang I, Wong HH, Punzi L, Encarnacion A, Shamloo M, Goodman SB, Wyss-Coray T, Goldring SR, Banda NK, Thurman JM, Gobezie R, Crow MK, Holers VM, Lee DM, Robinson WH: Identification of a central role for complement in osteoarthritis. Nat Med 17: 1674-1679 (2011)

224. Wang X, Wu Q, Zhang R, Fan Z, Li W, Mao R, Du Z, Yao X, Ma Y, Yan Y, Sun W, Wu H, Wei W, Hu Y, Hong Y, Hu H, Koh YW, Duan W, Chen X, Ouyang H: Stage-specific and location-specific cartilage calcification in osteoarthritis development. Ann Rheum Dis 82: 393-402 (2023)

225. Wang Y, Miao Y, Gong K, Cheng X, Chen Y, Zhao MH: Plasma Complement Protein C3a Level Was Associated with Abdominal Aortic Calcification in Patients on Hemodialysis. J Cardiovasc Transl Res 12: 496-505 (2019)

226. Wang Y, Al-Dakkak I, Garlo K, Ong ML, Tomazos I, Mahajerin A: Atypical Hemolytic Uremic Syndrome Treated With Ravulizumab or Eculizumab: A Claims-Based Evaluation of Health Care Resource Utilization and Clinical Outcomes in the United States. Kidney Med 5: (2023)

227. Weng JJ, Su Y: Nuclear matrix-targeting of the osteogenic factor Runx2 is essential for its recognition and activation of the alkaline phosphatase gene. Biochim Biophys Acta 1830: 2839-2852 (2013)

228. Wu MC, Brennan FH, Lynch JP, Mantovani S, Phipps S, Wetsel RA, Ruitenberg MJ, Taylor SM, Woodruff TM: The receptor for complement component C3a mediates protection from intestinal ischemia-reperfusion injuries by inhibiting neutrophil mobilization. Proc Natl Acad Sci USA 110: 9439-9444 (2013)

229. Wu X, You D, Pan M, Weng M, Xie Q, Guan Y, Zheng J, Lin S, Zhang X, Hao C, Wan J: Knockout of the C3a receptor protects against renal ischemia reperfusion injury by reduction of NETs formation. Cell Mol Life Sci 80: (2023)

230. Xiang XN, Zhu SY, He HC, Yu X, Xu Y, He CQ: Mesenchymal stromal cell-based therapy for cartilage regeneration in knee osteoarthritis. Stem Cell Res Ther 13: (2022)

231. Xie CB, Jane-Wit D, Pober JS: Complement Membrane Attack Complex: New Roles, Mechanisms of Action, and Therapeutic Targets. Am J Pathol 190: 1138-1150 (2020)

232. Xu JX, Xu FZ, Furbish A, Braxton AM, Brumfield B, Helke KL, Peterson YK: Inhibition of complement C3 prevents osteoarthritis progression in guinea pigs by blocking STAT1 activation. Commun Biol 7: (2024)

233. Yamaguchi K, Sakiyama H, Matsumoto M, Moriya H, Sakiyama S: Degradation of type I and II collagen by human activated C1-s. FEBS Lett 268: 206-208 (1990)

234. Yan JF, Qin WP, Xiao BC, Wan QQ, Tay FR, Niu LN, Jiao K: Pathological calcification in osteoarthritis: an outcome or a disease initiator? Biol Rev Camb Philos Soc 95: 960-985 (2020)

235. Yang CY, Chanalaris A, Troeberg L: ADAMTS and ADAM metalloproteinases in osteoarthritis - looking beyond the 'usual suspects'. Osteoarthritis Cartilage 25: 1000-1009 (2017)

236. Yang L, Tsang KY, Tang HC, Chan D, Cheah KS: Hypertrophic chondrocytes can become osteoblasts and osteocytes in endochondral bone formation. Proc Natl Acad Sci USA 111: 12097-12102 (2014)

237. Zhang W, Jones A, Doherty M: Does paracetamol (acetaminophen) reduce the pain of osteoarthritis? A meta-analysis of randomised controlled trials. Ann Rheum Dis 63: 901-907 (2004)

238. Zhou P, Shi JM, Song JE, Han Y, Li HJ, Song YM, Feng F, Wang JL, Zhang R, Lan F: Establishing a deeper understanding of the osteogenic differentiation of monolayer cultured human pluripotent stem cells using novel and detailed analyses. Stem Cell Res Ther 12: (2021)

239. Zhou X, von der Mark K, Henry S, Norton W, Adams H, de Crombrugghe B: Chondrocytes transdifferentiate into osteoblasts in endochondral bone during development, postnatal growth and fracture healing in mice. PLoS Genet 10: (2014)

240. Ziegler DV, Wiley CD, Velarde MC: Mitochondrial effectors of cellular senescence: beyond the free radical theory of aging. Aging Cell 14: 1-7 (2015)

Acknowledgment

Acknowledgments have been removed for privacy reasons.

Statutory declaration

Declaration:

I hereby declare that I wrote the present dissertation with the topic:

Involvement of anaphylatoxins and their corresponding receptors in cartilage calcification during osteoarthritis progression

independently and used no other aids that those cited. In each individual case, I have clearly identified the source of the passages that are taken word for word or paraphrased from other works.

I also hereby declare that I have carried out my scientific work according to the principles of good scientific practice in accordance with the current „Satzung der Universität Ulm zur Sicherung guter wissenschaftlicher Praxis“ [Rules of the University of Ulm for Assuring Good Scientific Practice].

Ulm,

_____

Leonie Ruths